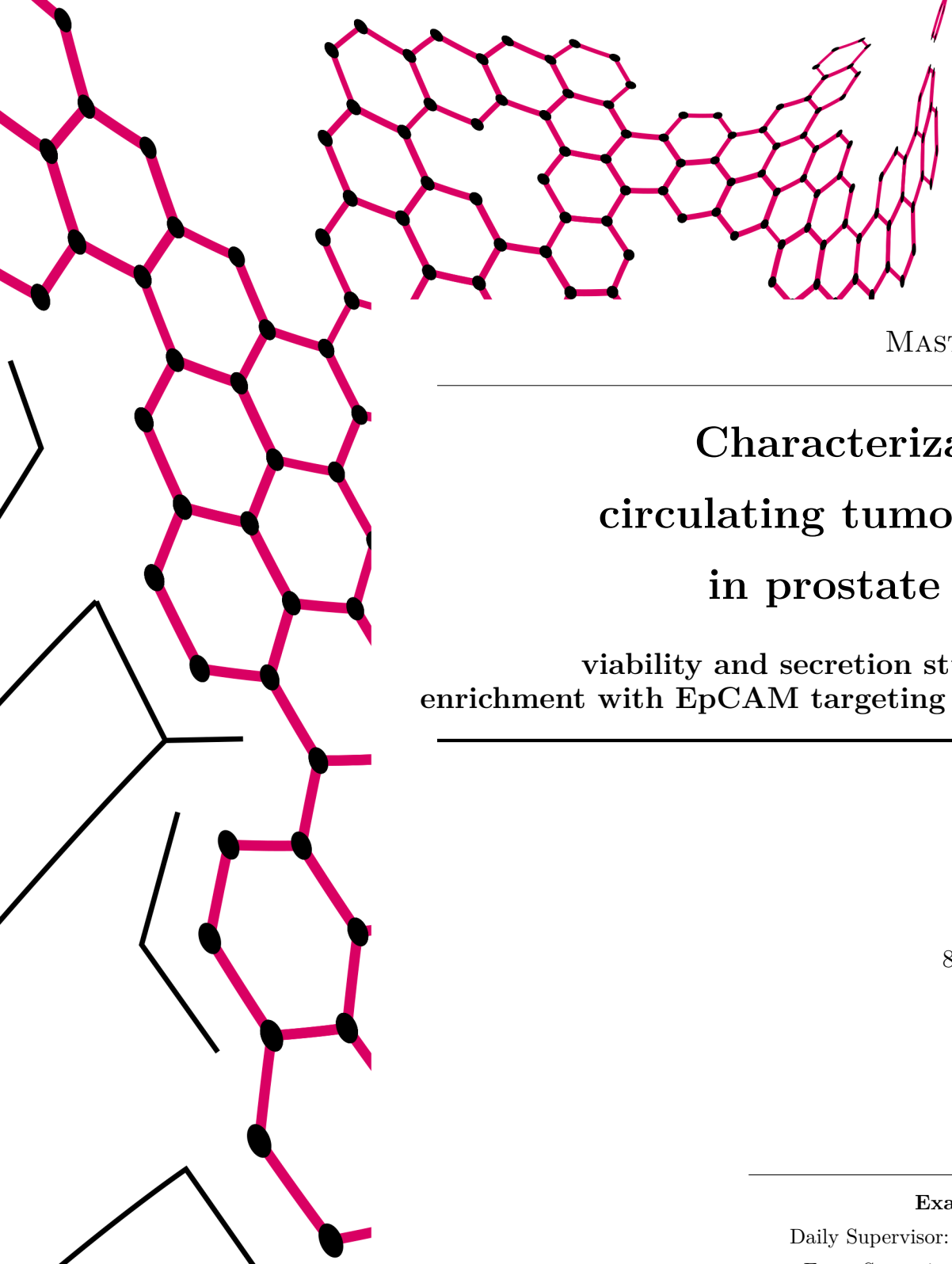

Master Thesis

Characterization of circulating tumour cells in prostate cancer:

viability and secretion studies after enrichment with EpCAM targeting ferrofluids

G. Bante

8 October 2022

Exam Committee:

Daily Supervisor: Ir. E. Dathathri

Extra Supervisor: Ir. M. Stevens

Extra Supervisor: Ir. F. Abali

Head Supervisor: Prof.Dr. L.W.M.M. Terstappen

External Supervisor: Prof.Dr. A. Kocer

Medical Cell BioPhysics (MCBP)

Faculty of Science and Technology (TNW)

University of Twente

Enschede

The Netherlands

Contents

1 Abstract

1.1 Abstract English

Prostate cancer (PCa) is the most common cancer among men in the USA and the second most death causing cancer when looking at total numbers. Primary PCa has nowadays 5 year survival rate of 100%, however metastatic PCa only has a 32% 5 year survival rate. Different PCa types need different treatment depending the stage of the cancer, AR dependency, aggressiveness, and mutations. That causes many prescribed treatments to be unresponsive or only partly responsive. More personalised treatment is needed which counters the huge heterogeneity issue of PCa.

We believe that CTCs are the key to understanding a patients exact disease profile. Therefore we developed a method to look at these CTCs individually. The biggest problem with CTC is their extreme rarity, there is maybe 1 CTC in a 7.5 mL blood sample. By use of DLA, immunomagnetic enrichment, and a microwell chip which causes cell isolation we tackle this needle in a haystack problem.

In this research we look at if the use of immunomagnetic ferrofluids (FF) for enrichment influences the CTCs. With Live/Dead stainings and flowcytometry we determined that there is some cell dead among CTC caused by FF. Next to that, metabolic activity was measured with Alamar Blue Assays which pointed out that metabolic activity did not decrease. Which is counter-intuitive with the lower viability results. Cell death was not on a level that it would make the single CTC analysis unworkable.

Chips from Vycap were used to make the first start towards single cell secretion analysis where patterns of Prostate Specific Antigen (PSA) were found. Optimization of current protocols will likely result in images that can be analysed and compared. We also observed that there was no visual difference between cells and enriched cells (with FF). Again, with optimization this can give a platform for analysis and comparison. Lastly we worked with PCa patient DLA samples in order to catch CTC on the Vycap chip. This proved to be difficult and even though some CTCs were found, secretion was not seen. In order to improve the CTC numbers that were found, we recommend using an extra enrichment method to filter out even more cell debris and leukoctyes of the DLA sample. That will open the future to secretion analysis of single CTC. Future work with PCa cells will make it possible to 'punch out' these cells of the chip and culture them for medicine testing. Which will lead to personalised medicine, better treatment decisions and more survivors of metastatic prostate cancer.

1.2 Abstract Dutch

Prostaatkanker is de meest voorkomende kanker bij mannen in de VS en de op één na meest dodelijke kanker als we kijken naar het totale aantal sterfgevallen aan kanker. Primaire prostaatkanker heeft tegenwoordig een 5-jaars overlevingskans van 100%, maar gemetastaseerde prostaatkanker heeft slechts een 5-jaars overlevingkans van 32%. Verschillende prostaatkanker-typen hebben een verschillende behandeling nodig, afhankelijk van het stadium van de kanker, AR-afhankelijkheid, agressiviteit en mutaties. Dat zorgt ervoor dat veel voorgeschreven behandelingen niet of slechts gedeeltelijk werken. Er is een meer gepersonaliseerde behandeling nodig die het enorme heterogeniteits-probleem van prostaatkanker oplost.

Wij denken dat CTC's de sleutel zijn tot het begrijpen van het exacte ziekteprofiel van een patiënt. Daarom hebben we een methode ontwikkeld om deze CTC's afzonderlijk te bekijken. Het grootste probleem met CTC is hun extreme zeldzaamheid, er is misschien 1 CTC in een bloedmonster van 7,5 mL. Door gebruik te maken van DLA, immunomagnetische verrijking en een microwell chip die cel-isolatie mogelijk maakt, pakken we dit speld in een hooiberg probleem aan.

In dit onderzoek kijken we of het gebruik van immunomagnetische ferrofluids (FF) voor verrijking de CTC's beïnvloedt. Met Live/Dead-kleuringen en flowcytometrie hebben we vastgesteld dat er extra celdood plaatvindt onder tumor cellen veroorzaakt door FF. Daarnaast werd de metabolische activiteit gemeten met Alamar Blue Assays waaruit bleek dat de metabolische activiteit niet afnam. Dit is contra-intuïtief met de lagere levensvatbaarheids-resultaten. Desalniettemin was Celdood was niet op een niveau dat de geisoleerde CTC-analyse onwerkbaar zou maken.

Chips van Vycap werden gebruikt om de eerste stap te zetten met de analyse van de secretie van één cel, waarbij patronen van prostaat-specifiek antigeen (PSA) werden gevonden. Optimalisatie van de huidige protocollen zal waarschijnlijk resulteren in beelden die kunnen worden geanalyseerd en vergeleken. We observeerden ook dat er geen visueel verschil was tussen cellen en met FF verrijkte cellen. Nogmaals, met optimalisatie kan dit een platform bieden voor analyse en vergelijking van geisoleerde cellen. Ten slotte werkten we met DLA-monsters van prostaatkanker-patiënten om CTC op de Vycap-chip te vangen. Dit bleek lastig en hoewel er enkele CTC's werden gevonden, werd er geen secretie gezien. Voor het verbeteren van het aantal gevonden CTC's, raden we aan om een extra verrijkingsmethode te gebruiken om nog meer celresten en leukocyten uit het DLA-monster te filteren. Dat zal de toekomst openen voor secretie-analyse van geisoleerde CTC's van patienten. Toekomstig werk met prostaatkanker-cellen zal het mogelijk maken om deze cellen uit de chip te 'stoten' en te kweken voor medicijntesten. Dit zal leiden tot gepersonaliseerde medicijnkeuzes, betere behandelbeslissingen en meer overlevenden van patienten met uitgezaaide prostaatkanker.

2 Introduction

2.1 Goal of the research

This research is part of the PICTURES project: Probing Intercellular Heterogeneity in Circulating TUmor cells of de novo metastatic Hormone Sensitive Prostate CanceR patiEntS. Treatment options for cancer patients are increasing, however factors to predict which treatment option will be the correct one for a patient are lacking. We aim to get a better insight in the cancer a patient has, so that treatment can be chosen more effectively.

The goal is to isolate and identify viable Circulating Tumour Cells (CTC) in Diagnostic Leukapheresis (DLA) products and measure their secretion, the readout is Prostate Specific Antigen (PSA). First the patient will undergo DLA, in which cells are selected based upon size and density. Then the DLA sample will be enriched by CellSearch or by in house developed immunomagnetic beads. This will be done via immunomagnetic ferrofluids (FF) which bond to the Epithelial Cell Adhesion Marker (EpCAM) on CTCs, see Chapter 4.1.1. Initially experiments will be done with selected cell lines, see Chapter 3.1.1. Cell lines will be used for developing a model to improve EpCAM characterisation and evaluate FF influence on the viability and secretion of cancer cells. The EpCAM characterization will be discussed in Chapter 3. The influence of FF on the viability and secretion of the CTCs will be discussed in Chapter 4. The enrichment procedure will allow us to reduce volume, which allows cost effective staining of chosen markers of the cells. After enrichment the cells are ready to be seeded in a microwell chip. Seeding on this chip will result in isolation of cells. Then cells will be cultured while isolated in the microwell chip. The chip and its principles will be discussed in Chapter 5.1.2. The final step and focus point of this research will be the secretion analysis that follows, this will be discussed in chapter 5. The final read out will be secreted PSA from isolated CTC from a DLA sample of a Prostate Cancer (PCa) patient.

2.2 Prostate Cancer (PCa)

Some background information on the disease, the different types of the disease, the societal impact, and current treatment is needed to understand the disease itself and the necessity of better and faster treatment. Lets start where it all begins, the place of origin of PCa.

2.2.1 The prostate

The prostate is part of the accessory glands next to the paired seminal glands and bulbo-urethral glands and plays a role in the production of semen. It is enclosed by connective tissue and made up of 20 to 30 compound tubuloalveolar glands. These are embedded in smooth muscle and connective tissue. The prostatic fluid is around 1/3 of the total volume of the semen and activates the sperm. Next to citrate and several enzymes, this fluid contains PSA[1]. There are other problems that might arise involving the prostate. There are many factors that might cause inflammation of the prostate, like bacteria, immune cells, and other unknown factors. For us Benign prostatic hyperplasia (BPH), or hyperthrophy of the prostate, should be mentioned since almost every male will have this at a certain point in his life and it causes rising PSA levels[2] (a prominent PCa marker discussed in Chapter 5.1.1). If cancer develops in the prostate it is called PCa, however the place of origin within the prostate determines the type of PCa.

2.2.2 Types

The most common form of PCa is adenocarcinoma, they are composed of small glands with almost no intervening stroma and make up almost 95% of all PCa[3]. The main aim of the overlapping PICTURES project is de novo metastatic PCa, however adenocarcinoma are often not very aggressive and therefore less often found in de novo metastatic PCa. There are 5 other types of PCa which are of interest since they are often more aggressive and therefore are more often found while already metastasized.
Small cell carcinoma of the prostate is one of the most lethal forms of cancer, the median survival rate is 1-2 years. Since small cell carcinoma is often hormone independent and therefore androgen therapy resistant, next to being more prone to metastasize earlier, correct diagnosis is very important.[4] A study shows that the median time between previous diagnosis of PCa and the new diagnosis of small cell carcinoma of the prostate is 25 months[5]. Squamous cell carcinoma is a cancer that arises in squamous cells. This cancer occurs at 0.5-1% of PCa patients and is known to be very aggressive[6, 7]. Bone, liver, and lungs are the most prominent places of metastasis[6]. The median survival time after diagnosis is 14 months[8]. Transitional cell cancer in the prostate is a carcinoma with urothelial origin and with pathology that has some or many aspects of prostatic tissue. It is rarely the primary tumor[9]. These tumors come to existence from urothelium linings of the prostatic urethra and the proximal portion of the prostatic ducts[9], it is also suggested that malignant transformation of the prostatic urothelium is the cause of these tumours[10]. There are also very rare forms of PCa like Neuroendocrine tumors and Soft tissue sarcoma. Neuroendocrine tumors can form in the neuroendocrine cells that produce hormones in the prostate. Soft tissue sarcomas start in the supportive tissue and is extremely rare.[11]
There are many different types of PCa and all types have different characteristics. Therefore, there is not 1 specialised way of treatment, but there are many different treatment option available.

2.2.3 Treatment

Primary and local tumours

Many PCas are slow growing and do not metastasize[1]. Therefore they often do not result in death[1]. To be more specific, the 5 year relative survival rate according to the SEER in the USA is 100% by localized (confined to primary site) and Regional (Spread to regional lymph nodes) cases[12]. The older a person, the less likely a new found PCa will be the cause of death[1]. However they should be monitored, and regular tests should be conducted[1]. Tests will involve palpating and PSA level checks[1]. If possible, surgery will be performed in order to remove the tumor(s), which is often followed by radiotherapy[1].

Distant tumours

If PCa has reached a higher stage and has metastasized to distant areas, the cancer poses a threat to the patients. Metastases are detected by MRI scans.[1] The 5 year survival rate of patients with distant metastasised areas is 32.3%[12]. If surgery is not possible which might be the case when there are metastases, other treatment option are looked into. Many PCas are hormone sensitive. This opens the option for removing Androgen from the patient. This can be done with drugs that block the androgen receptor (AR), but if needed castration is also an option.[1] Of course this has many side effects, and is rather avoided.

There are many different treatment option for advanced PCa wherein metastases are present. In order to come to a general consensus, 72 prominent figures in PCa research be it physicians or scientists came together in the 2019 Advanced PCa Consensus Conference (APCCC)[13]. They reached consensus (84%) that a primary tumour in metastatic setting and diagnosed with low-volume/burden metastatic M1 castration sensitive or naive PCa should be treated locally with radiotherapy.

In case of multiple metastasis, or an oligometastatic setting, bone scintigraphy and imaging by CT is not sufficient to determine further treatment (79% consensus). In patients who received radical treatment and had afterwards rising PSA levels, PSMA PET-CT or MRI should be used to confirm if they are oligorecurrent(75% consensus). Then patients should be treated with systemic therapy and lesion treatment (75%).

Treatment for newly diagnosed hormone sensitive patients was still undecided, however 77% agreed it should not involve castration. 95% agreed on the need for tissue research to determine the type of cancer, but also 96% agreed on starting ADT treatment in symptomatic patients before histopathological confirmation. Additional treatment for patients with high-volume metastatic (M1) castration-sensitive/naïve PCa (newly diagnosed or relapsing) or relapsing low volume patients, next to ADT treatment is needed. However many opinions on the best additional treatment exist.

Treatment for castration resistant patients is different. In M0 patients the additional treatment next to ADT is an AR antogonist (86%). In patients with further developed stages of mCRPC, other combinations of drugs are recommended. Treatment also differs depending on where the metastases are. Lastly, checks for mutations should be carried out and also influence the best treatment option.

All in all lots of treatment options are available and should be applied largely depending upon the sort of cancer, the stage of the cancer, AR dependency, and the mutations of the cancer. All these tests and treatments are time and money consuming.

2.2.4 Societal impact

The Surveillance, Epidemiology, and End Results (SEER) who monitors the cancer statistics in the USA estimates 34.500 deaths in 2022 due to PCa. That is 5.7% of all cancer deaths in the USA. Next to that they expect 268.490 new cases in 2022 which is 14% of all new cancer cases and thereby the second most common cancer after breast cancer. The 5 year survival rate that was determined between 2012 and 2018 was 96.8%.[12] However, the big factor that determines the 5 year survival rate is the stage of the cancer. Primary and regional PCa resulted in a survival rate of 100% compared to 32% from distant metastases[12]. This points out the importance of improving the treatment for metastatic PCa patients.

The burden on society is hard to calculate and dependent on the type and stage of PCa. However we try to illustrate the societal burden by giving the number of the most common form of metastatic PCa. The sites at which metastases are present are bone (84%), distant lymph nodes (10.6%), liver (10.2%), and thorax (9.1%)[14]. So looking at metastasis to bone, in 2016 the extra costs of a patient was calculated to be 21.191$[15].
However when trying to get a grasp of the difference between the economical impact of non-metastatic patients versus metastatic patients, inpatient costs (patients who are required to stay at the hospital for at least 1 night) provide us with a comparison. In 2019 treatment related costs for non-metastatic PCa inpatients was 265$ versus 7854$ for metastatic PCa inpatients[16], a 2963% difference. Therefore, most financial impact can be made for PCa when focusing at metastatic patients. Unresponsive treatment options can be prevented which highly impact patient well being and accumulates costs.

More knowledge is needed to decide on treatment for PCa patients. This knowledge is already in circulation, the blood circulation of patients. There, the so called Circulating Tumour Cells (CTC) can be found which are the cells that potentially result in metastases and which hold information about the tumour they originate from. We just need to find a way to extract this information unchanged due to the extraction method.

2.3 Circulating Tumour Cells (CTC)

Circulating tumor cells (CTCs) are a rare subset of cells in cancer patients which might potentially function as seeds for metastasis[17]. These tumour-derived epithelial cells might prove a solid alternative for highly invasive biopsies by enabling liquid biopsies[18]. Liquid biopsies are easier to collect with less consequences for the patients. Also the costs of performing a simple liquid biopsy are lower. The problem with liquid biopsies is finding the target of interest due to the often low target concentration and abundance of other material.

The importance of the viability of these CTCs has already been pointed out in 1975 by literature research of Salsbury [19], where it's been pointed out that CTCs are most likely 5-6 hours viable.

CTCs are proven to have prognostic value for metastatic castration-resistant prostate cancer by De Bono et all, [20] looking at overall survival of patients. Next to looking at PSA levels of serum, it is already looked into if the specific PSA levels of CTCs can be helpful in diagnosis of patients[21].

A major problem of liquid biopsies is the before mentioned rarity of finding CTCs in blood especially in small blood samples taken. These blood samples of around 7.5ml have on average 1 CTC[22]. To solve this Diagnostic Leukapheresis is a solution as a study showed it can detect more than 90%(compared to 5-24%) of nonmetastatic breast cancer patients with a median of 7500 CTCs per patient[22]. However since there is still an enormous abundance of leukocytes, the sample should be further enriched. This process will be done with use of immunomagnetic beads, manually or via the Cellsearch protocol and machinery, see Chapter 4.1.1. This will give purer, but still not pure samples. That's why we will use the microchips from Vycap for cell isolation, as will be discussed in chapter 5.1.2. The enrichment after DLA will be done with FF targeting EpCAM. Therefore, the EpCAM characterization of prostate cancer cells will be discussed in the next chapter, Chapter 3.

3 EpCAM characterization of prostate cancer cells

The enrichment process to decrease the number of non-CTC cells present in samples is based upon FF that target EpCAM. Therefore, a better understanding of EpCAM is necessary to come to the best approach of enrichment and staining the CTCs. In this chapter exploratory research is done towards EpCAM characterization.

3.1 Theoretical Background

3.1.1 PCa Cell Lines

Before going to the processing of DLA samples from patients, all experiments will be validated with samples that do not involve patients. Initially, experiments will be done with just cells gathered from cell line cultures. Then, we'll progress to experiments in which we use blood spiked with cells from the cell line cultures. After that, DLA samples (from non PCa patients) will be spiked with cells from the cell line cultures with which we will experiment. Finally, we will move on the DLA samples from patients with CTCs. All our experiments were primarily done with the LNCaP cell line before moving on to other cell lines. The most used cell lines for prostatic cancer are discussed here with focus on the ones used in our research. An overview of the most used prostatic cancer cell lines can be found in Table 1.

LNCaP

The LNCaP cell line is a human cell line which is isolated from a lymph node with metastasized prostate adenocarcinoma[23]. The cell line is hormone responsive [25], has PSA RNA[24], PSA Protein[24], androgen recepter (AR) RNA[24], AR Protein[24] and has the following markers[24]: Vimentin, E-cadherin Monoclonal Antibody (HECD 1), a- b- and g-catenin, and prostatic acid phosphatase (PAP). LNCaP cells have a mutated AR and are androgen sensitive[26]. They are not just androgen responsive but are dependent on androgen[27].

There are many derivatives from the original LNCaP cell line from which some stand out. LNCaP-LN3 and LNCaP-LN3-4 have a higher likelyhood to to have regional lymph node metastases[26]. The LNCaP-pro cell lines have been created by reinjecting tumours that were harvested and originaly from the LNCaP line(the number means the number of cycles)[33]. These cell lines derivatives could be of use if aggressiveness is a factor of interest. For investigating AR influence LNCaP-abl cells could be useful. They are derived by passaging in androgen depleted medium in order to mimic androgen ablation. That resulted in 4x more AR protein and 30x increase in AR transciptional activity. [29]

The cell line C4-2 is derived from the LNCaP cell line and already has its own derivatives. LNCaP cells were coinjected with osteosarcoma fibroblasts in a nude athymic mouse, after 8 weeks castrated, and then after 4 weeks collected. Then again co-injected with osteosarcoma fibroblasts but in a castrated mouse, and after 12 weeks harvested as the new C4-2 cell line. This was repeated after which harvest was done in a metastasis in bone tissue(C4-2B), lymph node (C4-2Ln), or the primary tumor (C4-2Pr) These cell lines have shown to have higher metastatic capacities but are also androgen independent[30] and are of interest when conducting research into the metastatic mechanism of PCas. [40]

PC-3

The PC-3 cell line is a human cell line which is established in 1979 and derived from a human prostatic adenocarcinoma metastatic to bone[31]. It is an androgen independent cell line[31, 27, 28], next to being

Table 1: Commonly used cell lines of prostatic cancer origin and their characteristics. A blank space means that no information was available in the sources. Resp. - stands for negative response in growth while resp.+ stands for positive response in growth. + stand for low, ++ for moderate, and +++ for high expression found.

Cell lines											
Cell Line name	Derived from	Origin or characteristic	PSA (RNA and/or protein)	AR (RNA and/or protein)	Cyto-ke-tarin	Androgen depen-dence	EGF	TGF-α	IGF-I	bFGF	TGF-β
LNCaP		lymph node with metastasized prostate adenocarcinoma [23]	V (V, V) [24]	V (V, V) [24]	8, 18, 20 [23]	Dependent and responsive [25, 26, 27]	++ [28]	++ [28]	++ [28]	- [28]	- [28]
LNCaP-LN3/4	LNCaP	likelyhood for regional lymph node metastases [26]									
LNCaP-pro	LNCaP	reinjecting tumours									
LNCaP-abl	LNCaP	passaging in androgen depleted medium [29]		4X higher protein and 30X higher transcip-tional activity [29]							
C4-2	LNCaP	coinjected with os-teosarcoma in cas-trated mouse, higly metastatic				Independent [30]					
PC-3		prostatic adenocarci-noma metastastic to bone [31]	V [32]	-[26]	5 [27], 8 [28], 18 [28]	Independent [31, 27, 28]	+ [28]	+ [28]	+++ [28]	+ [28]	++ [28]
PC-3-AR	PC-3	Transfected with AR[26]		V[26]							
PC-3M Pro4/LN4	PC-3	Reinjected, high metastatic [33]									
VCaPs		vertebral body of hor-mone refractory PCa [34]	V (V, V) [27]		8 [27], 18 [27]	Independent but respon-sive [27]					
CWR22 (R)		Shows regression bet-ter	Low and even-tually fading								
DU145		prostate adenocarci-noma metastic from the brain [35]	V [32] low/ nonex-istent [27]			Independent [27]					
DU145-AR	DU145					Dependent [36]					
LAPC-4		Lymph node [37]	V [37] (V, V) [27]	V (V, V) [27]		Dependent[27]					
RWPE-2	RWPE-1	Ki-ras transformation using murine sarcoma virus [38, 28]	V [28]	V [28]	8, 18 [28]	Responsive [28]	resp. + [28]			resp. + [28]	resp. - [28]
DuCaP		metastatic lesion con-nected to the dura mater [39]	V [39, 39, 27]			Independent but respon-sive [39, 27]					

unresponsive to glucocorticoids[31].

There are many different cell lines derived from the original PC-3 line. For example when selecting for high metastasizing cell lines, the derivative cell lines PC-3M-Pro4 and PC-3M-LN4 were created after re-injecting tumours created by the original cell line[33]. next to that the PC-3 cell line is AR negative, the derived PC-3-AR cell line is AR positive[26].

Since experiments were already difficult to conduct with the high levels of PSA expressing cell line LNCaPs, only a few experiments have been conducted with this relatively low PSA expressing cell line.

VCaPs

The VCaP cell line is a human cell line which is derived from a lumbar vertebral body of a patient with hormone refractory PCa. This tissue was xenografted in SCID mice and later harvested.[34] VCaP cells are androgen independent but responsive. Androgens are not required, but do stimulate growth. They do secrete PSA, PSA protein and mRNA was found in these cultures.[27]

Alternatives

There are other cell lines which are well suited for experiments. However they were not used in these experiments since they were not present in house for various reasons (mainly due to low or non present PSA, which will be used in the secretion studies, and because they were not in house available). Some examples are:

1. CWR22(R): A PCa cell line that shows more regression after androgen deprivation compared to LNCaP and PC-3 and thereby mimics the patient response better. This cell line shrinks more and shows lower PSA values that only sometimes come back months later when tested in mice (the cell line is then called CWR22R). [41] There are also derivatives from these cell lines which might be interesting. For example the 22Rv1 cell line which is a derivative after it was serially propagated and relapsed[42].

2. DU145: One of the 'classical' PCa cell lines. This cell line is derived from a human prostate adenocarcinoma metastic from the brain[35] Not used in our research due to their androgen Independence and therefore low/nonexistent PSA presence[27], while we were already having the PC-3 cell line with many overlapping characteristics but higher metastatic potential[26]. A cell line which is hormone sensitive has already been developed based upon this cell line, namely the DU145-AR cell line[36] which can be used to research AR influence and compared to DU145.

3. LAPC-4: 8 LAPC PCa cell lines have been established, from which LAPC-4 proved most useful for PCa research. The LAPC-4 cell line comes from a PCa found in the lymph node of a patient. Tumours grow in 3 months and were PSA positive, quantitated at the same level or less than LNCaP tumours however this was on very small scale. [37] The LAPC-4 cell line is positive for AR proteins and mRNA. It is also androgen dependent which means it requires androgen for its growth. Next to that is is tested positive for PSA proteins and mRNA, and DD3 mRNA.[27] Sublines have been established which become androgen independent or less dependent. That is a normal course of PCa after androgen depletion and therefore relevant for research to the mechanisms of androgen dependent to androgent independent cancers.[37]

4. RWPE-2: The RWPE-2 cell line is created by transformation with Ki-ras using the murine sarcoma virus of the RWPE-1 cell line. It does have the ability to form tumours.[38, 28] This line is AR and PSA positive, and androgen responsive.[28]

5. DuCaP: DuCaP cells are originated from PCa tissue present in a metastatic lesion that was connected to the dura mater[39]. They share the same primary tumor with the VCaP cell line, but are derived from a different metastasis[27]. PSA is detected in media, and PSMA was detected with RT-PCR[39]. DuCaP cells are androgen independent but responsive. Androgens are not required, but do stimulate growth. They also do express PSA. [39, 27]

Also of interest are the cell lines: TSU-PR1, ALVA 101, and P69SV40T. However, they are less well known. There were other cell lines that looked interesting, but turned out to be cross contaminated by cell lines that are already discussed before. PP-C1, DuPro-1, Alva-31, Alva-41, Alva-55, Alva-101, are contaminated by PC-3[43, 44, 27, 45]. ND-1 and BM1604 are contaminated by DU145[43, 44].

There are also Epithelial prostate cell lines, which could be used as controls. The undermentioned cell lines are positive for cytokeratin 8 & 18, PSA, AR and have an Androgen response.[46] The ones most extensively described in literature and therefore of most interest are:

1. RWPE-1: The RWPE-1 cell line is created by transfecting with the papilloma virus 18 and has no ability to form tumours.[38]

2. PWR-1E: Cells were immortalised by infection of the adenovirus 12-simian virus 40 hybrid virus (AD12-SV40).[46]

Also of interest are the cell lines: BPH-1, PNT1, pRNS-1-1, and PZ-HPV-7. However they are less well known and therefore less fit as control.

Just like CTC, all of these cell lines have the EpCAM molecule expressed which can be used to catch them.

3.1.2 EpCAM and its epitopes

Cell adhesion molecules (CAM)
Cell adhesion molecules (CAM) have a couple functions. Firstly they are there to attach cells to molecules and each other. Secondly, they are the handles or arms that cells use to migrate themselves. Thirdly, they warn in case of injury and infection by signalling to the immune system by sticking out of blood vessel lining. They also function as mechanical sensors and as transmitters of intracellular signals regarding specialisation, proliferation and migration. [1]

Epithelial cell adhesion molecule (EpCAM)
Epithelia are 'Sheets of cells covering an external surface or lining an internal body cavity'[47], or 'Pertaining to a primary tissue that covers the body surface, lines its internal cavities, and forms glands'[1]. The epithelial cell adhesion molecule (EpCAM) is different from the major adhesion molecules super families: the integrins, cadherins, selectins and the immunoglobulin[48, 49, 50]. For the detailed structure of EpCAM, see Figure 1. EpCAM is calcium independent, homophilic, intercellular, transmembrane adhesion glycoprotein also known as EGP40[51]. EpCAM is 40kDa and consists of 314 amino acids. Of these 314 amino acids, 265 belong to the extracellular domain, 26 belong to the intracellular domain, and the rest to the transmembrane domain[51, 50]. Since we are intested in viable cells and do not want to disturb the secretion processes, we are interested in the extracellular domain.

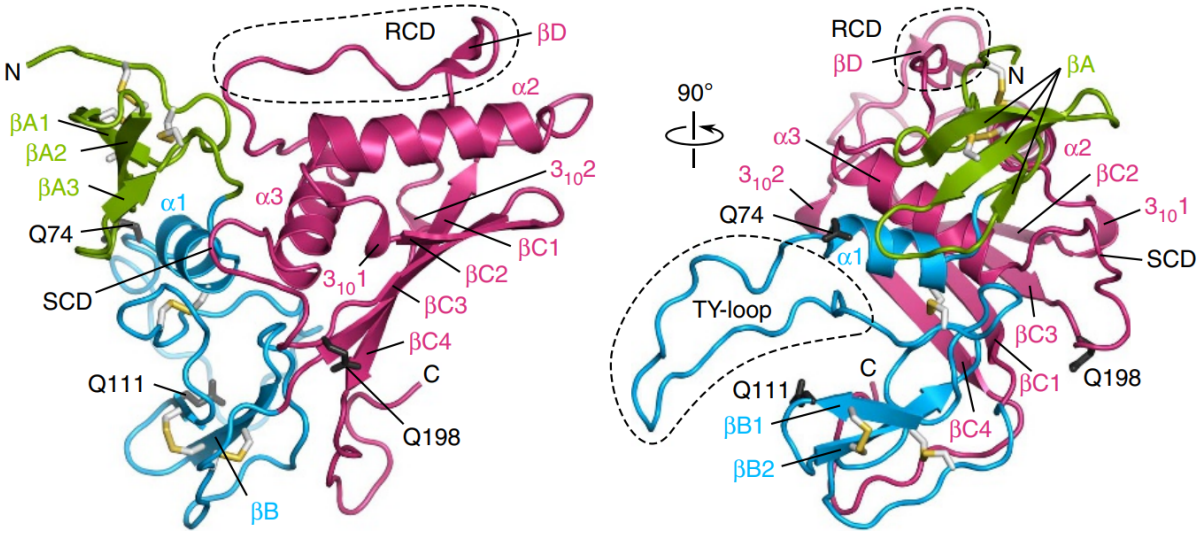

Figure 1: The complete EpEX (EpCAM extracellular) chain contained in the asymmetric unit. Two different orientations are shown. EpEX is composed of N-domain (ND, green), TY domain (blue) and CD (dark pink). It lacks the TM and EpCAM intracellular part (EpIC) of full-length EpCAM. Secondary structure elements are labelled from N to C terminus (for example, bA for b-sheet A, bA1 for first strand in bA sheet, a1 and 3101 for first a- and 310-helix).[52]

EpCAM is already known for more than 40 years as a cancer cell marker. It is widely recognized as the way the detect CTCs, wherein EpCAM is used as the positive and CD45 as the negative selective criterium[53]. The only FDA approved CTC detection device for PCa[54] (and breast[55], and colorectal cancer[56]), is CellSearch which is based upon anti-EpCAM antibodies. However, there are also some voices that say that the EpCAM age has come to an end because ' the inadequacy of EpCAM as universal marker for CTCs detection is unquestionable', basing that assumption on the mesenchymal-epithelial transition (MET) and epithelial-to-mesenchymal transition (EMT) and the thereby changes in EpCAM expression[57]. Nevertheless, EpCAM is especially highly expressed in adenocarcinomas (which is the most common form of PCa) and squamous cell carcinomas[58]. EpCAM is involved in a lot of processes in a lot of different stages in the body. To name some of them: cell adhesion, cell cycle regulation (repair, maintenance, cell proliferation, cell differentiation), signal transduction, organogenesis, and cell migration[58].

In mice lacking EpCAM tight junction are less well formed next to having more barrier function disruption[59]. It also caused downregulation of Claudin 1[26] and 7[26, 59] which is a major contributor to cell-cell junctions, downregulation of claudin 2 and 15 which play a part in paracellular permeability[59]. EpCAM also plays a role in interacting with the underlying layers like the basal membrane[58]. These factors indicate how EpCAM might play a major part in the aggressiveness of cancer and the propagation[26]. Interesting for our research is that LNCaP cells have higher EpCAM expression levels than PC-3[32].

Epitopes and Antibodies

An EpCAM molecule has different epitopes that antibodies can bind to. Research has been done to multiple epitopes in order to determine the best combination of antibodies when targeting EpCAM. Targeting different epitopes has also been done in studies aiming at the lysis of CTCs[60], which showed differences between targeted epitopes. Other studies are focused on detection of CTCs with antibodies. Binding affinity of these antibodies is determined with the dissociation equilibrium (K_D). Of the 4 tested antibodies, the K_D from highest to lowest affinity is EpAb3-5 (K_D=2.6E-11 M), HO-3 (K_D=4.0E-11

M), VU1D-9 (K_D=2.7E-10 M), and MJ-37 (K_D=2.8E-9 M)[61]. EpAb3-5 was found to abrogate Vu1D9 signal, whereas HO-3, MJ-37 and VU1D-9 seem to use different or non-interfering epitopes[62, 61]. The non-interfering target epitopes of Vu1D9 and HO-3 are supported by literature which points out they have different target domains[52], see Figure 2 for an schematic overview of antibodies and epitopes. VU1D9 targets the N-domain (ND), while HO-3 targets the thyroglobulin type-1A (TY) domain[52]. MJ-37 and VU1D9 seem to both target the ND[52], however since they are non interfering they likely target different epitopes of the ND[62, 61]. From those antibodies, HO-3 seemed to be most efficient in binding to EpCAM followed by Vu1D-9 and EpAb3-5 with a significant difference with MJ-37[62, 61]. Further in house research showed that the combination of HO-3 and VU1D-9 was the most compatible combination, which are therefore the respective epitopes targeted in our research.

The HO-3 antibody (in combination with the catumaxomab drug)) target epitope extends from the part of ND through TY loop to part of the CD, which suggests that HO-3 recognizes EpCAM in the cis-dimeric form, but also that the antibody-drug combination might bind to adjacent regions to the complementary determining region[52]. Even though antibodies might target different epitopes, depending on what is attached to them they might still be interfering with each other. Different epitopes are already targeted with drugs: HO-3, 17-1A, and MT201 are corresponding to drugs Catumaxomab, Edrecolomab, and Adecatumumab, respectively[52].

Theoretically it seems like you can target the same molecule but different epitopes with different antibodies. However, something is needed to differentiate between those antibodies if used at the same time or simply to know if a cell is positive for an antibody.

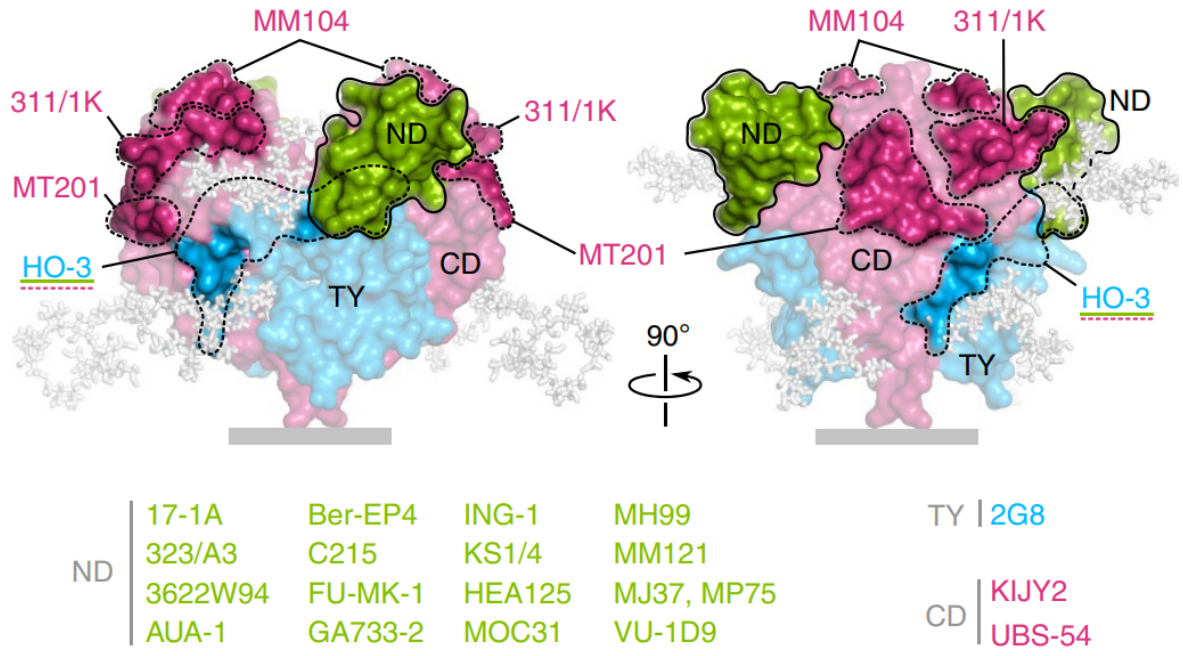

Figure 2: Epitopes of anti-EpEX antibodies on a glycosylated EpEX cis-dimer. The identified epitope regions and the most antigenic N-domain are depicted as intensively shaded surface regions. The antibodies listed below are antibodies of whose exact target epitope are unknown, only the target domain is known. Antibody names are color-coded by the domains they recognize. Of our special interest are HO-3, a TY-domain binding antibody. VU1D9, a ND-domain binding antibody. And also mentioned in our literature research, MJ37, a ND-domain binding antibody. [52]

3.1.3 Fluorophores

The fluorophores attached to the antibodies are also very important, since this is the factor that determines the brightness per bound particle. We looked into BV421 and BV605, and the corresponding filter cubes were bought. Since this excitation spectrum fitted in our pallet of other fluorescence used later on.

BV421

The optimal excitation wavelength is 405nm, and the optimal emisssion wavelenght is 421, see Figure 3. Biolegend gives this fluorophore a brightness of 4 out of 5.[63]

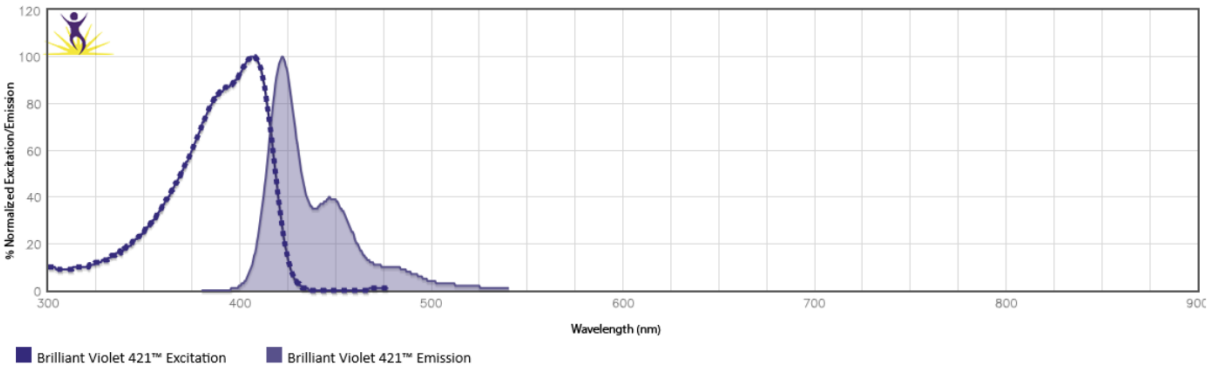

Figure 3: Emmision(solid line) and excitation(dotted line) spectra of the fluorophore Brilliant Violet 421. The optimal excitation wavelength is 405nm, and the optimal emisssion wavelenght is 421. Biolegend gives this fluorophore a brightness of 4 out of 5.[63]

BV605

BV605 is a tandem dye, based upon a BV421 polymer core[63]. A tandem dye is based upon a donor and an acceptor fluorescent molecules which are covalently bound. This principle is based on Förster resonance energy transfer (FRET). Which simply means that the excitation energy of the donor is passed to the acceptor which emits a photon. This can be done having the emission energy of the donor overlap with the excitation energy of the acceptor. When using two fluorescence molecules, like this case, FRET is also called fluorescence resonance energy transfer. Transfer does not actually occur via fluorescence between the molecules.[64] The optimal excitation wavelength is 405nm, and the optimal emisssion wavelenght is 603nm, see Figure 4[63]. Biolegend gives this fluorophore a brightness of 3 out of 5[63]. Since it is a tandem dye, there is a small emmission spectrum on the left side of the graph of Figure 4 which completely overlaps (however lower in intensity) with the emmission spectrum of BV421 that is seen in Figure 3.

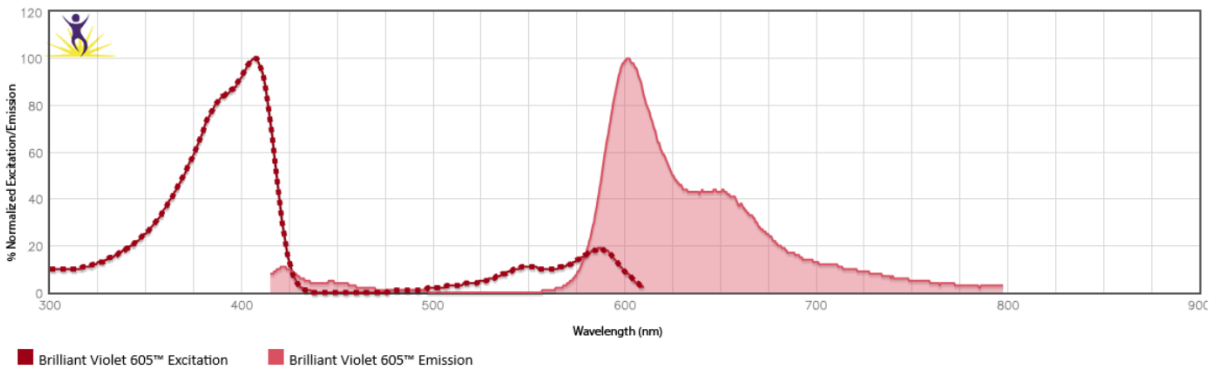

Figure 4: Emmision(solid line) and excitation(dotted line) spectra of the fluorophore Brilliant Violet 605. BV605 is a tandem dye, based upon a BV421 polymer core. The optimal excitation wavelength is 405nm, and the optimal emisssion wavelenght is 603nm. Biolegend gives this fluorophore a brightness of 3 out of 5.[63]

Cell Tracker Orange

Cell tracker dyes are made specifically to track cells. The principle is that they are freely passing through cell membranes, however when they are inside the cell they are transformed in impermeant(for the cell membrane) reaction products, which are fluorescent. There is a whole scala of colours which can be used, but in this chapter we work with Orange (PE) since this is one of the brightest and does not cause major overlap in the spectra which are important for the other fluorophores we combine them with. The specific molecule that we use is 5-(and-6)-(((4-chloromethyl)benzoyl)amino)tetramethylrhodamine. Celltracker dye stays in cells and is detectable for multiple generations(according to the manufacturer 3-6 generations). Naturally, it is non toxic at the working concentration. It is also stable and should emit fluorescence for at least 72 hours. CTO was used in order to be sure that we are dealing with cells and since it's an established staining, it can also function as reference. [65]

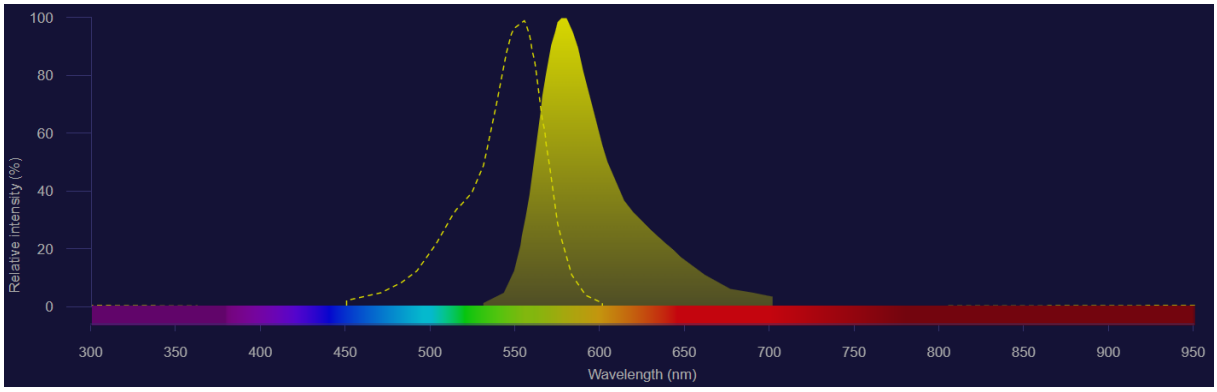

Figure 5: Emmision(solid line) and excitation(dotted line) spectra of Cell Tracker Orange. The optimal excitation/emission wavelength is 541/565nm.[65]

A standard fluorescence microscope can be used to visualise these fluorophores, but fluorescence can also be measured with a more quantitative method like flowcytometry.

3.1.4 Flowcytometry

Flowcytometry is a well known technique used for rapid analysis of a sample consisting of particles or cells, see Figure 6 for an schematic overview of a flowcytometer. Flowcytometry uses lasers that hit 1 target at the time, made possible by the narrowing of the tubing and the sheath fluid surrounding the sample causes the cells to line up, also called hydrodynamic focusing[66]. The sheath fluid and sample are incompressible liquids. The sheath fluids moves fast and thereby accelerates and focuses the slower moving sample fluid.[66] Cells are analysed primarily by their Forward Scatter (FSC) and Side Scatter (SSC). FSC is measured in the forward direction and is a measurement tool for the size of the cells (relative size). SSC is measured by a detectors at a 90 degree angle, the more granularity or complexity, the more side scatter there will be. Secondary, the targets can also be analysed for one or multiple fluorescence parameters.[67] For fluorescence measurements we will use fluorescent dyes, or fluorescent labeled antibodies.

Next to the analysis of cell populations, an application is cell sorting based on electrical loads given to cells depending on characteristics measured by the flowcytomer itself[67]. We will not make use of this.

Data analysis is traditionally done in a histogram with two parameters, also called the dot plot. With gating certain subgroups can be selected for analysis. However with the increase of measured parameters there is more need of cluster analysis.[67] For our application dot plot analysis is sufficient.

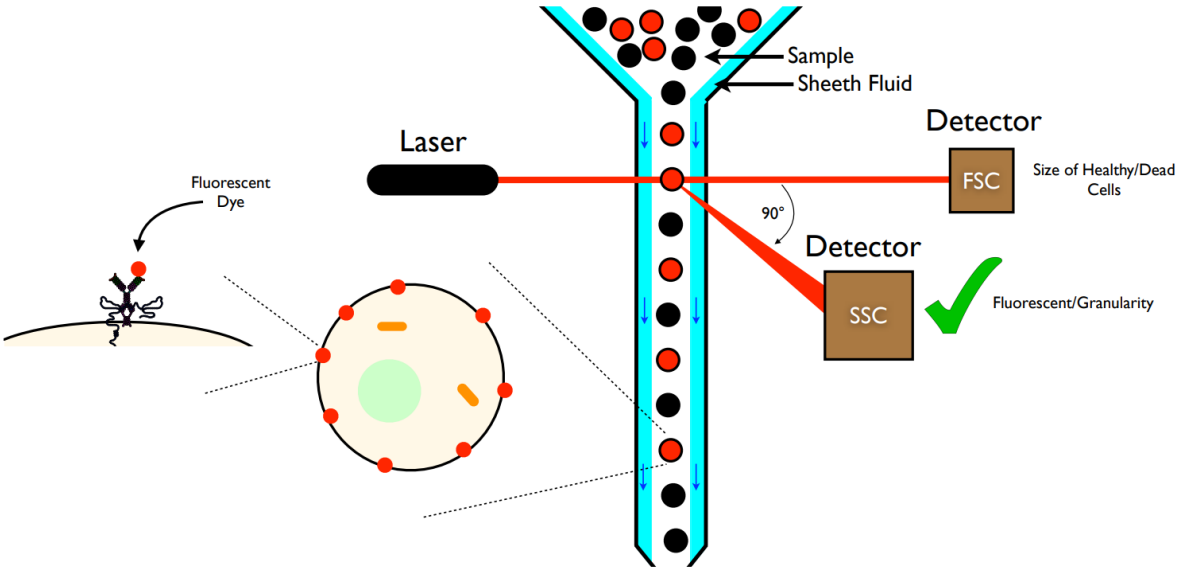

Figure 6: This figure is showing a representation of flow cytometry. Cells in a sample are fluorescent labeled. They are put in the flowcytometer and made into a single line of cells (or other target) by use of a small opening and sheath fluid surrounding the sample. The primary measurements from flowcytometry are Forward Scatter (FSC) and Side Scatter (SSC) which measure size and granularity, respectively. Sample is passed through a laser beam and at the moment of contact between sample and the laser beam the FSC and SSC are measured by detectors. Fluorescence measurements will be implemented for our research. [68]

3.2 Goals & Hypotheses

The goals for this chapter are the following:

1. Investigate the compatibility of the EpCAM epitopes HO-3 and VU1D9.
2. Determine which fluorophore between BV421 and BV605 gives the best signal.
3. Verify that LNCaP cells are higher expressing EpCAM compared to PC-3 cells.
4. Optimize the staining protocol used for staining cells with HO3-BV605.

Epitope compatibility, HO3 vs. VU1D9

In order to look at the compatibility of different epitopes, the epitopes HO3 and VU1D9 were compared. In order to see if they are compatible, different fluorophores were attached to the antibodies targeting the mentioned epitope regions.

We hypothesised, based upon our literature research, that VU1D9 and HO3 can be targeted at the same time without interference[62, 61].

Fluorophore comparison

The goal of the fluorophore comparison was to determine which fluorophore gives the best signal. Two fluorophores were chosen to be compared: BV421 and BV605. In order to compare these fluorophores, the same antibody was chosen and will be bound to one of these fluorophores in different conditions.

We hypothesised, based upon our literature research, that BV421 is brighter than BV605[63].

EpCAM expression: LNCaP vs. PC3

The goal of the EpCAM expression comparison test between the LNCaP and the PC3 cell lines was to verify theory. From literature we know that LNCaP are higher expressing EpCAM than PC3. The simple way to do this is following the exact same staining procedures with the exact same antibodies and fluorophores and see if there is a difference in intensity of the cells.

We hypothesised that the LNCaP cells are higher expressing EpCAM than PC-3 cells in accordance with literature.

Optimizing protocol

The goal of optimizing the protocol was to gain better images. There were some factors from which we did not know it they influenced the stainings and also not how much they influenced stainings. This was primarily done due to long exposure times of the samples we work with in Chapter 5 and the huge variation in those depending if procedures were working smoothly or not. Parameters that were looked into are:

1. The time of incubation
2. The temperature of incubation
3. The exposure to light

We hypothesize that the the longer the incubation time, the better the staining results. We expect the temperature of incubation to be better at 37 degrees compared to 20 degrees because the conditions for the cells are better. Lastly, we expect the exposure to light the negatively effect the stainings.

3.3 Materials & Methods

In order to realise our goals the following Chapter will give an overview of the materials used, followed by the methods of how the experiments were carried out.

3.3.1 Materials

Cell lines

Both the LNCaP cell line and the PC-3 cell line were obtained from the American Tissue Culture Collection (ATCC). Cells were maintained in an incubator kept on 37 degrees Celsius in 5% CO_2. The cells were kept in T25 culture flasks which were treated for better adhesion of the cells. They were passaged and/or harvested when cells reached around 80% confluency for PC-3 and since LNCaP grows as clusters when clusters of LNCaP became too big. Before passaging, LNCaP and PC-3 were washed with pre-warmed phosphate-buffered saline (PBS) (Sigma Aldrich, St. Louis, USA). Then, 0.5 mL of pre-warmed 0.05% trypsin-EDTA was added and incubated for 1 minute at 37C. If cells were detached, 2mL of pre-warmed medium was added to deactivate the trypsin. Otherwise a small snap against the flask was used to detach the cells. If this was also not sufficient, another incubation minute was used. Then cells were counted using the using the Luna-FLTM automated cell counter (Westburg B.V., Leusden, The Netherlands). LNCaP cells were passaged in a new flask with a seeding density of 5.000 cells/cm^2 whereas PC-3 cells got passaged with a seeding density of 2.000 cells/cm^2. The cell culture medium was replaced every 2-3 days. Culture medium consisted of Dulbecco's Modified Eagle Medium (DMEM) from Gibco, ThermoFisher Scientific. With 10% Fetal Bovine Serum (FBS) of Sigma Aldrich, and 1% Penicillin/Streptomycin of Lonza.

Mycoplasma tests were performed for all used cell lines as a routine check for mycoplasma contamination in the lab, all cell lines came out as negative.

Epitopes and antibodies

See Table 2 for the overview of the used antibodies in this Chapter.

Table 2: All antibodies used in Chapter 3, their working concentration, their stock concentration, and their manufacturer information.

Antibody	**Working Concentration**	**Stock Concentration**	**Manufacturer**
Brilliant Violet 421 custom conjugation clone HO-3-9	2.25 μg/mL	0.45 mg/mL	Biolegend, Greenwood Place, UK
Brilliant Violet 605 Custom Conjugation Clone HO-3-19	2.25 μg/mL	0.45 mg/mL	BioLegend, Greenwood Place, UK
Hoechst	1 μg/mL	1 mg/mL	
Mouse anti EpCAM PE clone VU1D9	20 μL per 100μL, unknown	2 mL, unkown	Sigma, Saint Louis, MO, USA
Cell Tracker Orange (CTO)	2μM	10mM	Thermofisher, Waltham, MA USA

3.3.2 Epitope compatibility, HO3 vs. VU1D9

Cells from the LNCaP cell line were collected on which stainings were performed with HO3 and VU1D9 antibodies, see Appendix 8.9 for the protocol. HO3 was attached to BV421: HO3-BV421. VU1D9 was

attached to a PE emitting fluorophore; VU1D9-PE. Pictures were taken in the PE channel and the DAPI channel (we do not have the specialised filter for BV421). Per channel, an optimal exposure time was determined and used. There were 4 conditions, LNCaPs stained with:

1. VU1D9-PE
2. HO3-BV421
3. 'both' VU1D9-PE and HO3-BV421
4. Control (no staining)

The conditions were visually compared between each other if there is no spill over and if signal is less bright when multiple antibodies were used. Next to that, it was looked into if the same cells will give signal for both antibodies when stained with both antibodies. There, the intensities were compared of different cells between the condition, and the relative intensities of the cells of the same 'both' condition were compared. The working concentration was based upon previous in house experiments.

3.3.3 Fluorophore comparison

Two fluorophores were chosen to be compared: BV421 and BV605. The antibody that was used for this comparison was HO3. Cells from the LNCaP cell line were stained with or the HO3-BV421 or the HO3-BV605. Pictures of the BV421 condition were taken with the DAPI filter since the specialised filter for BV421 was not available on the standard fluorescence microscope. Pictures of the BV605 condition were taken using the specialised BV605 filter.

The comparison was made based upon visuals. Next to that the exposure time which is needed to make a proper image was quickly looked into, and the relative intensity of the imaged cells was briefly looked at.

3.3.4 EPCAM expression: LNCaP vs. PC3

LNCaP and PC3 cells were stained with HO3 antibodies. The fluorophore attached to this antibody was BV421. The difference in intensity of the staining of the cells was compared, both visually and by relative intensity. Images were taken with the DAPI filter while exposure times and the way of adjusting the gray scales were exactly the same for both conditions. Cells to be compared were chosen randomly.

3.3.5 Optimizing protocol

The staining protocol (see Appendix 8.9) as previously used was followed with some varying parameters in order to deduce the best conditions for the staining.

The incubation time and exposure of light were tested in the same experiment. LNCaPs would be stained by HO3-BV605 and Celltracker Orange. Images were taken with brightfield, BV605, and PE channels. Exposure time was kept the same for every specific channel. After taking pictures, analysis by flowcytometry was done. The cell population was determined by a non stained condition, which was also used to set the gates to determine which cells are stained or not for the stained conditions. The conditions tested in the experiment were the following:

1. 1 hour incubation closed from light on room temperature.
2. 4 hours incubation closed from light in a waterbath of 37 degrees celsius.

3. 4 hours incubation exposed to light on room temperature.

Every one of these factors will be tested by 4 groups of differently stained cells:

1. No stain control (NSC)
2. Stained with Cell Tracker Orange (CTO)
3. Stained with HO3-BV605
4. Stained with CTO and HO3-BV605

With the temperature of incubation, temperatures of 20 and 37 degrees Celsius were tested. The BV605 staining was chosen to do these tests. Tests were done with LNCaP cells. Pictures were taken with a 10X objective magnification in brightfield, BV605, and DAPI channels. Exposure times were varied with, and then kept the same for 1 or 2 chosen times for all the other conditions.

Conditions:

1. Unstained
2. HO3-BV605, 20 degrees Celsius
3. HO3-BV605, 37 degrees Celsius
4. HO3-BV605 + Hoechst, 20 degrees Celsius
5. HO3-BV605 + Hoechst, 37 degrees Celsius
6. Hoechst, 20 degrees Celsius

3.4 Results

3.4.1 Epitope compatibility, HO3 vs. VU1D9

Epitope compatibility looks into targeting the same molecule with 2 different antibodies.
Cells stained with only VU1D9-PE and with both VU1D9-PE/HO3-BV421 antibody were visible in the PE channel. HO3-BV421 and non stained cells were not visible in the PE channel. Meaning that HO3 does not block VU1D9 signal in such a degree that visibility disappears. See Figure 7.

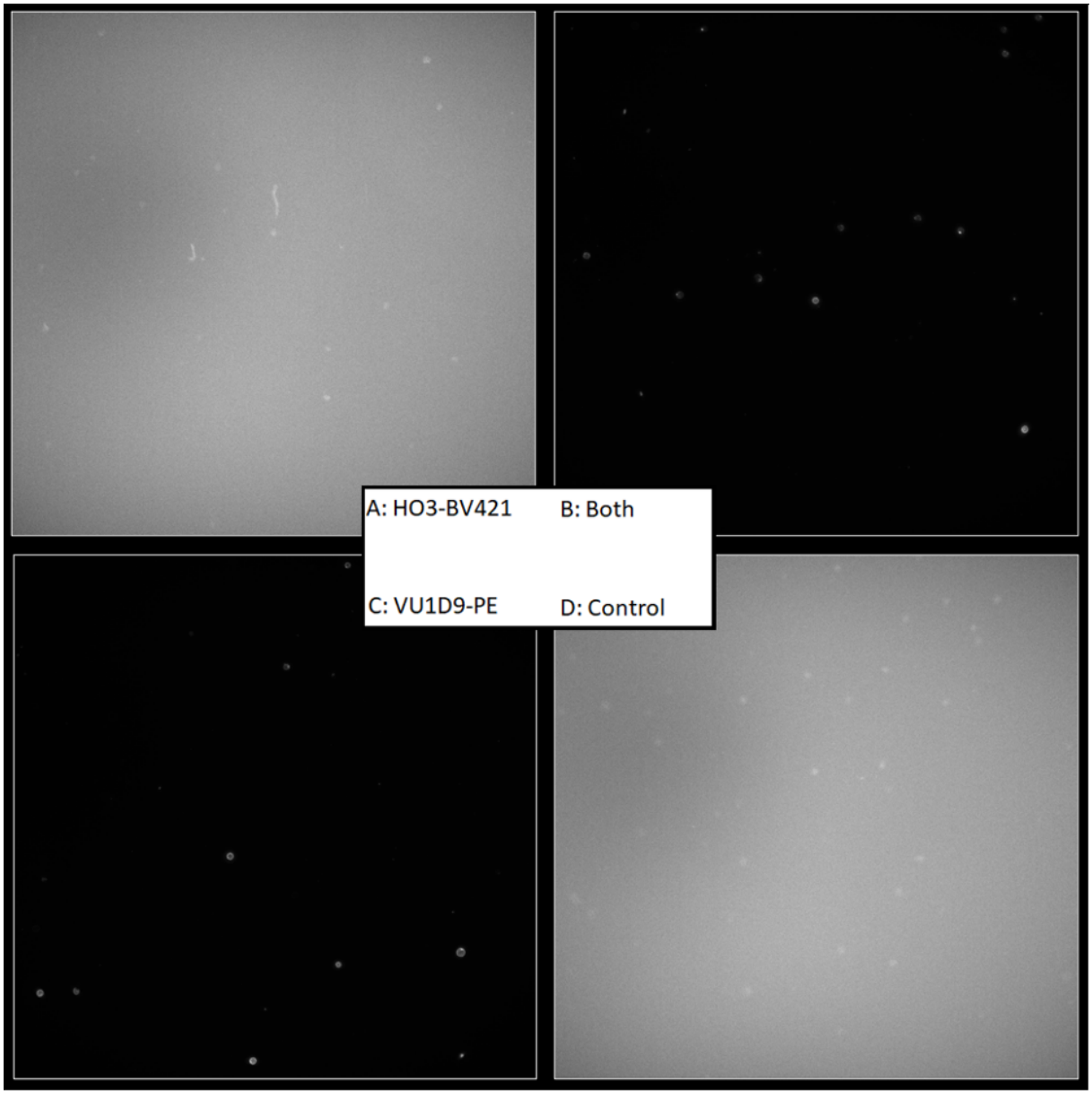

Figure 7: Epitope comparison; PE channel. Images taken from Lncap cells stained by HO3 and VU1D9 antibodies. HO3 is attached to BV421 and VU1D9 is attached to a PE emitting fluorophore. A: cells stained with HO3-BV421. B: cells stained with both antibodies C: cells stained with VU1D9-PE. D: cells which were not stained. Cells were expected to be visible at the B and C. All pictures are taken with a magnification of 10x the objective, an exposure time of 0.075s, and are displayed with the same LUT.

Cells stained with a HO3-BV421 and with both VU1D9-PE/HO3-BV421 antibody were visible in the DAPI channel. VU1D9-PE and non stained cells were not visible in the DAPI channel. Meaning that VU1D9 does not block HO3 signal in such a degree that visibility disappears. See Figure 8.

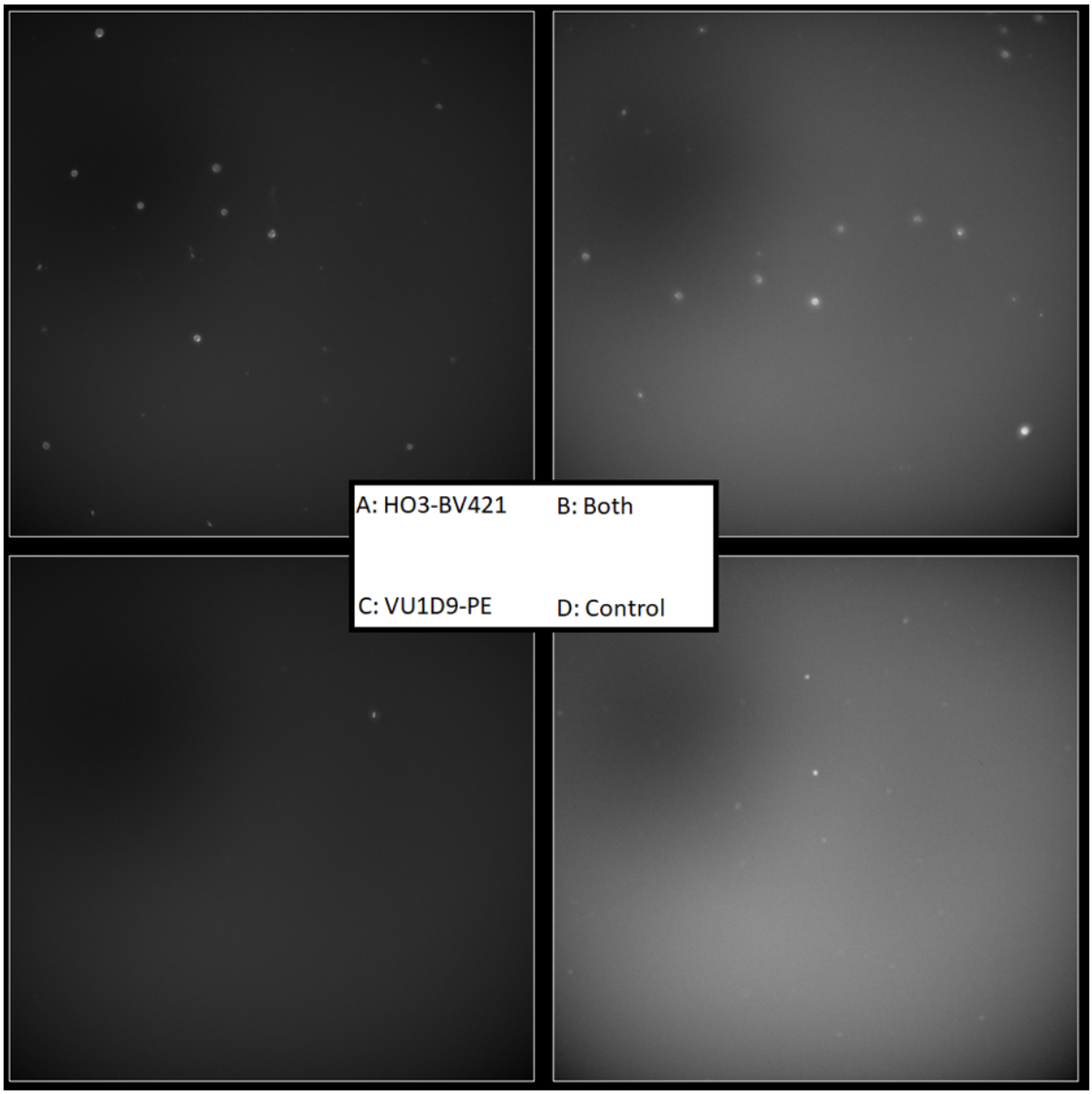

Figure 8: Epitope comparison; DAPI channel. Images taken from Lncap cells stained by HO3 and VU1D9 antibodies. HO3 is attached to BV421 and VU1D9 is attached to a PE emitting fluorophore. A: cells stained with HO3-BV421. B: cells stained with both antibodies C: cells stained with VU1D9-PE. D: cells which were not stained. Cells were expected to be visible at A and C. All pictures are taken with a magnification of 10x the objective, an exposure time of 1s and are displayed with the same LUT.

The BV421 was less bright than the PE staining. The exact same cells are visible in the PE and the DAPI channel in the condition that is stained with both antibodies. When comparing Figure 7D and Figure 8D, the exact same pattern is visible. Which means that the same cells emit fluorescent light from both fluorophores and thus bound both antibodies.

To add a quantitative value to the visual results, a small comparison was made in fluorescence intensity levels. Fluorescence signal was plotted through 2 randomly chosen cells in the PE channel (see Appendix 8.10 for the plots), and through 2 randomly chosen cells in the DAPI channel. This was done for all conditions.

PE

- VU1D9: 4060 and 4072
- HO3: 236 and 237
- Both: 2951 and 4447
- Control: 226 and 239

DAPI

- VU1D9: 908 and 945
- HO3: 1342 and 1332
- Both: 1081 and 1321
- Control: 961 and 901

Next to that, in the condition with both antibodies we compared the same cells in both channels. There was the assumption that if there were to be interference and blockage, that if 1 antibody type bound to a cell the other wouldn't be able to bind as efficiently. Which would result in cells that would give high fluorescence in one channel and low fluorescence in the other channel. When comparing 6 randomly chosen cells, the lower expressing cells were low expressing for both antibodies and the high fluorescent cells were high fluorescent for both channels. See Appendix 8.10 for the plots.

3.4.2 Fluorophore comparison

Now that we knew that EpCAM could be targeted by two different antibodies, which opened up the possibility to stain EpCAM even though it was also targeted in enrichment, deciding on the best fluorophore was important.
BV421 gave better signal even though the filtercube used for imaging BV421 (DAPI) was not optimized for BV421 fluorophores. BioLegend already stated that BV421 is brighter, so that was within expectations. Moreover, the exposure time used for BV421 was only about half of the exposure time used for BV605 and the resolution is better. When extracting the background noise, the signal from the cells was 2x as intense from the BV421 as from the BV605.

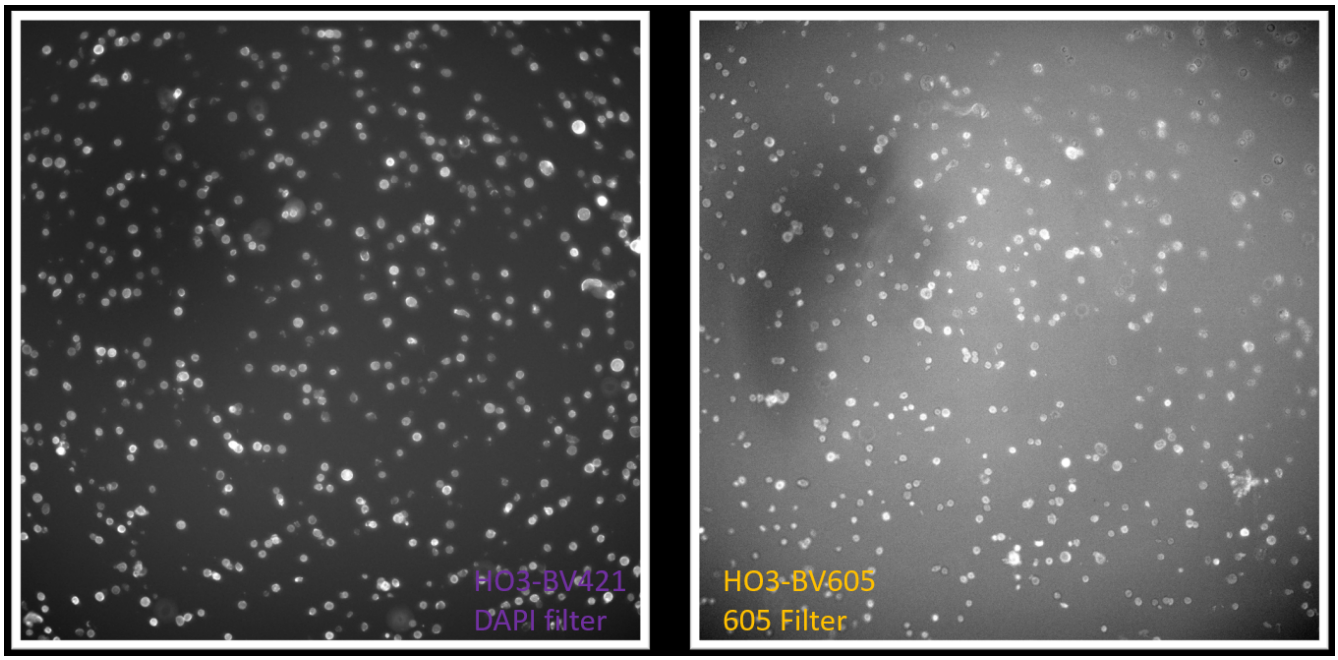

Figure 9: Images taken from Lncap cells stained by HO3 antibodies attached to BV421 imaged with the DAPI filter (left) and BV605 imaged with a 605 filter (right). The signal from the HO3-BV421 is brighter and better visible.

3.4.3 EPCAM expression: LNCaP vs. PC3

LNCaP and PC3 cells were compared in EPCaM expression. LNCaPs gave visibly better results, there is more contrast and intensity when using the same microscope and image analysis tools. PC3 cells are hard to distinguish while LNCaP cells are easily visible. The BV421 intensity values that we find on average of 8 LNCaP cells is 1284, while the average for 3 PC3 cells it is 833. Background for both images is on average around 725. See Figure 10 for the images taken in the DAPI channel and see Appendix 8.11 for the intensity plots of the DAPI channel.

The BV605 intensity values that we find on average of 6 LNCaP cells is 2733, while the average for 5 PC3 cells is 2594. Background for both images is on average around 2400. For the pictures and intensity plots when the cells were stained with BV605 as fluorophore, see Appendix 8.11.

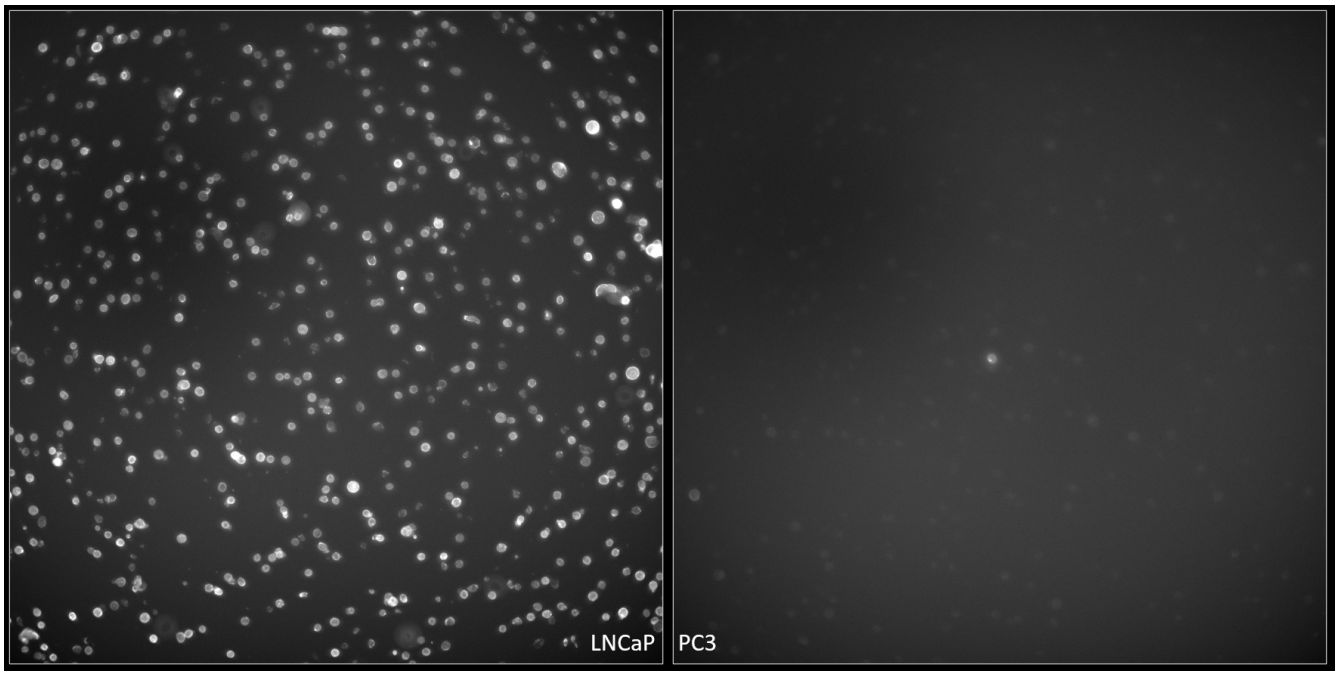

Figure 10: Images taken from Lncap cells (left) and PC3 cells (right) stained by HO3 antibodies attached to BV421 imaged with the DAPI filter. The signal from the the LNCaP cells is brighter and better visible. Both pictures are taken with a magnification of 10x the objective, the same exposure time exposure time and are displayed with the same LUT.

3.4.4 Other parameters

These experiments were started with setting the gates with the No Stain Condition. After setting the gates, the no stain control has 0% detection of both cells stained with CTO and/or cells stained with BV605 after longer exposure to light or longer incubation times. The combination of the conditions that were stained for a fluorophore is discussed here and shown in Table 3 and Figure 11. For the individual overview of all condition with their specific stainings, see Appendix 8.23 Table 6 for the CTO results and Table 7 for the BV605 results.

Effect of exposure to light

When looking at the cells stained with HO3-BV605 of the standard '1 hour dark incubation' condition, 93.70% of cells was identified as stained. When comparing this with the '4h light exposure' condition, 7.15% less cells were detected as stained and the average intensity of those cells decreased by 48.26%.

When looking at the cells stained with HO3-BV605 of the '4 hour dark incubation' condition, 84.15% of cells was identified as stained. When comparing this with the '4h light exposure' condition, 2.40% more cells were detected as stained and the average intensity of those cells increased by 3.03%. See the purple values in Table 3 and see Figure 11.

When looking at the cells stained with CTO of the standard '1 hour dark incubation' condition, 98.35% of cells was identified as stained. When comparing this with the '4h light exposure' condition, 23.95% less cells were detected as stained and the average intensity of those cells decreased by 72.35%.

When looking at the cells stained with CTO of the '4 hour dark incubation' condition, 83.75% of cells was identified as stained. When comparing this with the '4h light exposure' condition, 9.35% less cells were detected as stained and the average intensity of those cells decreased by 9.42%. See the orange values in Table 3 and see Figure 11.

Table 3: Overview of the flowcytometer results of the incubation time and light exposure experiment. The median fluorescence intensity decreased of both CTO and BV605 after longer incubation times. This decrease was also seen in the percentage of cells that are selected as positive for a staining. In yellow the most important results for CTO. In purple the most important results for BV605.

	Median Intensity CTO	**% intensity vs. 1h dark inc.**	**% CTO+ cells**
4h light exposure	3829	27,65%	74,40%
4h dark incubation	5452,5	38,07%	83,75%
1h dark incubation	13890	100,00%	98,35%

	Median Intensity BV605	**% intensity vs. 1h dark inc.**	**% BV605 + cells**
4h light exposure	1440,5	51,74%	86,55%
4h dark incubation	1361	48,71%	84,15%
1h dark incubation	2800	100,00%	93,70%

Effect of incubation time

When looking at the cells stained with HO3-BV605 of the standard '1 hour dark incubation' condition, 93.70% of cells was identified as stained. When comparing this with the '4h dark incubation' condition, 9.55% less cells were detected as stained and the average intensity of those cells decreased by 51.29%. When comparing this with the '4h light exposure' condition, 7.15% less cells were detected as stained and the average intensity of those cells decreased by 48.26%. See the purple values in Table 3 and see Figure 11.

When looking at the cells stained with CTO of the standard '1 hour dark incubation' condition, 98.35% of cells was identified as stained. When comparing this with the '4h dark incubation' condition, 14.60% less cells were detected as stained and the average intensity of those cells decreased by 61.73%. When comparing this with the '4h light exposure' condition, 23.95% less cells were detected as stained and the average intensity of those cells decreased by 72.35%. ee the orange values in Table 3 and see Figure 11.

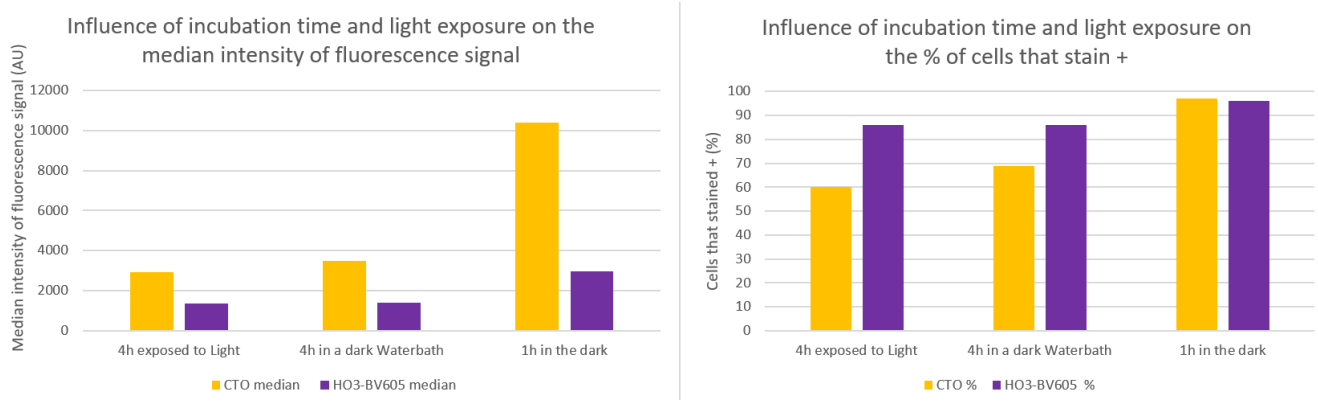

Figure 11: Overview of the flowcytometer results of the incubation time and light exposure experiment. The median fluorescence intensity decreased of both CTO and BV605 after longer incubation times. Decreases were also seen in the percentage of cells that are selected as positive for a staining.

Effect of incubation temperature

It was unclear if the small influence seen at the temperature is due to the temperature or due to the longer waiting time.

3.5 Conclusion & Discussion

Fluorophore comparison

Conclusion: The fluorophore BV421 is brighter than BV605 and if the staining cocktail allows, should be used to target EPCAM.

Discussion: Hoechst was so bright that it overlapped even in the BV605 spectrum. Therefore, combinations of these should not be used. If Hoechst is necessary, optimization with lower working concentrations of Hoechst can be performed till the overlap is not a hindrance in imaging the correct target.

Long exposure times of 0.5s gave better pictures than exposure times of 0.01s when imaging cells with BV605. However, when DAPI or Hoechst staining was used simultaneous, these were visible in the BV605 filter when using the longer exposure time of 0.5s. When looking at the ex/em max from BV605, DAPI, and Hoechst, this does seem indeed unlikely. For BV605 the optimal excitation wavelength is 405nm, and the optimal emission wavelength is 603nm[63]. For DAPI Excitation/emission is optimal at 358/461nm[69] with a max excitation wavelength of 405nm[70]. However, when using Thermofishers software Spectraviewer, it can be seen that the emission spectrum of DAPI and Hoechst has a very long tail likely even reaching the peak of emission of BV605 which is where we image[65]. Even though it's just a couple percent of the emission maximum, this might explain why we do see DAPI and Hoechst with very long exposure times.

Epitope compatibility

Conclusion: The epitopes HO3 and VU1D9 can be targeted at the same time with different fluorophores without interference of each other.

Discussion: The BV421 was less bright as the PE staining, as expected. That was most likely due to the filtercubes that were used. The correct filter for the PE staining was available, while the DAPI filter had to be used for the BV421 staining. This does influence the results but not in such a way that is changes the conclusion.

The optimal working concentrations were not determined in these experiments but based upon earlier in house research. These in house experiments were however not with the primary focus to optimize the working concentrations. If time and stock are present, we recommend to first optimize for the working concentrations before comparisons are made. Another factor that might influence the optimal working concentration is the cells of interest, different cells have different expression of EpCAM[32] and perhaps varying optimal working concentrations.

Epitopes might be compatible, if the antibodies are attached to larger bodies, there might still be steric hindrance depending on the shape and size. Which does not necessarily mean that we can stain the EpCAM which already has FF attached to them. Since the FF are bigger than the fluorophores (BV: 340 Kdalton[71]), antibodies (IgG: 150 Kdalton[72]), and EpCAM (40 Kdalton[73]), there is at least a 20x difference in diameter between FF and the others (see Figure 20).

We showed in our exploratory research that comparisons can be made and quantification can be done. However repeats should be added in all experiments based upon pictures of the fluorescent microscope. Next to that quantification should be done over a larger number of cells.

EPCAM expression: LNCaP vs. PC3

Conclusion: LNCaP cells have higher intensities of both fluorophores while using the same HO3 antibody. Therefore, LNCaP cells have higher expression of EPCAM compared to PC3 cells. Which is in line with our finding in literature[32].

Discussion: We know that LNCaP cells have lower metastatic behaviour than PC-3[74] cells. Tumours are characterized by high metabolism and very poor perfusion, this causes the tumour environment to become hypoxic and acidic[75]. An acidic environment causes more invasive behaviour[76]. Specifically in PC-3 cells, it caused more migration, vasculogenisis, improved colony forming in culture, and increased sizes and numbers of non-adherent spheres in culture[76]. This acidity stimulated the cleaving of EpCAM via Beta-site Amyloid Precursor Protein-cleaving Enzyme 1 (BACE1). Which causes it to become unavailable for staining the cell[77]. So the lack of staining does not necessarily mean there was less EpCAM, but that at present the extracellular part of EpCAM (the EpEX, shown in Figure 1) is simply no longer present. However it should be noted that cells were not kept in an 'acidic and hypoxic' environment. Therefore influence on cell line experiments is likely low, however it might have influence on CTC from the DLA samples which do directly come from a tumour environment which is likely acidic and hypoxic.

Protocol optimization

Conclusion: Dark chambers with long incubation times (4 hours) for CTO or HO3-BV605 give worse results than dark rooms with short incubation times (1 hour).

Discussion: The effect of long exposure to standard TL light was seen when using CTO, however in the staining we are interested in (BV605), no decrease was seen compared to 4 hours in a dark room. Note however that there was also a temperature difference between these conditions.

Temperature does seem to have influence on the intensity of the signal of both CTO and BV605. However, the difference between staining in 20 degrees Celsius and 37 degrees Celsius might also very likely have been due to longer incubation time.

Nothing can be concluded from this experiment in regard to light exposure and incubation temperature. Therefore, another experiment should be carried out with the same staining variations but other conditions (one of the conditions 2, 3, 4, or 5 is optional) with varying incubation temperature and light exposure, namely:

1. Unstained
2. HO3-BV605, 20 degrees Celsius, 1h dark incubation
3. HO3-BV605, 37 degrees Celsius, 1h dark incubation
4. HO3-BV605, 20 degrees Celsius, 1h light incubation
5. HO3-BV605, 37 degrees Celsius, 1h light incubation

All in all, we now know that the chosen epitopes do have different binding sites. We are also aware of the best fluorophores which can be used for staining and factors that might influence staining. Lastly, we know that there is different EpCAM expression on different sorts of PCa cells, which lets us know that there is variation to be expected in the CTC of PCa patients. Now that there is more understanding of our biomarker that we will target with FF, lets look into the actual targeting and the influence it might possible have on tumour cells in the next chapter.

4 Influence of ferrofluids on viability and metabolic activity

Ferrofluids (FF) will be used to enrich DLA samples in order to get the needed higher yield of CTCs. Naturally the influence of those FF on the cells is of our interest. Therefore this chapter looks into the influence of FF on the viability and metabolic activity of cells. Multiple ways of looking into these factors have been researched and will be discussed.

4.1 Theoretical Background

4.1.1 Ferrofluids (FF)

By binding magnetic particles to targets, the targets can be removed from a solution by magnetism. A liquid can also function as a magnet, this would be called a ferrofluid. A FF is a stable colloidal mixture of nanoscale magnetic particles with single domain ferro- or ferrimagnetic particles in a liquid carrier[78, 79]. The size of these particles is smaller than 10nm in diameter[79] and are coated in surfactant to prevent agglomeration and provide stabilisation[78].

The fluid doesn't exhibit any magnetic behaviour when there is no external magnetic field present[79]. But when there is an external magnetic field present, the particles aline with the field lines[79]. Side note is that a ferrofluid its particles will always stay in solution, however reality is often different and particles sink with time due to gravitational forces and interactions among particles (especially at higher densities[78]).

FF are frequently used in several applications, In our lab the use of FF to catch cells is of interest. Cell separation tests have been done based upon magnetism and labeled target cells from 1977 on [80] and continued through the ages[81, 82, 83, 84, 85]. Moreover, magnetic cell separation is even already applied on lab on chip applications[86] and applied for CTC enrichment[87]. Literature shows that 0.2 mg/mL is sufficient to quantitatively remove tumor cells from body fluids [85]. Furthermore this can be done within 1-2 minutes[85].

Figure 12 illustrates the mechanism of our separation method. First, the sample is mixed together with FF and left to incubate. Then an external magnetic field is created by a magnet which is held to the side of the tube. Then the remainder of the sample which is not bound to the sides of the tubes is aspirated, while the magnetic field is still applied. After that the magnetic field will be removed an the caught cells will be put in other medium or staining solutions.

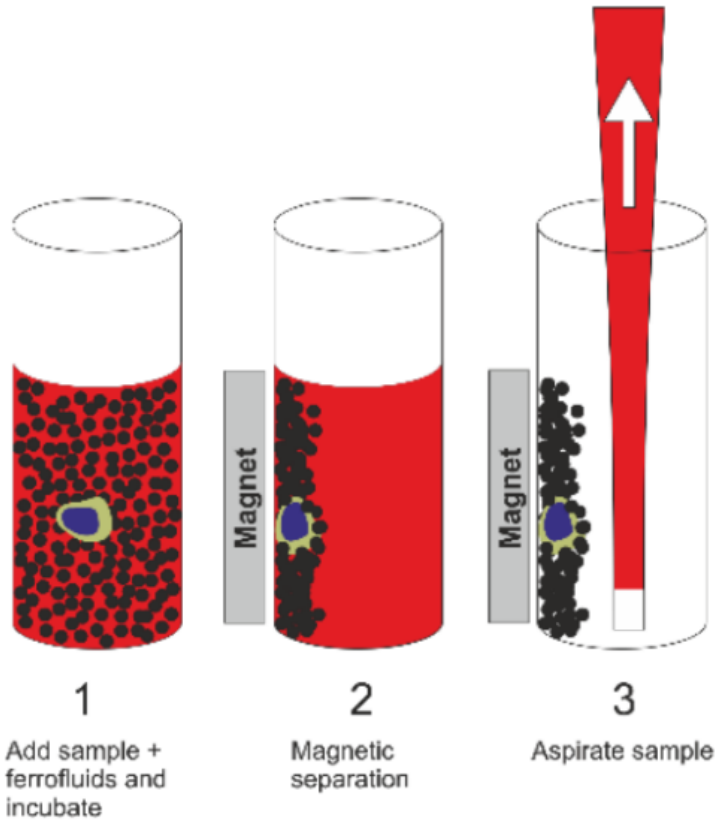

Figure 12: Schematic of the enrichment of the DLA sample with use of immunomagnetic ferrofluids. 1. Add the sample plus the ferrofluids and let this incubate. 2. Activate the magnet and let is stand, the bound cells will now be attracted to the magnet and accumulate there. 3. Aspirate the not caught fluid.

When using DLA samples, as will be done in Chapter 5, Figure 12 becomes a bit more complex. There will not only be cancer cells but also other types of cells, for example leucocytes, see Figure 13. Part of the leukocytes will also be present in the enriched sample, however in a much lower concentration when compared to a non-enriched sample.

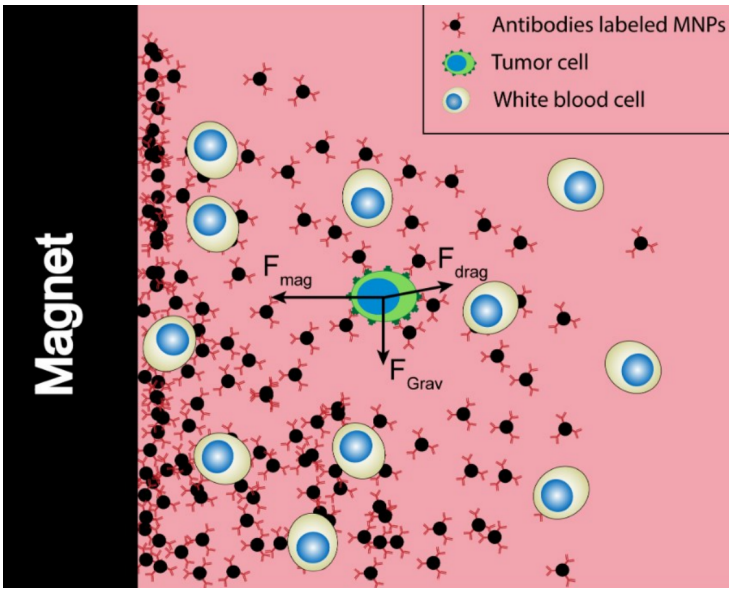

Figure 13: Schematic of the interaction between particles and surfaces during enrichment of the DLA sample with use of immunomagnetic ferrofluids. Plus a virtual force scheme of the target cells during immunomagnetic separation. Seen is that leukocytes likely will be caught up during the procedure due to being surrounded by the magnetic particles and unspecific binding. [87]

Of utmost importance is that the FF do not influence the CTC. If they were to secrete differently, behave differently, or perhaps not even survive the enrichment procedure, the information will not be extracted untouched. Therefore, the FF influence on the cells should be studied.

4.1.2 live/dead and apoptotic cell identification

Morphology

The most cost efficient way of investigating viability during small scale experiments is microscopically checking the morphology of the cells. By the standard procedure of culturing cells, those potential differences can be seen. Next to that, you can see if cells are attached or not to the culture flask. That is important for us since EPCAM is an adhesion molecule, the adhesive characteristics might change when these molecules are occupied by bound FF. Besides that, attachment of cells to surfaces is needed in the chip culture procedures when looking at secretion (extrapolation based on the characteristics of the cells from cell lines).

Morphology on its own doesn't give a quantitative value. Therefore other quantitative methods are also being used next to the morphological checks. A well known way of investigating viability during experiments is via fluorescent stainings. The most used method is Live/Dead stainings. We experimented with 1 sort of live staining, 3 different dead stainings (2 for flowcytometry and 1 for cell counter analysis), a DNA staining which we used in an alternative way as a dead staining, and an apoptotic tracker.

Live staining: Calcein-AM

The live staining that was being used is Calcein-acetoxymethyl(AM), a non fluorescent derivative from Calcein. Commonly used to determine if cells are viable. The Calcein-AM can enter cells, where it is converted to calcein after an ester hydrolisis reaction by intercellular esterases[88]. Calcein is has an emission/excitation spectrum of 495/515nm, see Figure 14. However is has been reported to have a negative effect on migration and adhesion in certain cell types (monocytes)[89]. Moreover, it has been

reported as cytotoxic for certain tumour cell lines[90, 91, 92]. Calcein-AM is also used as a marker for apoptosis[93].

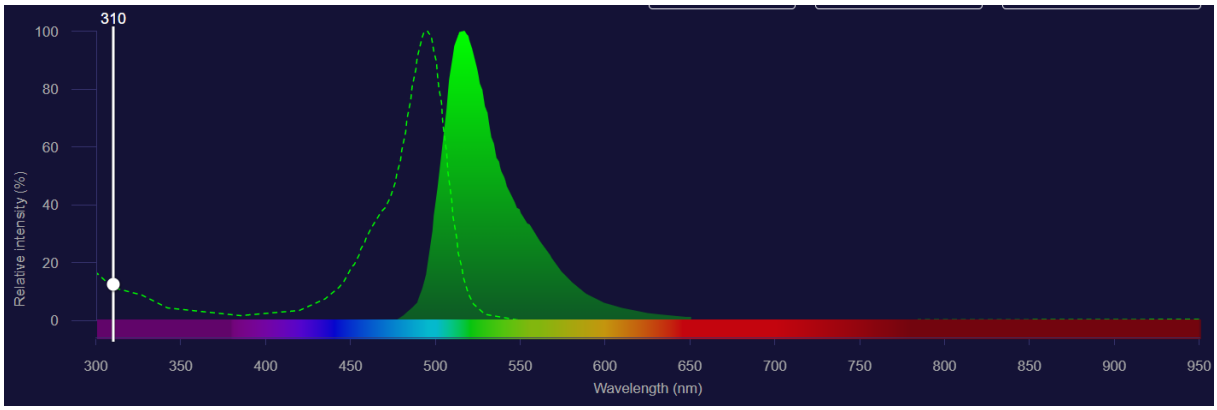

Figure 14: Emmision(solid line) and excitation(dotted line) spectra of Calcein, the fluorescent product after Calcein-AM reacts intercellular. The optimal excitation/emission wavelength is 495/515nm.[88]

Dead stainings: Propidium Iodine (PI) and Ethidium Homodimer (EH)

The dead stainings being used were Propidium Iodine (PI) and Ethidium Homodimer (EH), both often used in combination with Calcein-AM. Ethidium Homodimer-1, makes dead cells visible by entering via damaged membranes and binding to the nucleic acids. By binding to the nucleic acids, its signal is 40 times enhanced. This is a bright red signal with excitation/emission of 528/617nm, see Figure 15. The downside of this staining is that it does not detect cells that are effected in such a way that the cell membrane is not damaged.[94]

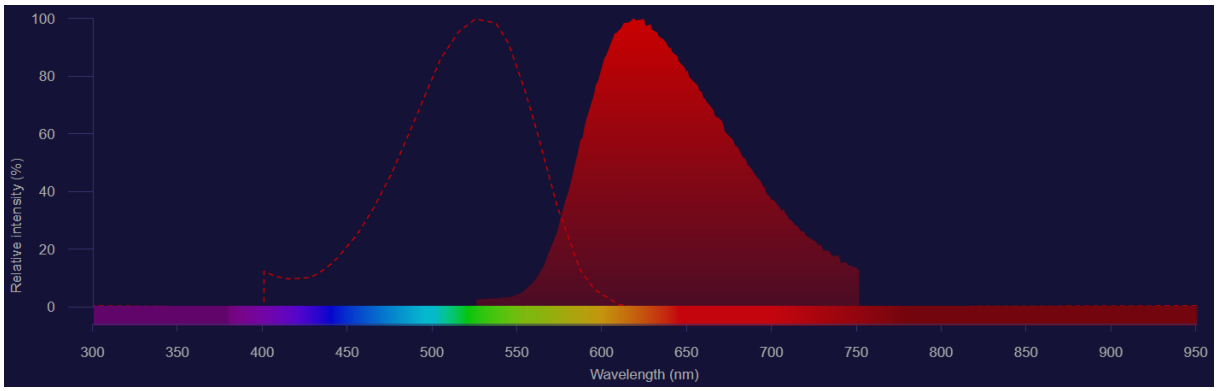

Figure 15: Emmision(solid line) and excitation(dotted line) spectra of Ethidium Homodimer-1. The optimal excitation/emission wavelength is 528/617nm.[94]

Propidium iodine (PI) works the same as EH, it also makes dead cells visible by entering via damaged membranes and binding to the nucleic acids. By binding to the nucleic acids, its signal is 20 to 30 times enhanced. The excitation and emission spectra are changed the moment it binds. from 493/636nm as maxima to 535/617nm as maximum excitation/emission wavelength, see Figure 16 for the initial spectrum.[95]

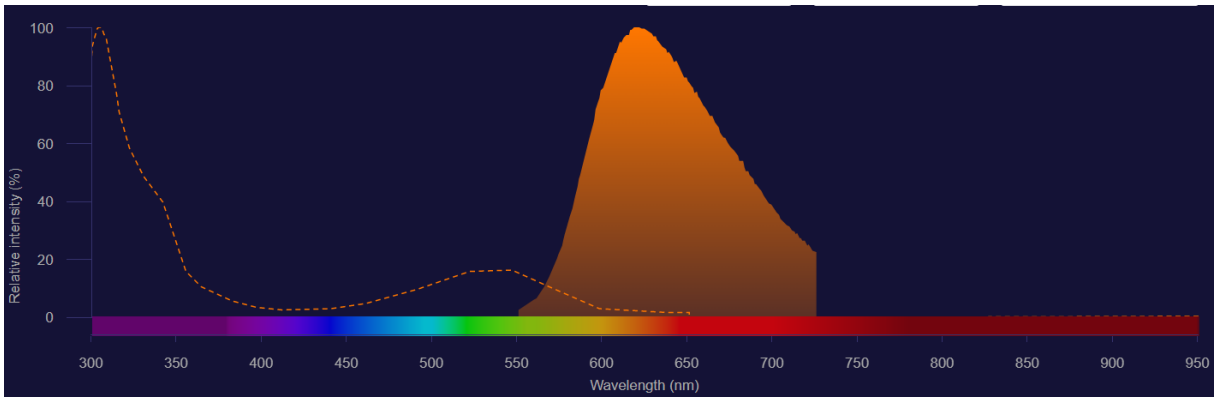

Figure 16: Emmision(solid line) and excitation(dotted line) spectra of Propidium iodine. The optimal excitation/emission wavelength is 304/622nm. However the moment the dye binds the max excitation/emmision changes to 535/617. [95]

Multi-use staining: DAPI

As the established protocol for the CTC staining uses DAPI 4,6-diamidino-2-phenylindole (DAPI) to evaluate the viability of the CTCs in the DLA samples, our later experiments were conducted with DAPI. DAPI is cell impermeant[70] and therefore normally used to stain the nuclei of fixated cells. Relying on that DAPI in not too high concentrations will not immediately enter viable cells since their membranes are intact, dead cells could be stained[96]. The blue fluorescence of DAPI will increase 20 fold when binding to the targeted AT regions of the DNA. Excitation/emission is optimal at 358/461nm[69] with a max excitation wavelenght of 405nm[70].

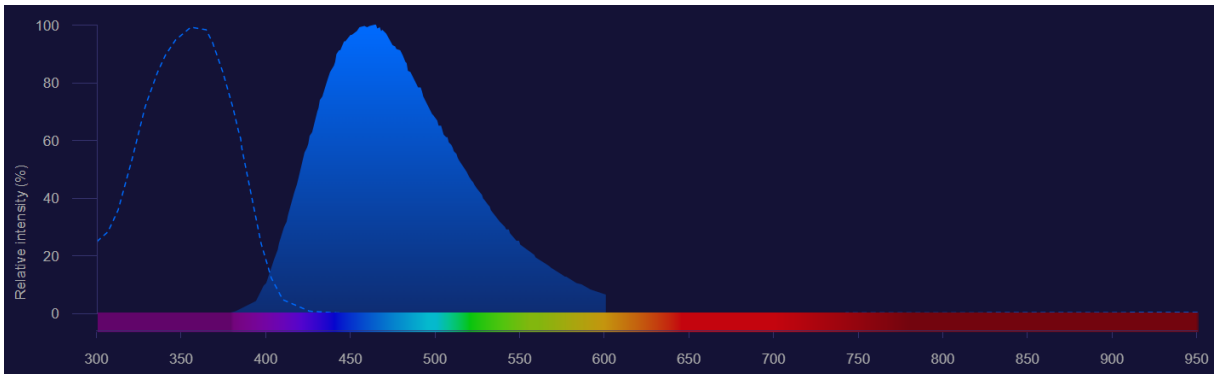

Figure 17: Emmision(solid line) and excitation(dotted line) spectra of DAPI. Excitation/emission is optimal at 358/461nm[69] with a max excitation wavelenght of 405nm[70].

Dead staining: Trypan Blue

Trypan blue is a dizoa (RN=NR) dye. Trypan Blue exlusion assays are based upon the same principle as the PI and EH dye[97]. Trypan Blue does not enter cells with intact membranes while it does enter cells with membrane discrepancies[98]. Trypan blue is negatively charged and thereby does not interact with the negatively charged membranes of cells[98]. The cells with damaged membranes do take up the dye, will become distinctive blue an can be easily seen under a simple microscope. Trypan blue has been used before to look into cell dead, apoptosis, and necrosis in LNCaP cells[99], which is the cell line most used in our research. It is also suggested to use Trypan Blue in the flowcytometer[100], but due to the nature of the dye we chose to use different life dead dyes for flowcytometry.

Apoptosis staining: Apotracker

In general tumour cells prefer to be attached, however when epithelial-to-mesenchymal transition (EMT) occurs and they lose their cell-cell adhesion next to improving migratory and invasive properties, integrins change and they detach[101]. This is a 'submicroscopic fraction' of the original cancer named the CTCs, which are as the name already suggests, circulating[57]. After EMT, CTCs are suddenly exposed to a lot of other external forces, therefore the condition of the CTCs in the DLA sample are not of high viability and could already enter the stage of apoptosis. Therefore, stainings that can detect apoptotic cells are of interest. The earlier discussed EH, PI, and DAPI do that as a secondary side effect of their nature, but are not specialised in it. Apotracker is a staining specially developed to detect apoptotic cells[102]. Apotracker Green is a calcium independent staining and detects the translocation of phosphatidylserine (PS) residues[102]. The translocation of PS is recognised due to it normally being present in the inner leaflet of the cell membrane[103]. During translocation it is randomized and can move to the outer leaflet of the cell membrane where is can be detected[103]. Apotracker gives a good indication of the viability state of the CTCs, which might also have influence on their secretion patterns and thus their PSA secretion which is of importance for us. However, there is another way to measure likely influence on secretion: metabolic activity measurements.

4.1.3 Metabolic activity

Metabolic activity is a parameter often used to indicate viability of cells. In order to investigate the metabolic activity, Alamar Blue Assays(ABA) were performed. ABA were used for the first time in 1929, but has been in use for the past 60 years for the use of investigating cell viability and cytotoxicity[104]. They are ready to use, permeable, non-toxic, assays to quantitatively measure viability[105]. It uses the chemical reaction of converting resazurin (7-hydroxy-10-oxidophenoxazin-10-ium-3-one) to fluorescent resorufin[105]. ABA is measured in fluorescent signals at an excitation/emission wavelenght of 530-560/590nm[104], see Figure 18.

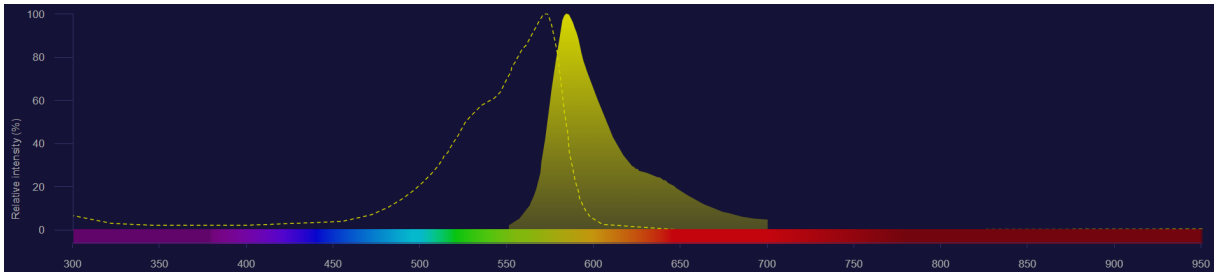

Figure 18: Emmision(solid line) and excitation(dotted line) spectra of resorufin, the fluorescent product measured in Alamar Blue Assays[105]. Excitation/emission is optimal at 530-560/590nm[104].

4.2 Goals & Hypotheses

Goals

The goals for this chapter are the following:

1. Investigate the influence of the enrichment procedure and the influence of FF on cell viability (live/dead).
2. Investigate the influence of the enrichment procedure and the influence of FF on cell metabolism.
3. Determine which live/dead stainings are best used in flowcytometry.
4. Investigate if FF have influence on the stainings next to investigating the best way of staining enriched cells.

In order to look at the influence of the enrichment procedure versus the influence of the FF themselves, multiple conditions were created: a control, a condition which was exposed to the procedure, and a condition that was exposed to the procedure with the use of FF.

A couple experiments will be done to investigate the viability of the cells will be checked. Morphology will be checked. For quantitative values, Trypan Blue staining will be applied which stains dead cells and is visible under a standard microscope. Also other Live, Apoptosis, and Dead stainings will be used and checked with flowcytometry. Multiple Live, Apoptosis, and Dead stainings will be tested to determine the optimal combination to have clearly distinguishable population, ideally a control staining, and without different subpopulations. Another important factor is to know if the FF have influence on the stainings, and what is the ideal order/protocol to stain cells to investigate FF influence.

In order to look into the metabolism, Alamar Blue Assays will be done. This will give quantitative value of metabolic activity.

Hypotheses

Since the FF do not interact with the interior of cells. We do not expect FF to impair the viability or metabolism of the cells. We can find reason to expect a slight influence of the enrichment procedure since the cells will be exposed to different pipetting and mixing steps. However, we expect these influences to be insignificant since they are part of standard manipulations performed by researchers and often done with cells.

We expect Calcein AM to be a good combination with EH or PI. However we expect more intense signal from DAPI staining, which might be interesting.

We know from previous in house experiments that FF changes the SSC plots majorly. We also know from previous in house experiments that FF change the FSC and increases background fluorescence from unstained cells. Next to that we expect that we can stain the cells by targeting different EpCAM epitopes (as we learned theoretically in Chapter 3.1 and proved in Chapter 3.4). We also expect to be able to stain the enriched cells by staining the FF. Both ways are visualized in Figure 19. However, if one of the options does not work (due to steric hindrance which is better imaginable when taking into account the sizes shown in Figure 20), it would be staining of the EpCAM after FF are attached. This will be because the body of the FF will be in the way of the EpCAM targeting fluorophore, but there will be other conjugated antibodies available which are attached to the FF body.

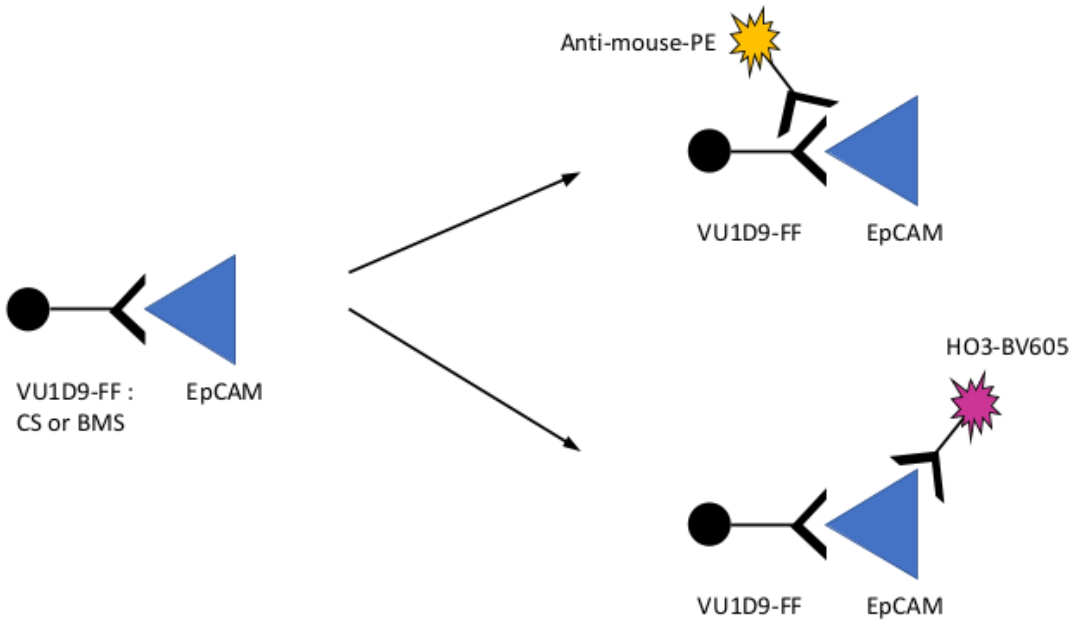

Figure 19: Off scale image of FF targeting the VU1D9 epitope of EpCAM for enrichment and different ways to visualize the enriched cells. Top: targeting the ff with fluorescent antibodies. The VU1D9 has a mouse area, this can be targeted with anti-mouse antibodies. The anti-mouse antibody can be attached to a fluorophore. Bottom: an epitope of EpCAM is targeted by an antibody focused on another epitope than the FF targets. This antibody is attached to a fluorophore, in this case resulting in HO3-BV605.

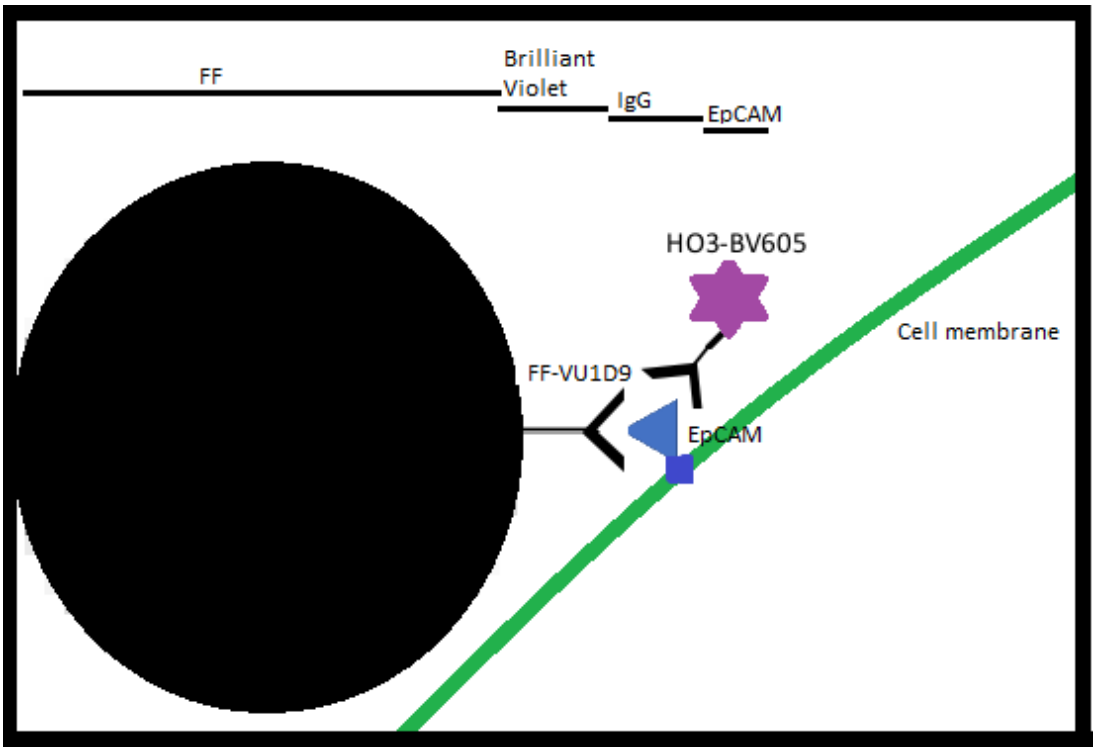

Figure 20: On scale image of antibody interaction of FF and fluorophore with EpCAM. FF might cause hindrance towards the other targeting molecules. Shapes are random. The size of the used FF is known. and the size of a IgG is known. The other sizes are estimates based upon their weight. FF: diameter = 200 nm. IgG: diameter = 10 nm[72], Weight: 150 Kdalton[72]. EpCAM: diameter = 6.2 nm, Weight = 40 Kdalton[73]. Brilliant Violet fluorophore: diameter = 13.2 nm, Weight = 340 Kdalton[71].

4.3 Materials & Methods

To achieve these goals, the following Chapter will give an overview of the used materials, followed by the different conditions that will be compared in every experiments that looks into FF influence on cells, and closed by all methods applied in the experiments to look into the FF influence on tumour cells.

4.3.1 Materials

Cell line

All experiments in this chapter have been conducted with the LNCaP cell line (see Chapter 3.3.1 for the specifics).

FF

During the current standard procedure a volume of 15 μL of Cellsearch FF was added on a total volume of 1 mL of sample. The exact concentration is unknown. While mimicking the Cellsearch system and filtering the CTCs from the DLA sample manually, a concentration of 3μg/mL of VU1D9-FF was used (Biotin VU1D9 SA BSAFF, Biomagnetic solutions, january 2020 batch, stock 0.5 mg/mL). On advise of experts, this manual procedure with a huge amount of (cancer) cells was done with 20 μg/mL which was applicable on the viability experiments which were always done with at least 100.000 cells.

Antibodies and stainings

See Table 4 for the overview of the used antibodies in this Chapter.

Table 4: All antibodies used in Chapter 4, their working concentration, their stock concentration, and their manufacturer information.

Antibody	**Working Concentration**	**Stock Concentration**	**Manufacturer**
Calcein-Am	0.005-0.125 μM	1 mM	Invitrogen eBioscience, San Diego, CA, USA
Propidium Iodine (PI)	1.5-3 μM	1.5 mM	HansaBioMed, Tallinn, Estonia
Ethidium Homodimer	4 (or 8) μM	1.17 mM	Invitrogen Life Technologies Corporation, Eugene, OR, USA
DAPI	3 μM	10.9 mM	Biolegend, Greenwood Place, UK
DAPI (Cell Search)	-	-	Immunicon, Huntingdon Valley, PA, USA
Apotracker	0.1-2.5 μM	0.08 mM	BioLegend, Greenwood Place, UK
Brilliant Violet 605 Custom Conjugation Clone HO-3-19	2.25 μg/mL	0.45 mg/mL	BioLegend, Greenwood Place, UK
anti-mouse PE IgG whole molecule R phycoerythrin antibody produced in goat	1-10 μg/mL	1 mg/mL	SigmaAldrich, Saint Louis, MO, USA

4.3.2 Conditions

After trypsinization with 0.05% trypsin of the LNCaP cells in culture, the following 3 different main conditions were created and used in all experiments:

1. *Cells.* This condition functioned as the control, these are just cells. Nothing was done with this condition during the incubation and separation process and this condition was held under the same

circumstances as the other conditions. Which means that they were put into a FACS tube and kept in the fumehood for the duration of this part of the experiments.

2. *Magnet.* These are cells which were put in a FACS tube which was put against the magnet. The same mixing procedures were done with this condition in order to identify if the mixing has a significant influence on the viability of the cells. Furthermore, if this condition showed divergent results compared to the control condition with only cells, it could be used without mixing in order to identify if the magnet has influence on the cell viability.

3. *FF.* These were cells with added FF. A concentration of 20 μg/mL was added to the cells. After this the standard protocol for incubation and separation was followed (see appendix 8.14).

These 3 conditions were used for all experiments that look into the influence of FF on tumour cells.

4.3.3 Morphology

We check on morphological differences while culturing with a standard microscope. We cultured the cells of the 3 conditions mentioned above and checked for morphological differences of the cells. Factors that were looked into were if there were visual differences for the eye in the size of cells, the growth pattern (clusters or single cells), the cell structure (intact membranes, shape of the cells). When looking into the adhesion abilities of the cells in enriched samples, we counted spread out cells as bound and circle like cells as not bound. The percentage of cells in those conditions was determined.

Looking into morphological changes was not an experiment on itself, but was routinely done before any of the other experiments that look into the influence of FF on tumour cells.

4.3.4 Trypan Blue

A total of 5 experiments were conducted in which viability was looked into by use of Trypan Blue staining.

After following the standard protocol for incubation and separation, the Trypan Blue measurement were done. After mixing the cells again, 10 μL of cellsuspension was mixed with 10 μL of trypan blue solution, this was done in duplo. This cell suspension was analysed by the LUNA cell counter using the same protocol for cell recognition as being used for cell counting when culturing the cells. The only difference was that the mode for recognizing trypan blue staining was switched on. Which means that all cells which stain blue were recognized as dead cells.

4.3.5 Alamar Blue assay

A total of 9 experiments were conducted in which metabolism was looked into by use of ABA. The first 6 were used to optimize the method, after which there were 3 last repeat experiments done in order to get the data.

The ABA followed directly after doing the Trypan Blue experiments, the same conditions were continued for ABA. These conditions were in principal seeded in duplo in the following densities; 5k, 10k, and 20k cells/cm^2. Sometimes there was a slight deviation from these values which will be adjusted for. Seeding was always done in a tissue culture 24 wells plate. Next to that there was always a zero control with just medium, like the producer instructs[106], which value can be substracted from the fluorescence values of the experiment wells. Also a condition in which the cells would be killed with MilliQ functioned as control, no activity should be seen here. Cells were incubated for 24 hours, after which 2 hours of

incubation with the ABA solution followed. 300 μL of ABA solution was used per well which consisted of 270 μL medium and 30 μL Alamar Blue Reagent Solution 10X. After those 2 hours, the ABA solution from 1 well of a 24 wells plate was put in 2 wells from a black 96 wells plate, 100 μL each. Then they were analysed using the Multimode Plate Reader Victor X3 from PerkinElmer using a standard ABA protocol of the MCBP group, excitation of the CW-lamp filter F555/38 and emission with filter F600/10. The value of the 'only medium' condition was extracted from the other found values, seeing this as background noise. Then the highest seeding conditions of 'Cells' was chosen as reference point, after which all values were taken relative to this point. This made comparison between experiments possible.

4.3.6 Live/Dead staining

Live/Dead staining concentrations

A concentration of 5-125 nM was tested for Calcein-AM. PI was tested for 1.5-3 μM. EH was used with 4 μM (also 8 μM was tested), the protocol of the manufacturer recommends between 0.1 and 10 μM[107]. DAPI staining was initially used in 3 μM but then was switched to 10 μL of Cellsearch DAPI solution on 1 mL of cells in PBS (final concentration unknown). In order to investigate the number of apoptotic cells, the staining Apotracker was used. A concentration of Apotracker of 0.1-2.5 μM was tested. See Table 4 for an overview of the antibodies.

Enriched cells and staining conditions

Investigating the best staining procedure/order and if targeting the FF used for enrichment with staining is possible was done with HO3-BV605 to stain EpCAM of the cells and anti-mouse PE to stain the FF (see Table 4. The following conditions were compared with use of fluorescence microscopy and flowcytometry.

1. Stain FF first, then enrich cells with FF.
2. Enrich cells first with FF, then stain FF.
3. Stain cells first, then enrich cells with FF.
4. Enrich cells first with FF, then stain cells.
5. Enrich cells first with FF, then stain both cells and FF (in both orders and simultaneous).
6. Stain FF first and cells first but separately, Then enrich cells with FF.

Flowcytometer

Stainings were performed on the cells from the LNCAP cell line with the before mentioned conditions in chapter 4.3.2. After testing with multiple staining agents, DAPI and Ethidium homodimer were chosen for a longer series of measurements since they were the most stable. Note that all other stainings showed the same results (differences between conditions) just less recognisable, overlapping, or more than 2 population for one staining (probably depending on the state of apoptosis). There were four staining variations that were continuously tested:

1. DAPI-, EH-
2. DAPI+, EH-
3. DAPI-, EH+
4. DAPI+, EH+

For the detection of EH+ cells the 488-585/42 filter was used. For detection of DAPI+ cells the 375-450/40 cell was used. The settings of the flowcytometer for the final 3 experiments were as follows:

1. FSC: 100V
2. SSC: 250V
3. 488-585/42: 290V
4. 375-450/40: 250V
5. amplitude: 15
6. frequency: 25
7. gap: 12
8. flow rate: 3.0

These settings gave the best recognisable results.

Then, a gate was set to filter out cell debris and other smaller non cell particles. This gate cut off an edge off the FSC/SSC plot at the lower values. Then, based on a non stained sample of Cells enriched with FF(the most fluorescent sample without staining) and the previous set gate to filter out cell debris, the gates were set for EH+ and DAPI+ cells. An extra gate was necessary to filter out FF or the threshold needs te be raised till they are not visible.

The positive control was a condition that was killed in order to see if the stainings worked. This was done with mixing 1 on 1 with 70% ethanol and performed for every repeat of the experiment.

For experiments of the ideal staining order with enriched samples the following filters were used: for HO3-BV605 the 375-605/20 filter, and for PE anti-mouse the 488-585/42 filter. The settings were chosen per repeated experiment and are noted next to the figures.

4.3.7 Statistical Analysis

In order to determine significance between groups, an Analysis of Variance (ANOVA) was carried out. We assume there were only normal distributions. The one-way ANOVA was followed by testing for pairwise differences in a post-hoc test. The post-hoc test that was used was the Tukey method. The Dunnett method seems interesting but we are also interested in differences between the conditions that are not the control group since that will give us information of the influence of the procedure and the FF. Especially T-tests on all pairs but also the Scheffee tests were not done because of the higher Alpha inflation. Newman-Keuls is subject to type 1 errors (just like t-tests) and was therefore not used.[108]

The results that followed from the experiments and analysis will be discussed in the next chapter.

4.4 Results

4.4.1 Viability of cells

Viability was determined with flowcytometry and with a cell counter. Flowcytometry proved to be most reliable and was studied most thoroughly. ***Flowcytometer***

In a serie of 20 experiments, all experiments showed higher percentage of dead cells in the conditions containing FF compared to the control without FF and compared to the condition with magnet exposure without FF, however not always significant. In the final 3 experiments significant difference was shown with DAPI staining between the 'Cells' and 'Cells enriched by use of FF' ($P<0.05$). Also significant difference was shown between the 'Cells exposed to the magnet' and 'Cells enriched by use of FF' ($P<0.05$). No significant difference was seen when looking at the EH results($P>0.05$). see Figure 21 for a depiction of the averages for the DAPI staining results. See Appendix 8.24 Figure 80 for an extensive overview of both DAPI and EH measurements without averaging conditions. EH staining did not show total staining of the population when the whole population was killed whereas DAPI did stain the majority of the population, see Appendix 8.16. An example of the results from the flowcytometer can be seen in Appendix 8.15.

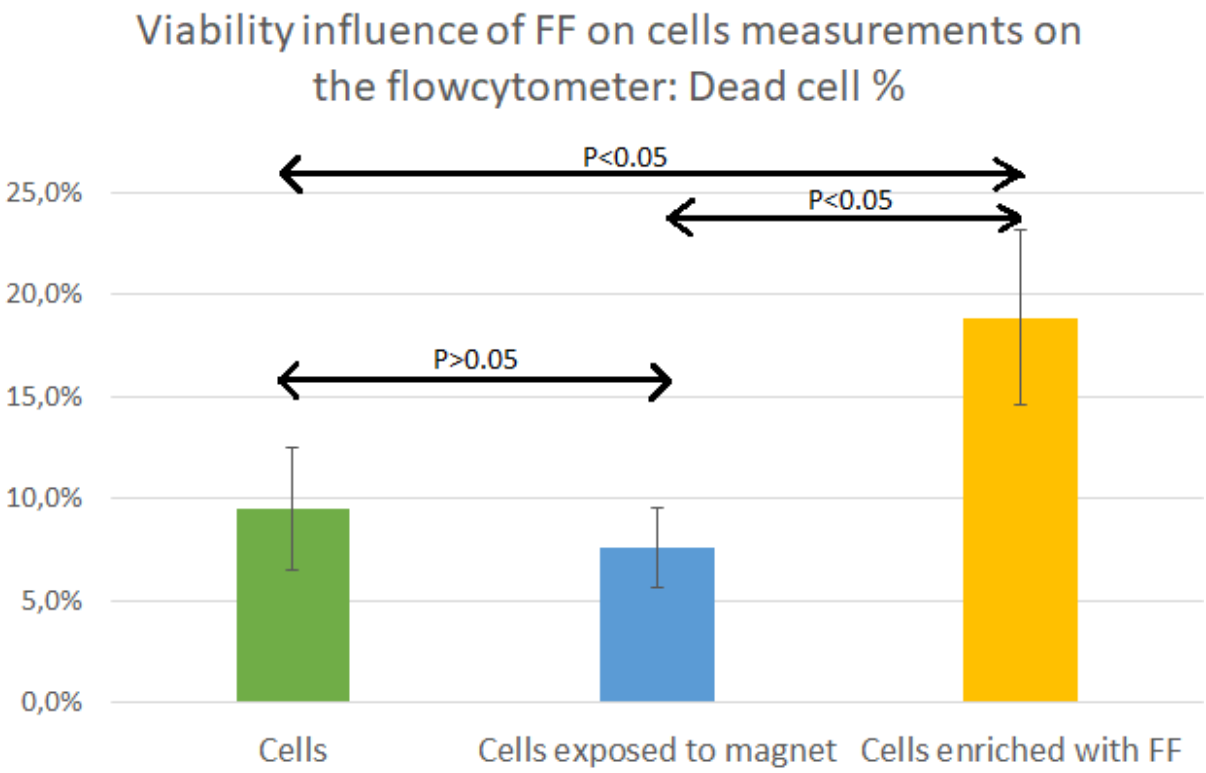

Figure 21: Flowcytometer measurements of cell dead levels and their standard deviation measured by DAPI. FF do cause cell dead. Significant difference was shown between the 'Cells' and 'Cells enriched by use of FF' ($P<0.05$). Also significant difference was shown between the 'Cells exposed to the magnet' and 'Cells enriched by use of FF' ($P<0.05$).

Flowcytometry gave clear results, FF do influence viability. The other method for determining viability was using the Luna Cell Counter and Trypan Blue staining.

Trypan Blue

In the Trypan Blue measurements there was a significant difference between the 'Cells' and 'Cells enriched by use of FF' condition (P=0.02019, P<0.05). This indicates that the use of FF had an effect on LNCaP cell viability. There were also slight differences between the 'Cells exposed to magnet' and the other 2 conditions, however not significant (both P>0.05). The conditions 'Cells', 'Cells exposed to magnet', and 'Cells enriched by use of FF' had respectively 88,2, 80,7, and 69,9% of viable cells. However, after analysing the sample by microscope, it was seen that a lot of questionable spots were coloured with the dye. These spots did not look like cells, or were only small part of what were ones cells. Which were however all counted as dead cells.

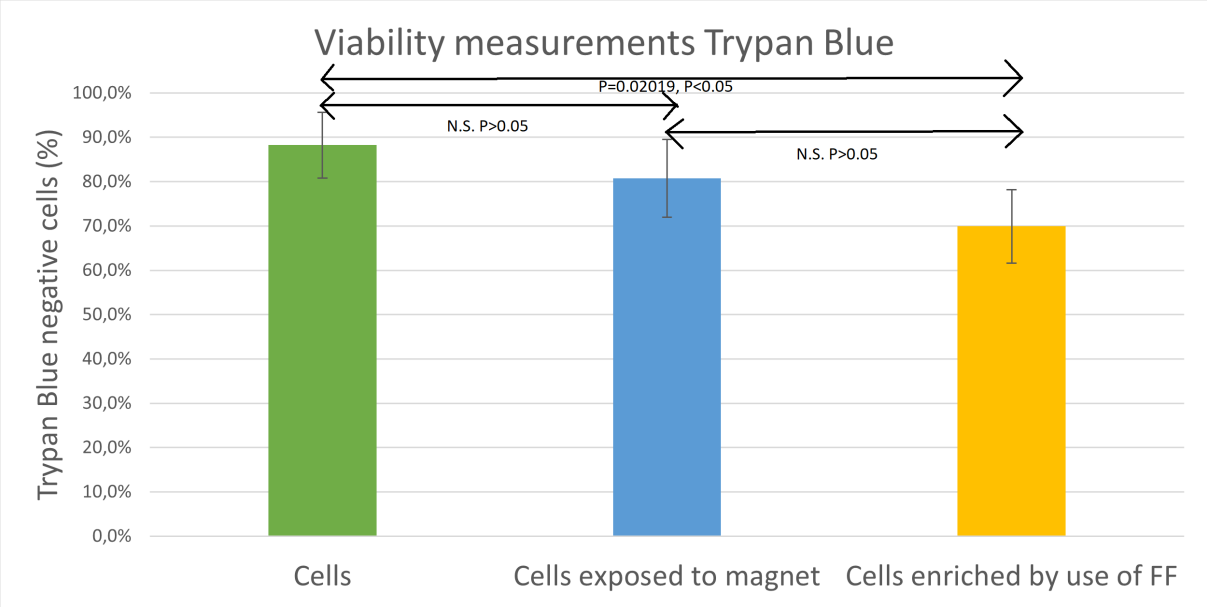

Figure 22: Trypan Blue measurements and their standard deviation. There was a clear difference between the 'Cells' and 'Cells enriched by use of FF' condition (P=0.02019, P<0.05). There were also slight differences between the 'Cells exposed to magnet' and the other 2 conditions, however not significant (both P>0.05). The conditions 'Cells', 'Cells exposed to magnet', and 'Cells enriched by use of FF' had respectively 88,2, 80,7, and 69,9% of life cells.

These were the live/dead staining that were chosen to be used in our experiments. There were others trackers which we did not use for varying reasons.

Other Live/Apotracker/Dead stainings

The best **Apotracker** concentration was hard to determine, very minimalistic subpopulations were seen when using 200nM in the first experiment, but the first recognisable peaks in the histograms became visible around 250nM in a second experiment with different concentrations. However, it was not of a intensity that we deemed it useful compared to other available dyes.

When using **Calcein-AM** there were often more subgroups found which both stained positive for Calcein-AM, see Figure 68 in Appendix 8.17. Therefore Calcein AM was not further used.

PI gave very lower intensity signal than EH when compared at their manufacturers standard concentration, see Figure 69 in Appendix 8.17.

Even though the results were not for all markers as obvious. Enriched cells do seem to have lower viability, of interest is now if that lower viability is also translated into lower metabolic activity.

4.4.2 Metabolic activity

Alamar Blue Assay

Relative metabolic activity of the conditions of Cells, Cells exposed to the magnet, and cells enriched by use of FF have a respective relative metabolic activity of 111,6, 110,6 and 99,5%. This is relative to the highest seeded density of untreated cells. The relative activity of all densities were taken together for each one of the 3 conditions. 9 experiments have been conducted to optimize the protocol and learn the necessary skills. These are the last 3 experiments. The conditions are not significantly different from each other (P=0.52549, p>0.05). The standard deviation of 'Cells exposed to the magnet' overlaps slightly with the standard deviation of the condition 'Cells enriched by use of FF'. See Figure 23 for an overview of this, and Figure 70 in Appendix 8.18 for a zoomed in version at the peaks.

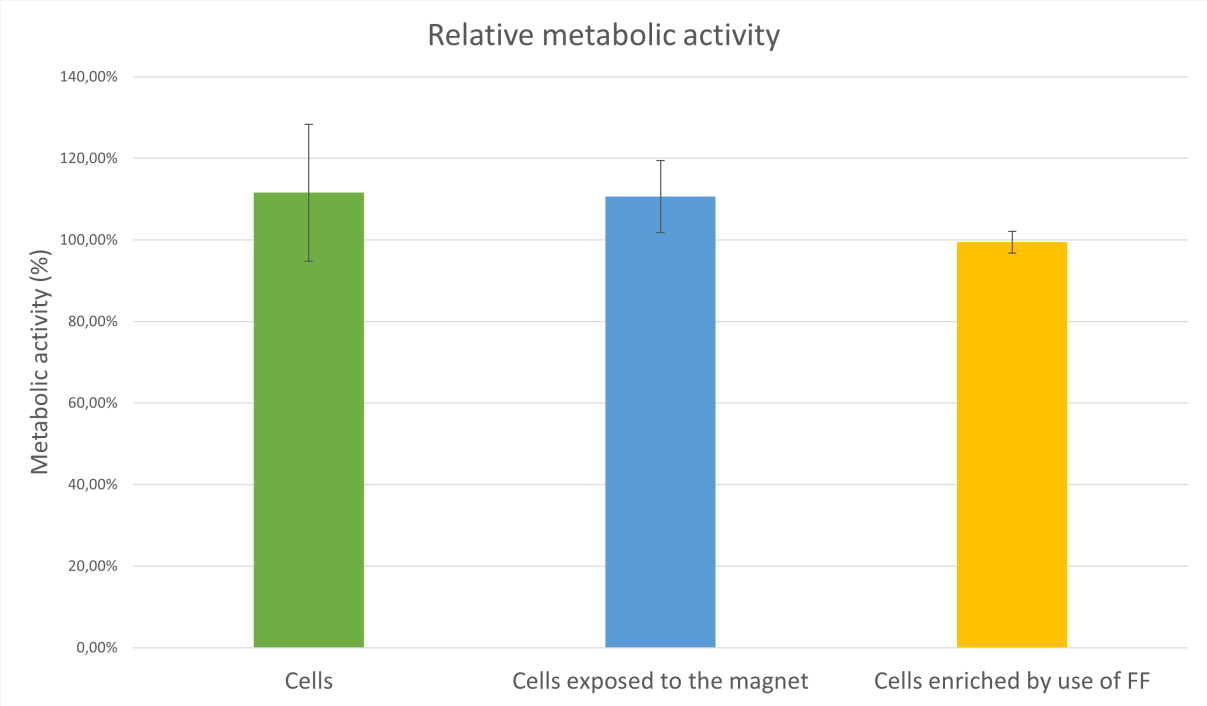

Figure 23: Relative metabolic activity of the conditions of Cells(green), Cells exposed to the magnet(blue), and cells enriched by use of FF(yellow) and their standard deviation. They have a respective relative metabolic activity of 111,6, 110,6 and 99,5%. This is relative to the highest seeded density of untreated cells. All relative densities were taken together for each one of the 3 conditions. These are the last 3 experiments, after the protocol was optimized and the procedure was well under control. The conditions are not significantly different from each other (P=0.52549, p>0.05).

Since slight differences could be seen, we tried to eliminate more uncertain factors. Another part of the calculation was eliminated. The multiplying of lower seeded densities to make them comparable with higher seeded densities was eliminated. Then, when mapping the higher seeded densities, all standard deviation shrank. However, also the averages were closer together. The difference between conditions was even less significant (P=0.721358, P>0.05). See Figure 24 for an overview of this, and Figure 71 in Appendix 8.18 for a zoomed in version at the peaks.

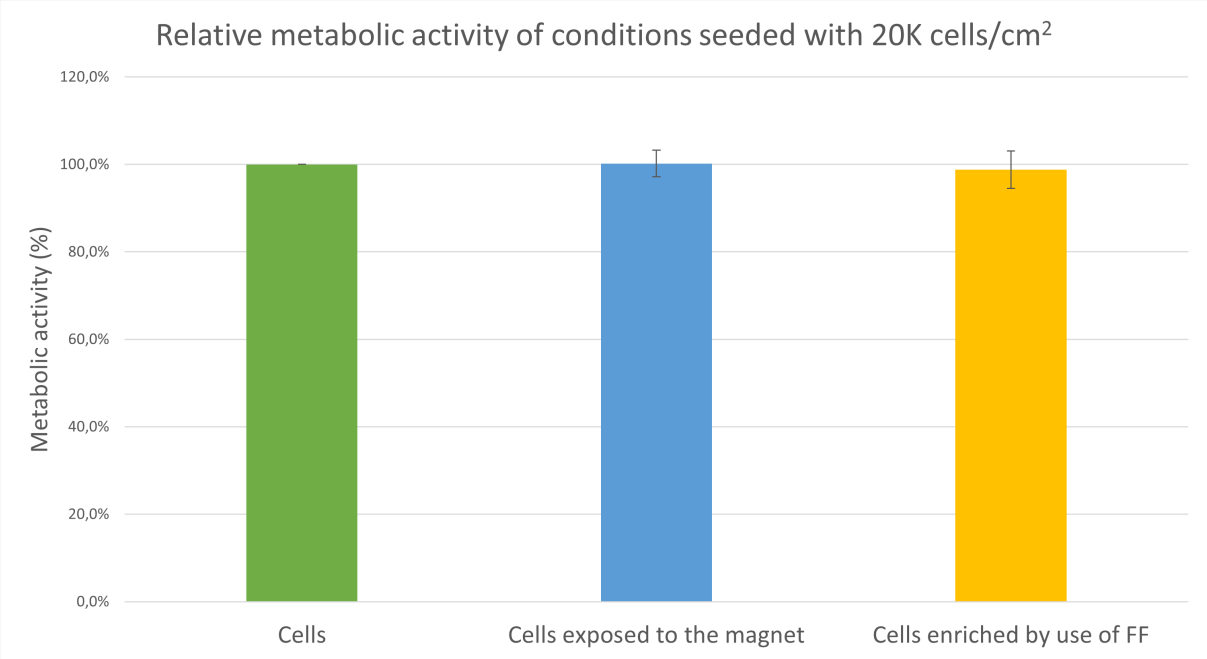

Figure 24: Only relative metabolic activity of conditions seeded with 20K cells/cm^2 are taken into account and their standard deviation. Cells(green), Cells exposed to the magnet(blue), and cells enriched by use of FF(yellow) have a respective relative metabolic activity of 100.0, 100.2 and 98.8%. This is relative to the highest seeded density of untreated cells, which is the 20K cells/cm^2 conditions(therefore it was set in every experiment as 100%). The difference between conditions was even less significant (P=0.721358, P>0.05).

Metabolic activity did not seem to be influenced, which was curious especially because viability seemed to be influenced. Next to looking at the influence of enrichment on the cells, some experiments were done in preparation of the next Chapter, in which enrichment with FF needs to go hand in hand with staining of cells.

4.4.3 FF and staining

We learned 4 valuable lessons from experimenting with FF, Cells, FF staining, and Cell staining.

Filter out FF

In order to measure cells, we have to filter out the free FF. This can be done by setting gates, see Figure 25.

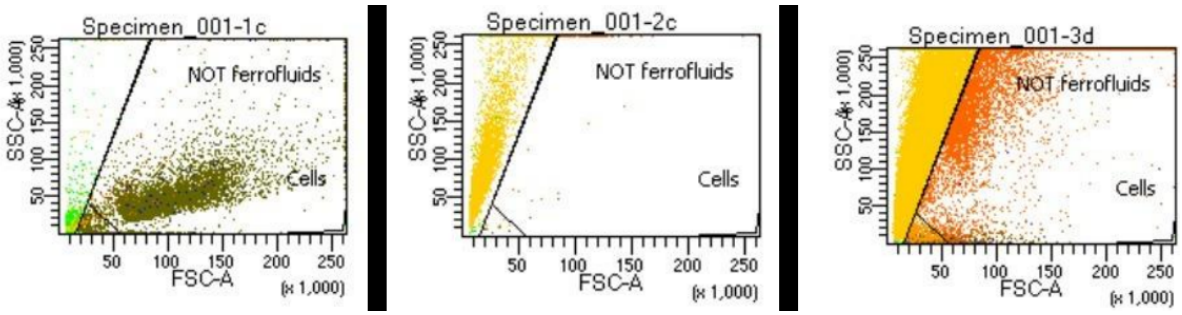

Figure 25: Flowcytometer results of a condition with only cell (left), only FF (middle), and enriched cells (right).

FF increase background fluorescence

When FF attach to cells their fluorescence increases. Gates have to be set in such a way that this should not be noticed. However, it is noteworthy that the populations were clearly distinguishable. That means that we were not measuring the increased background fluorescence. See Figure 26.

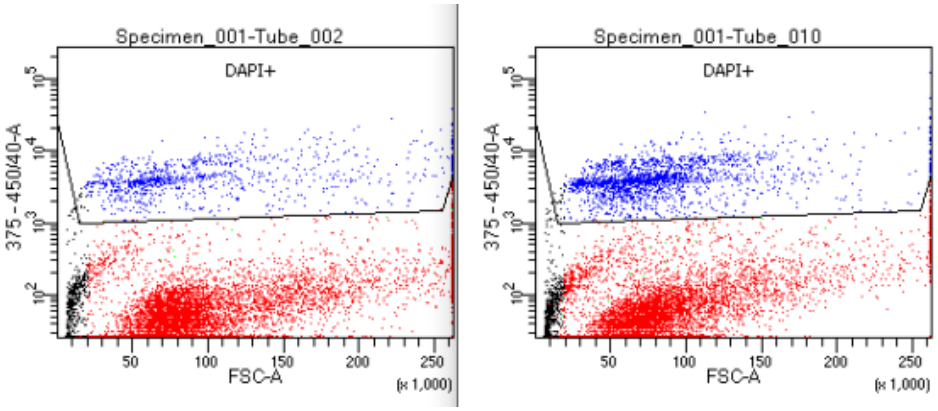

Figure 26: Flowcytometer measurements of cell dead levels measured for DAPI staining. Left. 'Cells' with DAPI staining. Right. 'Cells enriched by use of FF' with DAPI staining. Both show that what is gated is indeed a subpopulation and that background does not influence this.

FF bind to antibodies targeting the cells

Cell staining that is added, is caught or binds to the FF. When adding HO-3-BV605 staining to a sample with only FF, 17.4% of FF were detected as positive, see Figure 27 and see Appendix 8.19 Figure 72. Moreover, when also adding FF staining (PE anti-mouse) to the mix, 46.8% of FF stained positive for HO3-BV605, see Appendix 8.19 Figure 73. This could be prevented in 2 different ways. First, by staining the cells before adding FF, however that is undesirable for the endgoal as well as for viability studies with live/dead stainings. Secondly, FF needs to be filtered out for flowcytometric analysis. That is doable, however if stainings are added the SSC and FSC of the cells change drastically which should be taken into account.

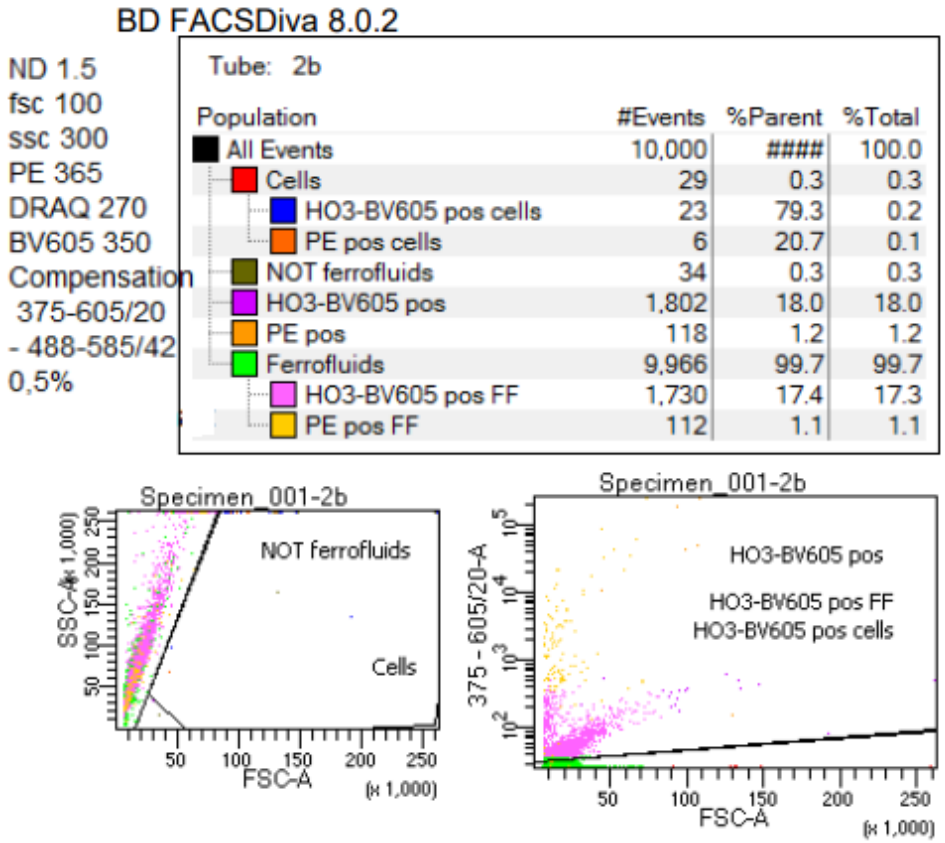

Figure 27: Flowcytometer results of FF mixed with HO3-BV605 which stains EpCAM at cells. 17.4% of FF was stained positive for HO3-BV605. HO3-BV605 was measured with the 375-605/20 filter and results are depicted in the graph at the right bottom. The graph at the left bottom shows the FSC vs. SSC and the gates set to differentiate between cells and FF.

Staining FF is more reliable than staining cells

Staining FF with PE anti-mouse is more reliable than staining cells with HO3-BV605, especially after enrichment. Staining enriched cells with HO3-BV605 worked and 82.6% of cells stain positive, see Figure 28 and Appendix 8.19 Figure 74. Staining enriched cells with PE anti-mouse worked and 95.9% of cells stain positive, see Figure 29 and Appendix 8.19 Figure 75.

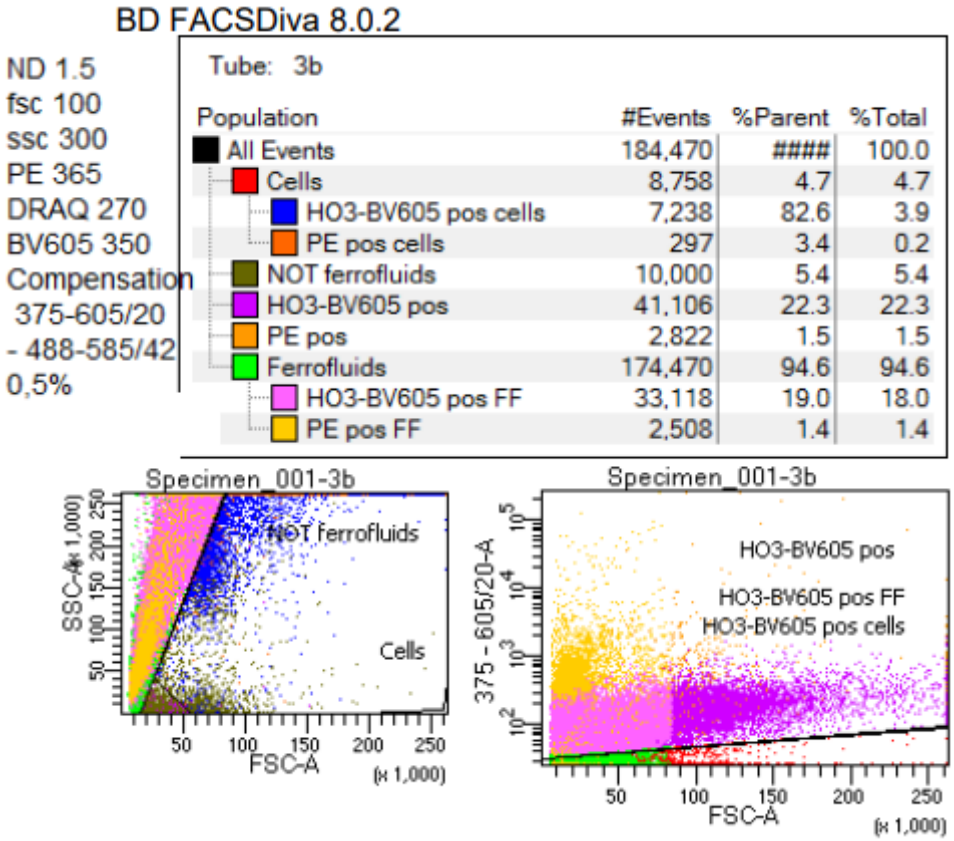

Figure 28: Flowcytometer results of cells enriched with FF. Then mixed with HO3-BV605 which stains EpCAM at cells. 82.6% of cells was stained positive for HO3-BV605. HO3-BV605 was measured with the 375-605/20 filter and results are depicted in the graph at the right bottom. The graph at the left top shows the FSC vs. SSC and the gates set to differentiate between cells and FF.

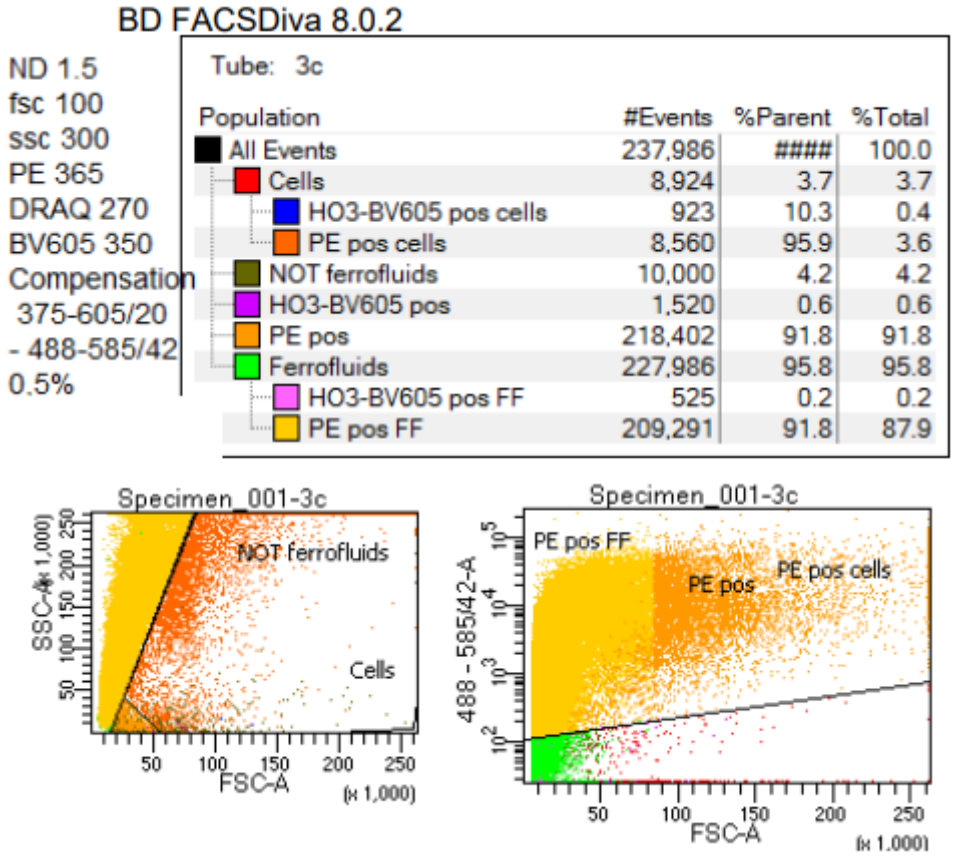

Figure 29: Flowcytometer results of cells enriched with FF. Then mixed with PE anti-mouse which stains the FF. 95.9% of cells was stained positive for PE anti-mouse. PE anti-Mouse was measured with 488-585/42. The graph at the left top shows the FSC vs. SSC and the gates set to differentiate between cells and FF.

4.5 Conclusion & Discussion

4.5.1 FF do cause extra cell death

Flowcytometer

Conclusion:

DAPI staining seemed to work best and showed a significant difference in cell death percentages between the condition involving FF and the conditions with just cells (exposed and non-exposed to the magnet and the procedure).

Discussion:

EH staining did not show total staining of the population when the whole population was killed whereas DAPI did stain the majority of the population, see Appendix 8.16. Even though the concentration of EH can stain part of the now bigger number of dead cells, this might indicate that when working with a higher concentration of cells also a higher working concentration should be used. Another explanation could be that the ethanol (partly) fixed the cells. EH is incompatible with fixed cells, it 'does not bind to any cellular components after fixation'[109]. Therefore, EH might not have stained all dead cells. In that case another way of killing the cells should be practiced, for example killing the cells with milli Q as is done in the ABA experiments.

Another viability staining had a noteworthy phenomenon. The extra subgroups found when using Calcein-AM can be explained due to that Calcein-AM is also used as a marker for apoptosis with a sharp increase in intensity before a decline[93] and this might indicate cells that are not dead yet but in the process of cell death. The subpopulations might also be explained by possible attachment of cells to each other and it being the signal of 2 cells at the same time.

Trypan Blue

Conclusion:

Trypan blue shows that FF influence the viability of the cells, a reduction of 18.3% was seen when cells were enriched with the FF.

Discussion:

Results varied between the same condition with sometimes outliers of 50% difference. With the microscope it was seen that a lot of spots were coloured with the dye, which did not look like cells or were only small part of what once were cells. These were however all counted as dead cells. Therefore analysis with the use of Trypan Blue was stopped and more focus came on the results from the flowcytometer and the ABA.

4.5.2 FF do not impede metabolic activity

Conclusion:

No significant difference between metabolic activity was seen between 'Cells' and 'Cells exposed to the magnet' in which we looked at the influence of the magnet and the procedure steps without using FF. We do see a tendency towards a little less metabolic activity in cells which were enriched using FF. However when we focus on the results of the highest density(20K cells/cm^2), which are the most reliable and repeatable, we also do not see a significant difference here.

Discussion:
We can't say much about the influence of the seeding density at the metabolic activity because the result got harder to repeat with lower densities. Likely due to the bigger influence of counting errors when determining the number of cells to be put in a conditions. Also other possible influences are increased due to smaller number of cells we work with.

We notice a significantly increased cell death of 8.8% and 18.3% by flowcytometry and trypan blue staining, respectivily. Therefore, the insignificantly decreased metabolic activity of 12.1% could be seen as another indicator of this cell dead but simply with not enough statistical power. More research should be welcomed. On another note, we hypothesize that when a significant difference will be seen this will likely not be because a cell enriched by use of FF is lower metabolically active. It will likely be the overall decreased metabolic activity because of the cell dead of a certain part of the cells.

4.5.3 Future research

An interesting topic for future research would be to look into which characteristics of the FF cause the decreased viability. Moreover, how we can chance these characteristics such that production of FF that do not influence viability is possible. We know it is not the handling of the samples during the procedure or exposure to a magnetic field. Some examples of matters that could be looked into are: the type of FF, the size of the FF, the binding spot of the FF, the concentration of the FF, and the force of the magnetic attraction during enrichment.

There are other promising ways to determine cell viability which are not discovered in this report. These methods can be very beneficial for more detailed insights in cell behaviour.

Mitochondrial activity
Another way to put a number on viability besides measuring the metabolic activity, is measuring the mitochondrial activity. This will not be done in our research but if a broader view of the viability of cells is wanted, extra measurements of mitochondrial activity might give more insightfull information.

Lactate dehydrogenase (LDH)
Another possible method is based on an enzyme of the matrix of the cytoplasms, the cytosolic enzyme named lactate dehydrogenase (LDH). It is rapidly released in the surroundings when there is damage to the plasma membrane[110, 111]. LDH can be measured extracellular and this protein is released when cells die due to apoptosis(or necrosis)[110], which occurs often in CTCs. Especially because it is hard to determine if a caught cell secreted a certain product or released already internally present proteins due to cell death. With negative LDH we will know that proteins are secreted, while positive LDH will mean that due to an already apoptotic state, proteins can already freely exit a cell. Quantification of extracellular LDH can be done by an coupled enzymatic reaction in which LDH functions as catalyser; the conversion of lactate to pyruvate via NAD+ reduction to NADH[110]. Then this NADH can be used in the formation of a fluorescent product[111]. For example, NADH is used in formation of a red formazan product, which is directly proportional to the released LDH amount[110] and thereby the number of dead or damaged cells[111]. Formazan can be best measured at a wavelenght of 492nm[111].

All in all, we now know that FF do decrease cell viability. However not in such a degree that a sample of CTCs is not useful anymore. The larger part keeps being viable. We also learned that metabolism does

not change, therefore the planned experiments in which we look into the PSA secretion are still very much of use.

5 Detection of PSA secretion from single tumour cells and the influence of ferrofluids

In the previous chapter we have looked into the influence of FF on the viability and the metabolism of tumour cells. In this Chapter we will lay the basis to investigate the influence of FF on the secretion of single cells by use of a self seeding microwell. We will also try to look into single cell secretion of CTCs found in DLA samples from PCa patients.

5.1 Theoretical Background

Here the techniques and principles where the research is based upon will be discussed. The enrichment procedure is already explained in Chapter 4.1.1. There it was not important to be able to differentiate between tumour cells and blood cells. In this chapter more complex samples will be used where other cells will also be present in abundance. Therefore, being able to differentiate between tumour cells and blood cells is of utmost importance.

5.1.1 Biomarkers

There were different kinds of biomarkers of interest for this research. For the selection of tumour cells, we looked into two prominent surface markers. The first marker was EpCAM, which is thoroughly discussed in Chapter 3.1.2. The other surface protein target of tumour cells was PSMA.

Prostate-specific membrane antigen (PSMA)

Prostate-specific membrane antigen (PSMA), also known as glutamate carboxypeptidase II when found in the central nervous system (CNS)[112], is a type II transmembrane glycoprotein[113, 114] which is a transmembrane protein with N_{in}-C_{out} ends[115]. The internal portion exists of 19 amino acids, the transmembrane portion of 24 amino acids, and the external portion is by far the largest with 707 amino acids[113] which gives possibilities to attach (multiple) antibodies without passing the cell membrane. PSMA exhibits enzymatic function and acts as glutamate preferring carboxypeptidase, however the impact of this remains unclear in cancers[113], although it is hypothesised and researched if that is stimulates angiogenisis[112]. Next to the prostate gland and specifically the apical epithelium of secretaory ducts, PSMA is naturally found in lacrimal and salivary glands, proximal renal tubules, epididymis, the ovary, the luminal side of the ileum-jejunum and astrocytes in the CNS[116].

PSMA is expressed on multiple sorts of cancers, like bladder carcinoma[112], schwannona[112], renal tumours[117], but especially on prostate cancers(where it is named after)[112, 116, 118, 119] and correlated with the aggressiveness of the tumor[120, 121]. In the phase of gaining androgen independence of prostate cancers, the PSMA expression is majorly upregulated and migrated to the plasma membrane[116]. The cell line that we use most in this thesis is the LNCaP cell line with 96.7% of its cells expressing PSMA[122].

PSMA is often used in the oncology and there are plenty of diagnostic and therapeutic trials going on. Radiopharmaceutical therapy has already been tested in clinical trials. Radio-immunoconjugate anti PSMA monoclonal antibody 7E11 is even already commercially available and FDA approved for diagnostics[113]. This is called the ProstaScintő (Cytogen Corporation, Princeton, NJ) scan. It also showed it use for other cancers beside prostate cancer[113]. Employing radionuclides which emit high energetic alpha particles, which are therefore cytotoxic, have been attached to monoclonal antibodies

that target PSMA[119]. This is called alpha therapy[119]. Radiotracers that target PSMA also seem to be effective in detection of prostate cancer with a focus on low PSA levels[118]. A recent study names Lutetium PSMA tracers as most promising radionuclide therapy, specifically ^{177}LU-PSMA-617[123]. A metastudy showed that there are more than 33 studies using GA-PSMA11 (Ga-HBED-CC) with positron emission tomography with a detection rate of 70.2%[118]. However radiopharmaceutical therapy has some non responders. For this a non-radioactive prodrug SBPD-1, a small molecule PSMA targeting moiety with a cancer-selective cleavable linker and microtubule inhibitor monomethyl auristatin E has been developed with high binding affinity to PSMA and selective cytotoxicity[120]. Other approaches are involving artificial T cell receptors that target PSMA which showed no cytotoxic effect on non-PSMA cells[124].

PSMA and EpCAM are well established membrane biomarkers for tumour cells. However in order to differentiate between the cells in DLA samples, also the blood cells needed to be stained. A surface biomarker which is present in almost all blood cells was used for that: CD45.

Protein tyrosine phosphatase receptor type C (PTPRC/CD45)

Protein Tyrosine Phosphatase Receptor Type C (PTPRC) is also known as Cluster of Differentiation 45 antigen (CD45) or Leukocyte Common Antigen and a member of the protein tyrosine phosphatase (PTP) family[125]. PTPRC is a transmembrane glycoprotein type I[126, 127] and present on the cell surface[127]. It exists of 2 domains, a transmembrane and an extracellular domain[127]. It is a large molecule of 180-220 KDa and takes up 5-10% of all glycoproteins B- and T-lymphocyte surfaces[128]. It is present on all nucleated, differentiated, hematopoietic, cells[126, 127]. It is also reported in peripheral blood insulin-producing cells (PB-IPC)[129].

PTPs are signalling molecules involved with cell growth, differentiation, mitosis, and oncogenic transformation[125]. PTPRC is a regulator of T- and B-Cell antigen receptor signalling[127] and has a role in innate immune cell recognition[130]. It also functions as a regulator of cytokine receptor signalling by suppressing Janus Kinase (JAK)[125, 128] and thereby plays a role in cytokine production[130]. CD45 is also involved in T-Cell/Macrophage interaction[131]. It may upregulate cytotoxic T-lymphocyte-associated protein 4 and the induction of T-cell tolerance[131].

CD45 plays a role in immune cell signaling which resulted into clinical interest in organ transplantation, autoimmune disease treatment, and Alzheimer disease associated microglial activation[128, 127]. Furthermore, CD45 antibody radioimmunotherapy is used in marrow transplantation for myeloablation[132], and CD45-positive leukemia treatment[133]. CD45 has also been marked as biomarker to indicate positive treatment response of patients with rheumatoid arthritis[134, 135].

Now that we know which markers can be used to differentiate between tumour cells and blood cells, we can focus on the secretion observations. The most well known PCa biomarker was used for this: PSA.

Prostate specific antigen (PSA)

Prostate specific antigen (PSA), also known as human kallikrein 3, is a 33-kDA serine protease[136] primarily produced in the prostate epithelium by the acinar and ductal cells[137]. It is also produced in the male periurethral glands[137]. PSA is production will in general increase during lifetime and is increased by patients with hyperplastic and neoplastic prostate tissue, is it most prominently present in the transition zone of BPH patients[2]. PSA is dependent on hormones, it is positively androgen regulated[138].

This serine protease plays a part in cleaving semenogeleins in the seminal coagulum[139]. There is no significant source of serum PSA outside of the prostatic ducts[138]. PSA itself isn't secreted into the prostatic ducts, the inactive version (proPSA) is. proPSA is then cleaved in PSA, however in patients with prostate cancer this mechanism is less efficient to different degrees. Next to that, PSA that enters circulation is bound by protease inhibitors unless they are proteolytic inactivated. Also proteolytic inactivation is induced in prostate cancer patients.[138] That might explain the lower expression of prostate cancer cells compared to normal prostate cells which is found in extracted tissue form patients[140, 141], altough certain mutation like the P53 mutation upregulate PSA secretion in prostate cancer[142]. However, increased PSA levels are a well known marker for increased risk at prostate cancer. The exact mechanism that causes this is much debated. A theory is that much more of the PSA, in different forms, enters the blood circulation due to the disruption of the glandular structures[138]. Mainly the lack of basal cells and basement membrane[138]. Also the increased size of the prostate likely causes higher PSA levels in the blood due to its volume, and the volume is also an indicator of more risk at prostate cancer. PSA might also play a role in cell migration since it is able to cleave extracellular matrix proteins, examples are fibronectin[139] and laminin[143]. Blocking PSA activity in vitro resulted in less invasive LNCaPs[143].

All in all, PSA is the most researched PCa biomarker and can be used to study the secretion of single cells. But in order to look into single cells, cells needed to be isolated first.

5.1.2 Self-seeding microwell chip

When cells can be isolated to individual cells, we can use the above mentioned biomarkers attached to fluorophores for staining in order to identify CTCs. Because of isolation they will also be easily available to take out for further testing/culturing/or analysis. Isolation will be achieved with the self seeding microwell chip from VYCAP. The self seeding microwell chip has 6400 individual microwells. Every well has a small pore at the bottom which allows flow through the chip, see Figure 30A. The moment a cell 'sits' on the pore, the flow through that particular well stops and a cell is isolated, see Figure 30C. See Figure 30B for a picture of a chip. The used pore size is 5um. In order to have flow, a small pressure difference should be established. Around 10mbar will be sufficient and was deemed to still keep the cells alive. The flow will be around 1mL/min but decrease linear with the percentage of blocked pores. The capture efficiency with this chip is already tested for 2 of the cell lines we are interested in, namely the LNCaP and PC-3 cell line with a capture efficiency respectively 58% and 71%. [144] Then, when cells are isolated from each other, secretion needs to be captured.

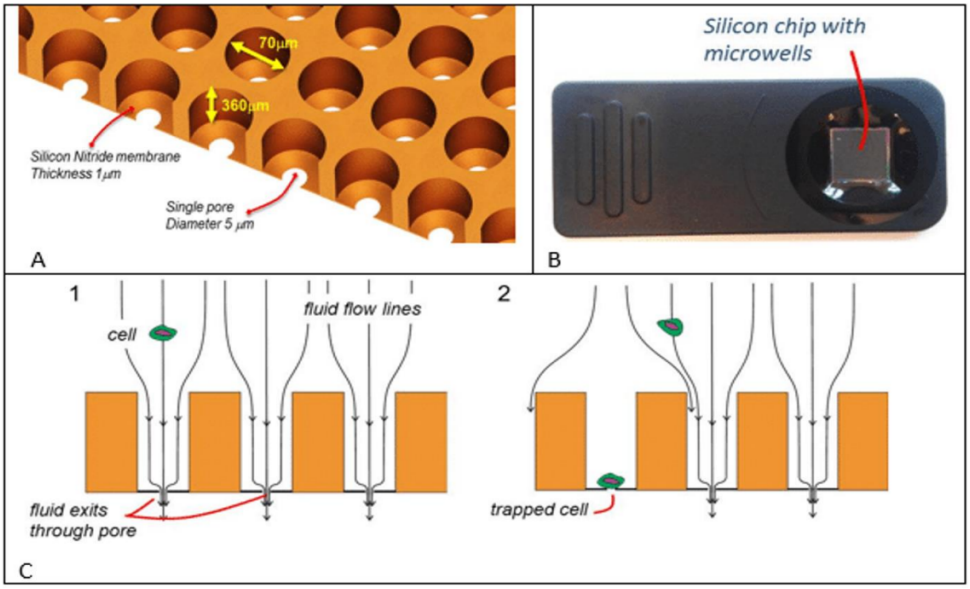

Figure 30: The self seeding microwell chip. A. Containing 6400 individual microwells of 70 um wide and 360 um high. Every well has a small pore at the bottom which allows flow through the chip. B. A picture of a chip, the left black structures are for grip when handling the chip. The black circle on the right is where the chip lowers in height with a gray square in the middle. The lower surface is in order to keep liquid on it. The gray square is the part that contains the wells. C. The moment a cell 'sits' on the pore, the flow through that particular well stops and a cell is isolated.[144]

5.1.3 Membrane

Capture of secretion was done on a membrane. The membrane being used is a Polyvinylidene fluoride (PVDF) membrane with a thickness of 0.1-0.2um. The membrane is activated by wetting in methanol for a short time since PVDF is extremely hydrophobic. The prewetting will improve the contact with the medium and increase the ability of immobilization from the membrane. Longer times will decrease protein binding capacity and mechanical strenght of the membrane itself[145]. Then the membrane will be functionolized with a ligand that will bind the cell secretion product of interest[146].

Once the Seeding is done and most microwells contain a cell (see Figure 31.1), the functionalised membrane is placed under the chip with the wells (see Figure 31.3). The secretion of the cell will come free in the medium, and part of it will move through the pore and meet the activated membrane where it will bind.[146] Then the membrane will be removed and incubated with antibodies targeted the cell product of interest, see Figure 31.

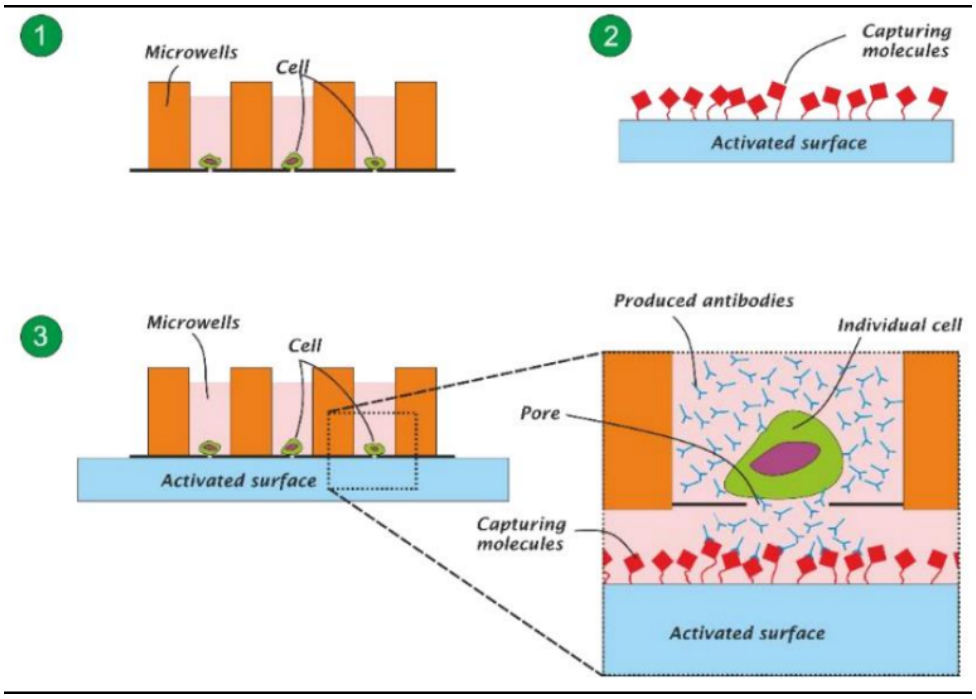

Figure 31: The secretion capture principle. 1. The Seeding is done and most microwells contain a cell. 2. The activated membrane. 3. The activated membrane is placed under the chip with the wells. The secretion of the cell will come free in the medium, and part of it will move through the pore and meet the activated membrane where it will bind.[146]

After the incubation time of the cells in the chip, the secreted particles will have been caught on the coated membrane, see Figure 32. Then this secretion of interest is stained with a polyclonal antibody that also targets other epitopes of the secreted product. This polyclonal antibody will make sure that PSA is bound and increases the number of available binding sites. Lastly, the polyclonal antibody will on its turn be targeted by an antibody, however now a fluorophore is attached to the targeting antibody. This fluorophore will make it possible to see signal of the secreted particle of interest under the microscope.

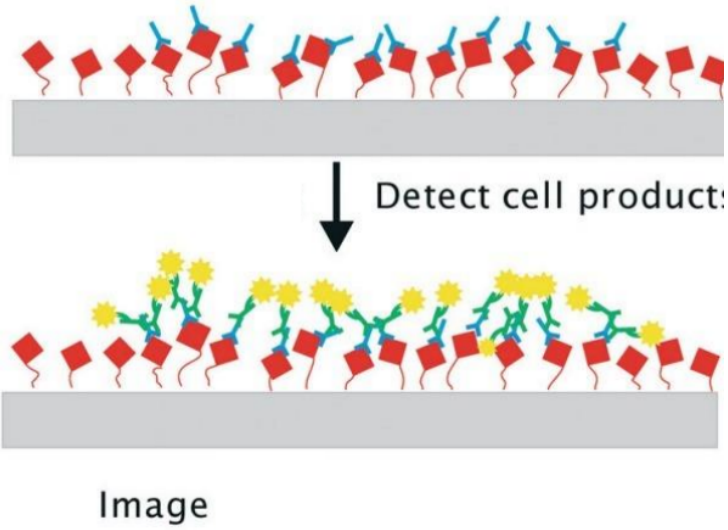

Figure 32: The membrane with caught particles of interest[146]. In gray the membrane. In red the ligands attached to the membrane specific for a chosen cell product. In blue the cell product of interest which binds to the ligand. Then with green yellow, the green part recognises a different epitope of the cell product (compared to the ligand), and the yellow part imitates the fluorescence part that might be excited and imaged after.

5.1.4 ELIspot

Visulatisation of the cells can be done of multiple fluorophores and markers. Biomarkers of cells will be labeled with different fluorophores which will be imaged each in their separate filter. The filters make the colour of the spot unimportant since in every selected wavelength pictures are taken which determine the outcome. The colour is only for graphical visualisation. Key is having the spot location recorded and being able to use the exact same location for pictures with different filters.[147]

5.2 Goals

The goals for this chapter are the following:

1. Investigate the influence of enriching cells on their secretion behaviour.
2. Visualize secretion of PSA of isolated cells.

We worked towards these goals in steps of small experiments. Working our way up from easy accessible Cell Line supernatant to later precious DLA samples from PCa patients. The goals were therefore divided in the following subgoals:

1. Prove that the membrane coating worked for collecting PSA secretion by using **supernatant** rich PSA of cells of a cell line in culture.
2. Prove that a smaller number of cells from a **cell line** secrete enough secretion to detect by seeding them directly on the membrane. Then seeding them on chip which causes isolation and looking into their secretion on a membrane at the bottom of the chip.
3. Investigate if a smaller number of **enriched cells of a cell line** influences secretion detection by seeding them directly on the membrane. Then seeding them on chip which causes isolation. Looking into how well the chip works with catching and isolating cells and looking into their secretion on a membrane at the bottom of the chip.
4. Prove that a smaller number of enriched cells from a cell line **spiked in blood** secrete enough secretion to detect by seeding them directly on the membrane regardless of the blood cells. Then seeding them on chip which causes isolation and looking into their secretion on a membrane at the bottom of the chip.
5. Prove that a smaller number of **CTC** from a DLA sample from a PCa patient secrete enough secretion to detect by seeding them directly on the membrane regardless of the blood cells. Then seeding them on chip which causes isolation. Looking into how well the chip works with catching and isolating CTCs and looking into their secretion on a membrane at the bottom of the chip.

5.3 Materials & Methods

There are 2 sorts of experiments that have been conducted. Experiments with cells seeded on the chips, and experiments with cells seeded directly on the membranes. Since it initially was hard to get signal on the seeded membranes, a control was always taken when seeding on chips in the form of seeding directly on the membrane. This proved if there were cells of interest at all.

5.3.1 Materials

Cells and Samples

All experiments in this chapter have been conducted with the LNCaP cell line (see Chapter 3.3.1 for the specifics). Blood samples were obtained form TNW TechMed Donordienst (Enschede, The Netherlands). DLA samples were obtained from the Erasmus Medisch Centrum (Rotterdam, The Netherlands).

FF

FF used for these experiments, were used in the same manner as described in Chapter 4.3.1.

antibodies and stainings

See Table 5 for the overview of the used antibodies in this Chapter.

Table 5: All antibodies used in Chapter 5, their working concentration, their stock concentration, and their manufacturer information.

Antibody	**Working Concentration (μg/mL)**	**Stock Concentration (mg/mL)**	**Manufacturer**
Anti-PSA mouse monoclonal antibody	25	6.41	Fitzgerald, Acton, MA, USA
Rabbit polyclonal Ab to PSA	14.16	7.58	Abcam, Cambridge, UK
Goat Ab to Rabbit IgG (PE)	0.2	0.1	Abcam, Cambridge, UK
aEpCAM-BV421 (HO-3)	2.25	0.45	
PE anti human PSMA (FOLH1) antibody	1.00	0.1	Biolegend, Greenwood Place, UK
aCD45-APC fire	4.00	0.025	Biolegend, Greenwood Place, UK
aCD45-PerCP	4.00	0.2	
Calcein-AM	4.00	0.623	Invitrogen eBioscience, San Diego, CA, USA

5.3.2 Methods

Seeding

Before being able to start the procedure, chips have to be degassed. Otherwise airbubbles will disrupt the seeding procedure. This will be done in a vacuum dome according to Appendix 8.12. The chip set-up is taken from the example that VyCap gives at their website[148]. First of all the cells will be seeded on the chip. For the set-up see Figure 33 The tube will be washed to remove any possible residue which could clog the chip. The chip is then wetted with ethanol, washed with PBS, washed with medium, seeded with cells, and washed with medium again. The seeding is done with a maximum of 10mbar. For the protocol see Apendix 8.4.

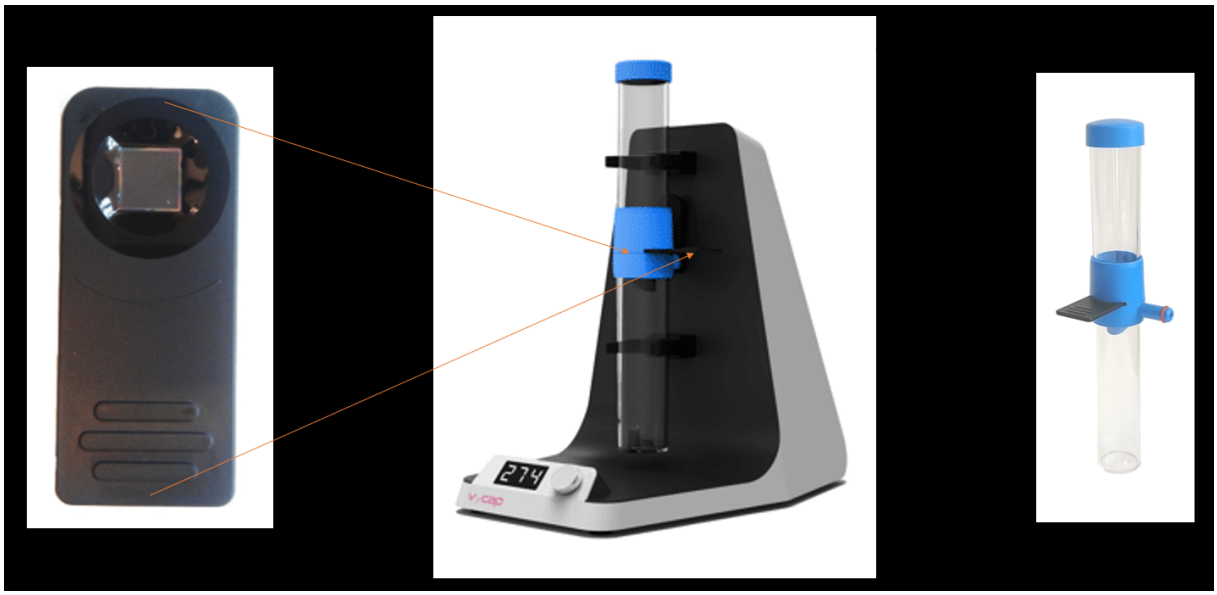

Figure 33: A microwell chip, a pump system and a tube. Left: the microwell chip with extra grip on the bottom and the square area with all the microwells on the top. Middle: the pump system that creates a pressure gradient. Right: the tubing in which the chip is put before attaching to the pump system. The top lit can be opened to put the sample in.[148]

Imaging of the seeded chip

In order to check if the seeding was successful, a quick check will be done under a microscope. If not enough cells are present yet, seeding is continued. If enough cells are present, the chip will be imaged by the channels of interest with the microscope, see Figure 34. Often Reflection (needed for later analysis), Brightfield (chip and cells), PE (PSMA to detect CTCs), PERCP (CD45 to detect leukocytes), and FITC (calcein, to determine viability). For the entire process of preparing a chip for imaging and the imaging itself, see Appendix 8.5.

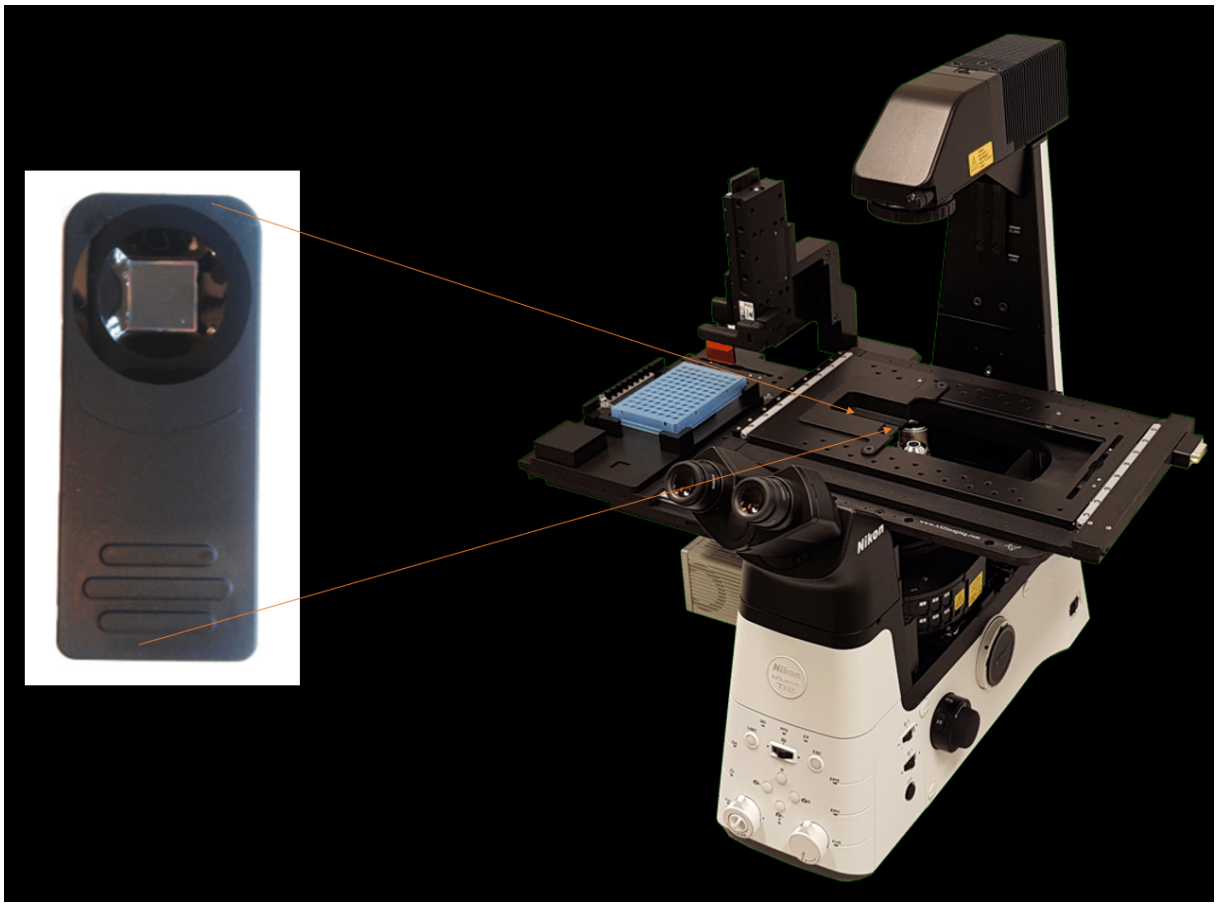

Figure 34: The microscope[148]. The chip is inserted in a holder which is desinfected which is then montaged on a microscope in a flowhood. Then the whole square area of the chip is scanned with microscopy for the fluorescence of interest.

After imaging the seeded chip, the chip will be put in a clamp unit in which there will be made contact between the seeded chip and a coated membrane, see Figure 35. Then the seeded chip will be incubated for a day. Due to the contact of the chip with the membrane, the secretion of interest will be caught. For the protocol, see Appendix 8.6.

After the incubation the seeded chip will be imaged again with the same channels as used prior. Also the membrane will be imaged as will be discussed in the next chapter.

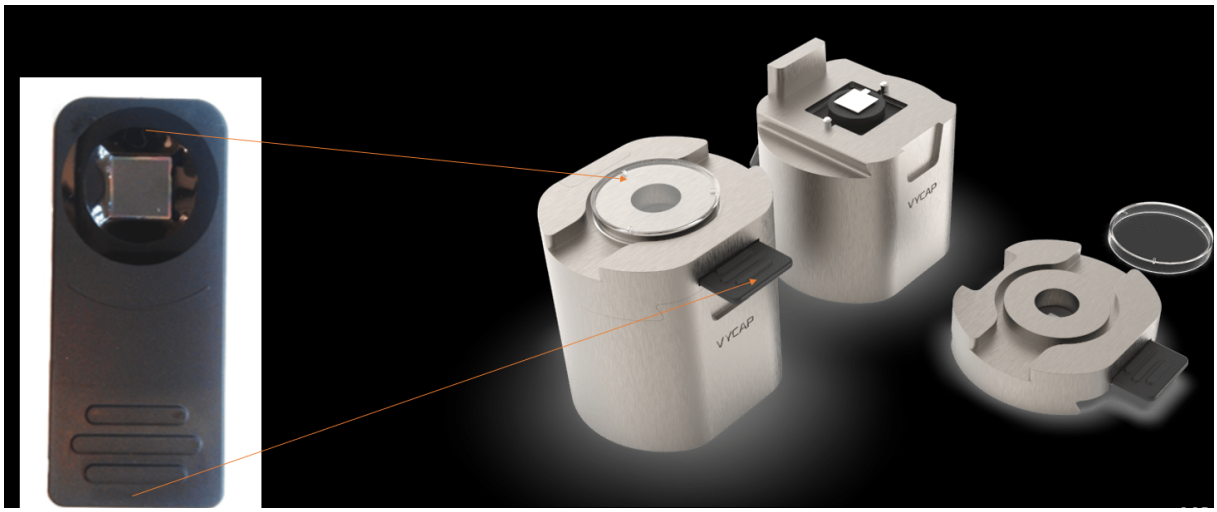

Figure 35: The clamp units. After imaging the chip, the chip will be put in a clamp unit. A coated membrane will be put on the designed area on the bottom part of the clamp unit, see the white membrane. Then the chip will be inserted in the top of the clamp unit after which the top will be put on the bottom of the clamp unit. Then the lever will be slowly put down to make contact between the chip and the membrane. Last, medium is put on top of the chip and covered with a small lit to prevent contamination during incubation in the incubators. [148]

Membrane

The membranes that were used were often self-cut or pre-cut. The self cut membranes were very slightly smaller than the size of 1 well of a 24 wells plate, which is approximately 1.9cm^2. The pre-cut membranes came also in that size, as well as a square size. The squar sized membranes were slightly larger than the chip wells area and had a small 'handle' which was used to place and remove the membranes while handling it with the pincer.

To activate the membranes, they are kept in methanol for 1 minute. Then they are washed twice with 1X PBS and covered with an 'O'-ring to prevent them from floating and reduce needed antibody. The membranes will then be coated with anti-PSA antibody with a concentration of 25 ug/mL and kept preferably overnight in 4 degrees Celsius (4h instead of overnight is also acceptable). See for the detailed protocol Appendix 8.1.

After removing the anti-PSA antibody, the rest of the membrane needs to be blocked in order to prevent aspecific binding. This will be done by blocking for 1 hour in 3%w/v BSA, after which they are washed with 1X PBS again. See for the detailed protocol Appendix 8.2.

After incubation, the chip and membrane will be removed from the clamp unit. Then the membrane will be stained by a primary and secondary antibody, see Appendix 8.7. As primary antibody Rabbit polyclonal antibody to PSA with a concentration of 15.16ug/mL will be used, which will be incubated for 1 hours. As secondary antibody, Goat antibody to Rabbit IgG PE with a concentration of 0.2ug/mL will be used, which will be incubated for 1 hour. After that, the membrane will be put on a glass microscopic slide and imaged with microscopy for PE and brightfield, see Figure 36. Quick focusing is of utmost importance here since bleaching occurs rapidly. See Appendix 8.8 for the protocol.

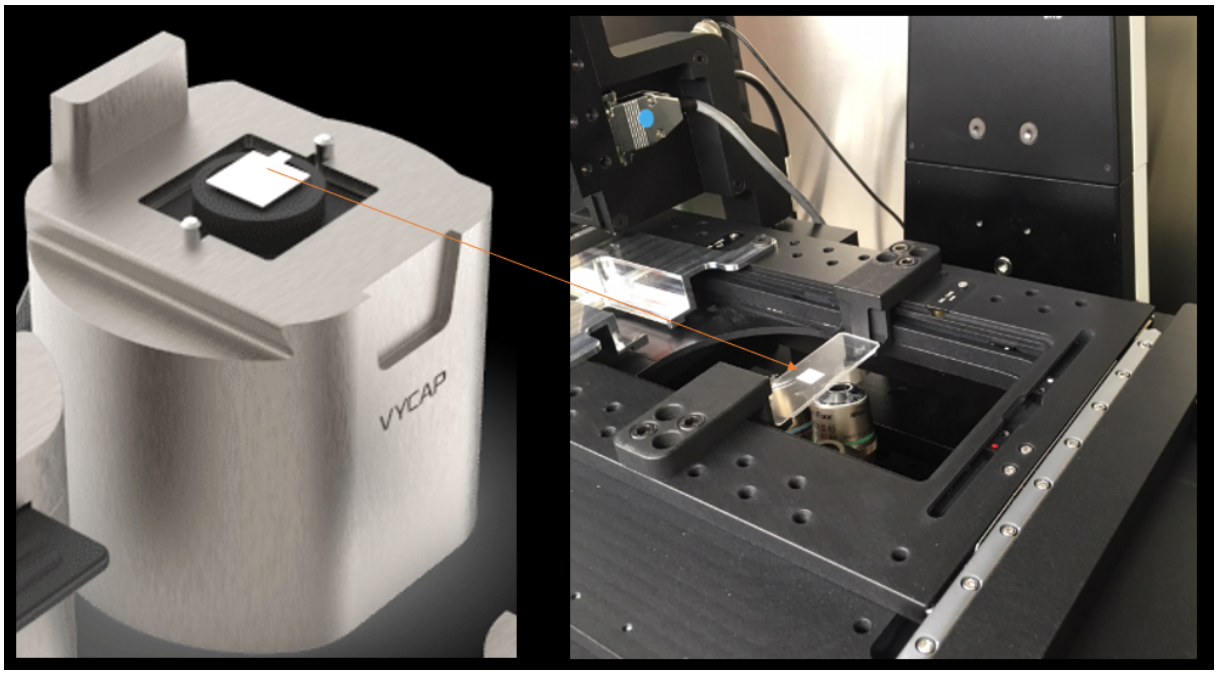

Figure 36: The software: outlining of the chip before scanning the whole chip. Reflection is used to determine the corners of the chip by selecting the most outlaying well on 3 different corners.

Software

The software which will be used for taking the pictures will be software developed by VyCap specially for the puncher microscope and the use of their chips. Since the software is under constant development, different version might be used during the experiments. The exposure time can be adjusted with the software. The chip will be briefly checked on brightfield after which reflection is used to determine the corners of the chip by selecting the most outlaying well on 3 different corners.The software will recognise the well shape and mark this with red lining.Then the focus will be checked at random points on the chip. During this, there will be briefly focused in all channels in order to determine if all channels are in focus (this will also be done beforehand with beads in order to be more sure of a smooth workflow). If not all channels are in the exact same focus, the channel focus will be changed in the settings of the coding of the software. The channels which will be imaged will be chosen.The wanted channels can be chosen and the exposure time for each channel can be selected. The exposure times are optimised at the start of all experiments and then largely kept the same in order to make comparison possible.

The pictures taken with this software are very high resolution and are shown in the next Chapter.

5.4 Results

Firstly we needed to prove that PSA was secreted and could be caught on the membrane and after that visualised. For that reason the exploratory droplet experiments were done.

Supernatant

The droplet experiments were done on 3 membranes and all showed positive results, see Figure 37 for an example of 1 membrane. In the left bottom of the picture there is some bleaching visible which taught us at an early stage the dangers of too long exposure while trying to find the correct focus.

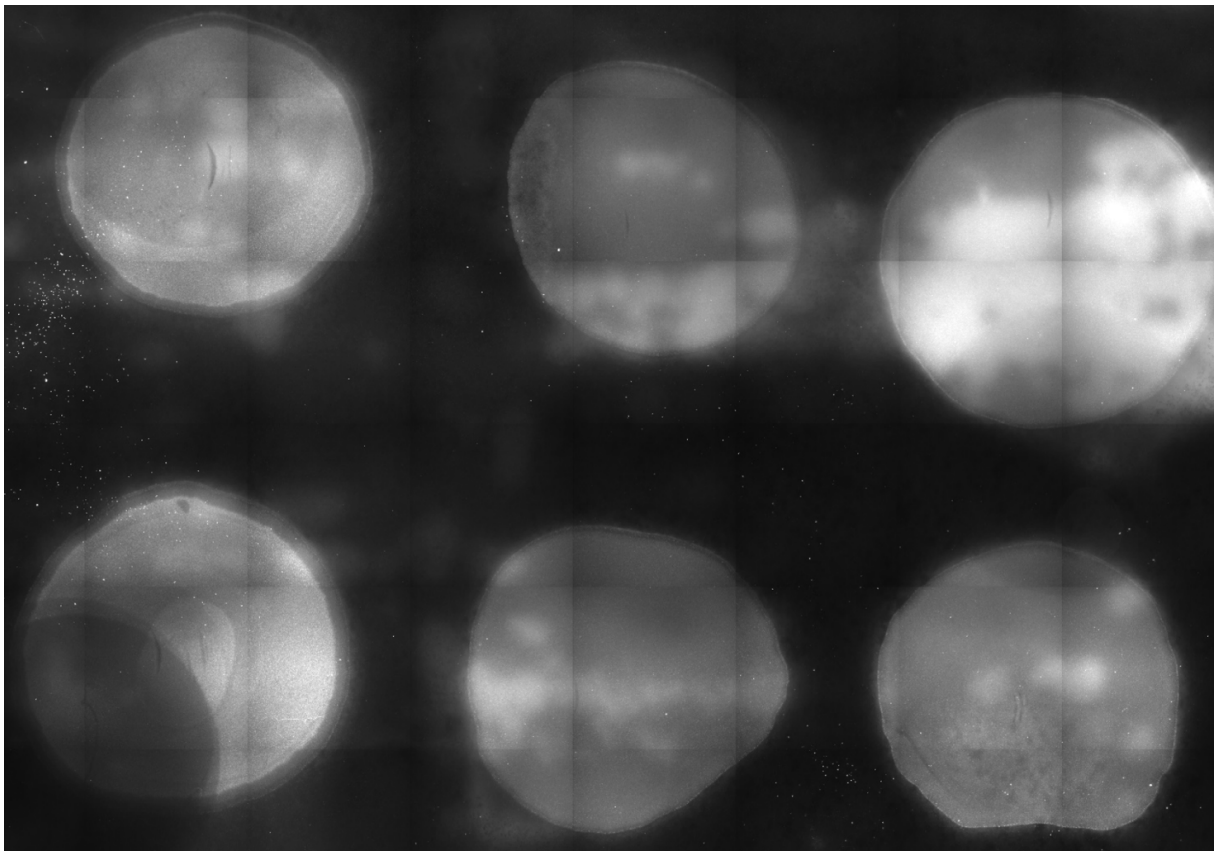

Figure 37: Drops of supernatant of LNCaPs on anti-PSA coated membranes. All the drops are clearly visible and much lighter than the dark background which was not exposed to medium with secreted PSA. Visualised by primary rabbit Ab to PSA staining and secondary goat Ab to rabbit IgG with PE fluorescence.

Secreted PSA can be imaged when collected from medium in which it is likely more abundant than working with a smaller number of cells. Therefore the next experiment was done with a specific number of cells themselves, instead of supernatant from a mass culture. This experiment was combined with the start of the FF influence experiments for efficiency sake.

5.4.1 FF influence on secretion

Both the 'medium control' and the 'FF control' (see Figure 38) show no staining on the membrane as expected. Both the 'Cells directly seeded on a membrane' (see Figure 39) and the 'Cells-FF directly seeded on the membrane' (see Figure 40) show staining, as expected.

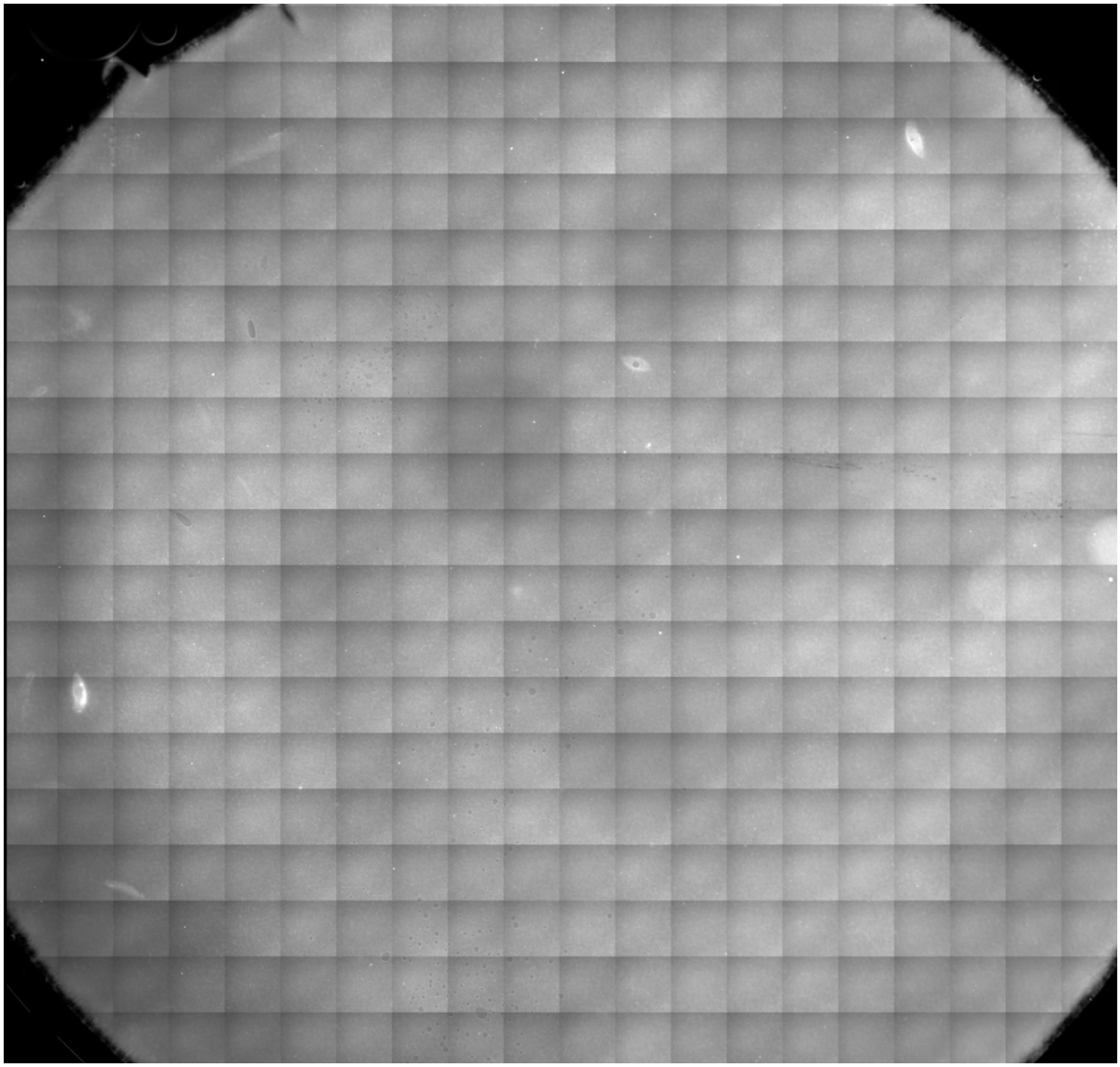

Figure 38: Control condition in which only FF were put on a mouse antibody anti-PSA coated membrane. No fluorescence signal was seen caused by the FF. The condition incubated for a day, was washed, and the membrane was stained with Rabbit polyclonal antibody to PSA, which on turn was stained with Goat antibody to rabbit IgG (PE).

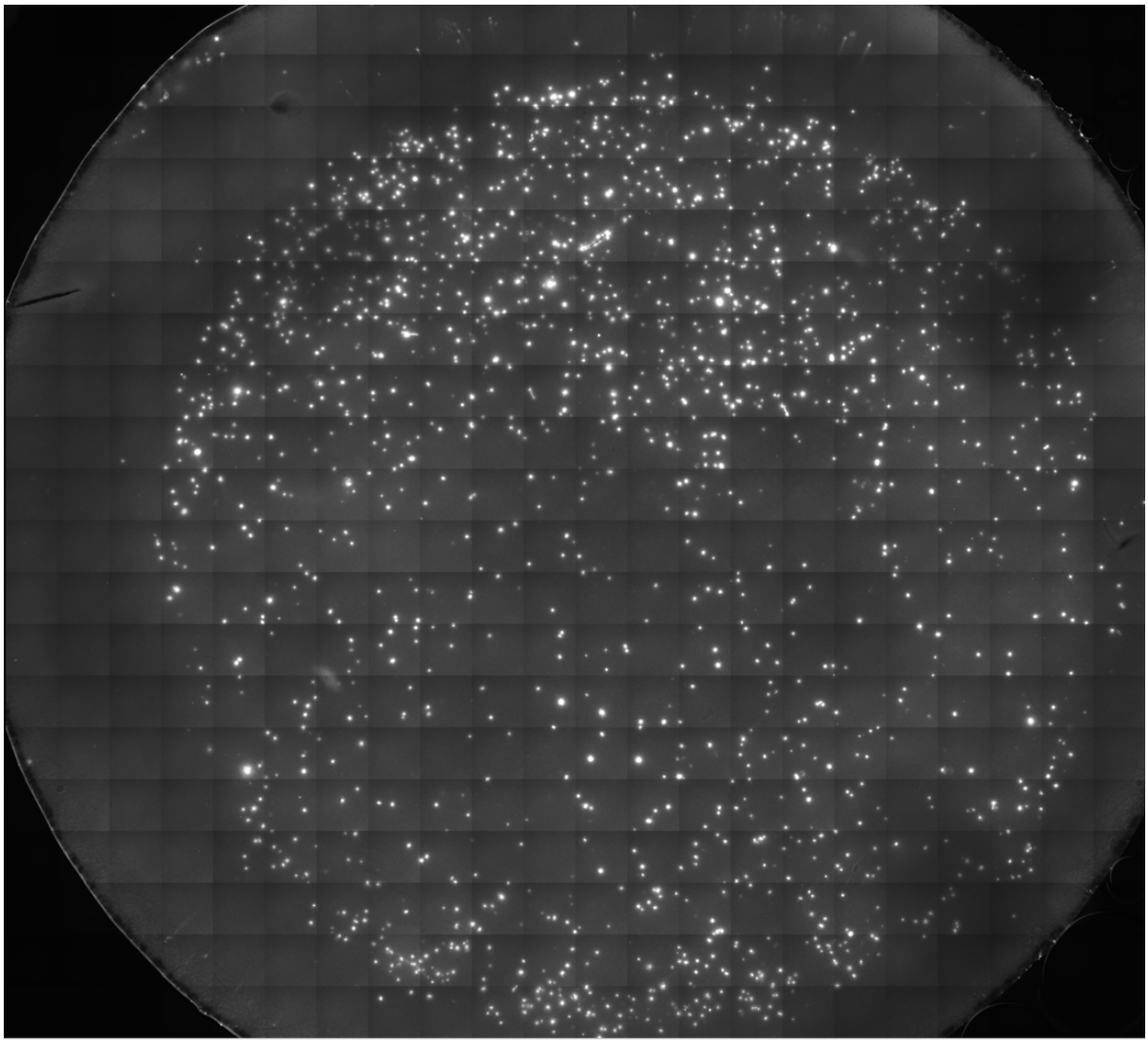

Figure 39: Condition 'Cells directly seeded on the membrane'. 6K cells were put directly on a mouse antibody anti-PSA coated membrane. They incubated for a day. Were washed off, and the membrane was stained with Rabbit polyclonal antibody to PSA, which on turn was stained with Goat antibody to rabbit IgG (PE). Cells or cell groups are seen.

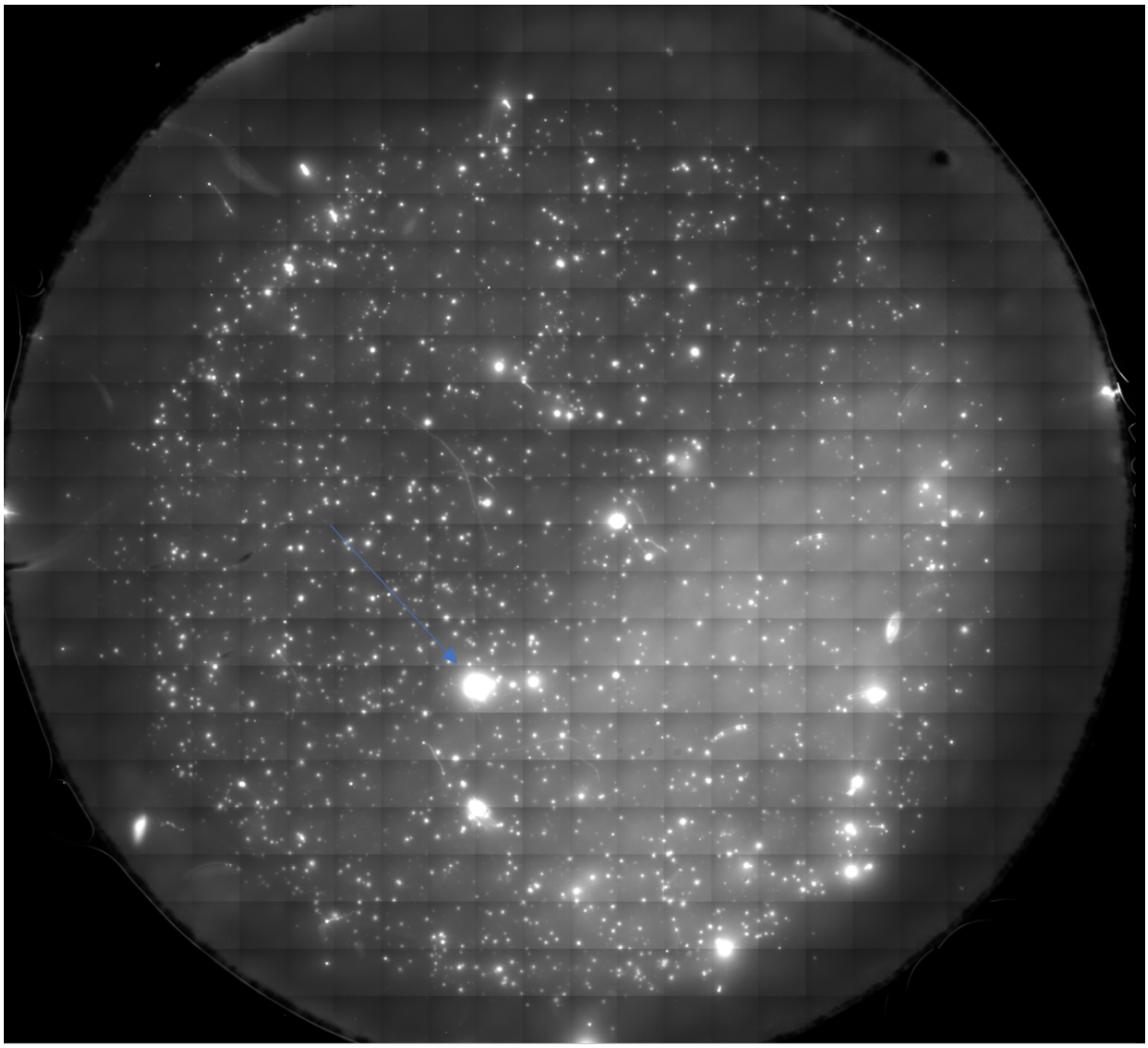

Figure 40: Condition 'Cells-FF directly seeded on the membrane'. 6K enriched cells were put directly on a mouse antibody anti-PSA coated membrane. They incubated for a day. Were washed off, and the membrane was stained with Rabbit polyclonal antibody to PSA, which on turn was stained with Goat antibody to rabbit IgG (PE). Cells or cell groups are seen. Clustering of cells is more common when using FF and is indicated with the arrow.

The next step was seeding the cells on a chip and retrieving their PSA footprint. Therefore the cells were first imaged after seeding, we also looked into how many cells were found in the chip.

Cells were stained with CTO and after seeding in the condition 'Cells-FF seeded on chip', approximately 2600 wells gave PE signal, see Figure 41. (see Appendix 8.21 Figure 78 for the PE signal and Figure 77 for the brightfield signal) of which approximately 90% was from cells. Therefore approximately 2340 wells (37%) were seeded with 1 or multiple cells.

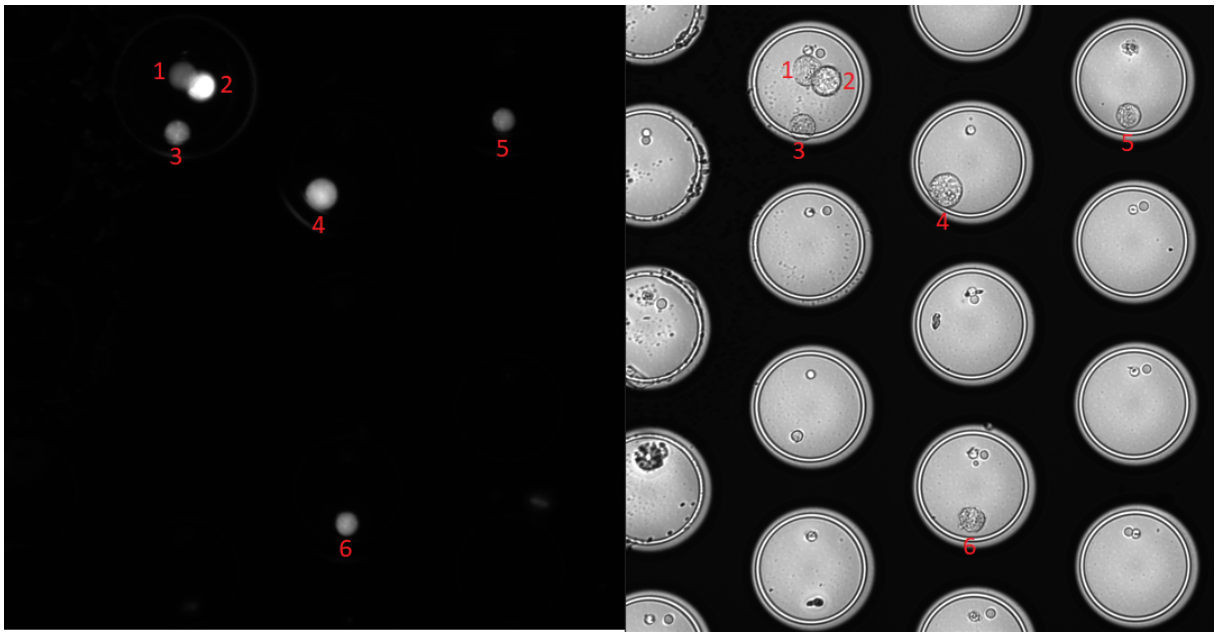

Figure 41: Condition 'Cells-FF seeded on chip', the zoomed in chip imaged with PE (left) and brightfield (right). Cells were stained with CTO. Approximately 2600 wells gave PE signal of which approximately 90% was from cells. The number indicate the same.

6K enriched cells were seeded on the chip with 5 mbar pressure. Since only 37% of wells was seeded and most commonly only 1 cell was present in a seeded well, this meant the chip was already 'full' (not flowing anymore under pressure) or some cells were not caught by the chip. Most wells are visible. When zooming in on wells, cells and debris can be seen in small amount in the right picture of Figure 41 See Appendix 8.25 Figure 81 and Figure 82 for more debris. Some cells remained in place and some cells moved during incubation, see Appendix 8.25 Figure 81 and Figure 82, respectively.

Both the 'Cells seeded on chip' (see Figure 42) and the 'Cells-FF seeded on chip' (see Figure 43) show positive staining on their membranes. A comparison could not be made since the pictures of the membrane of the 'Cells-FF seeded on chip' turned out blurry. In later experiments we lost the imprint of the wells, which made comparison impossible.

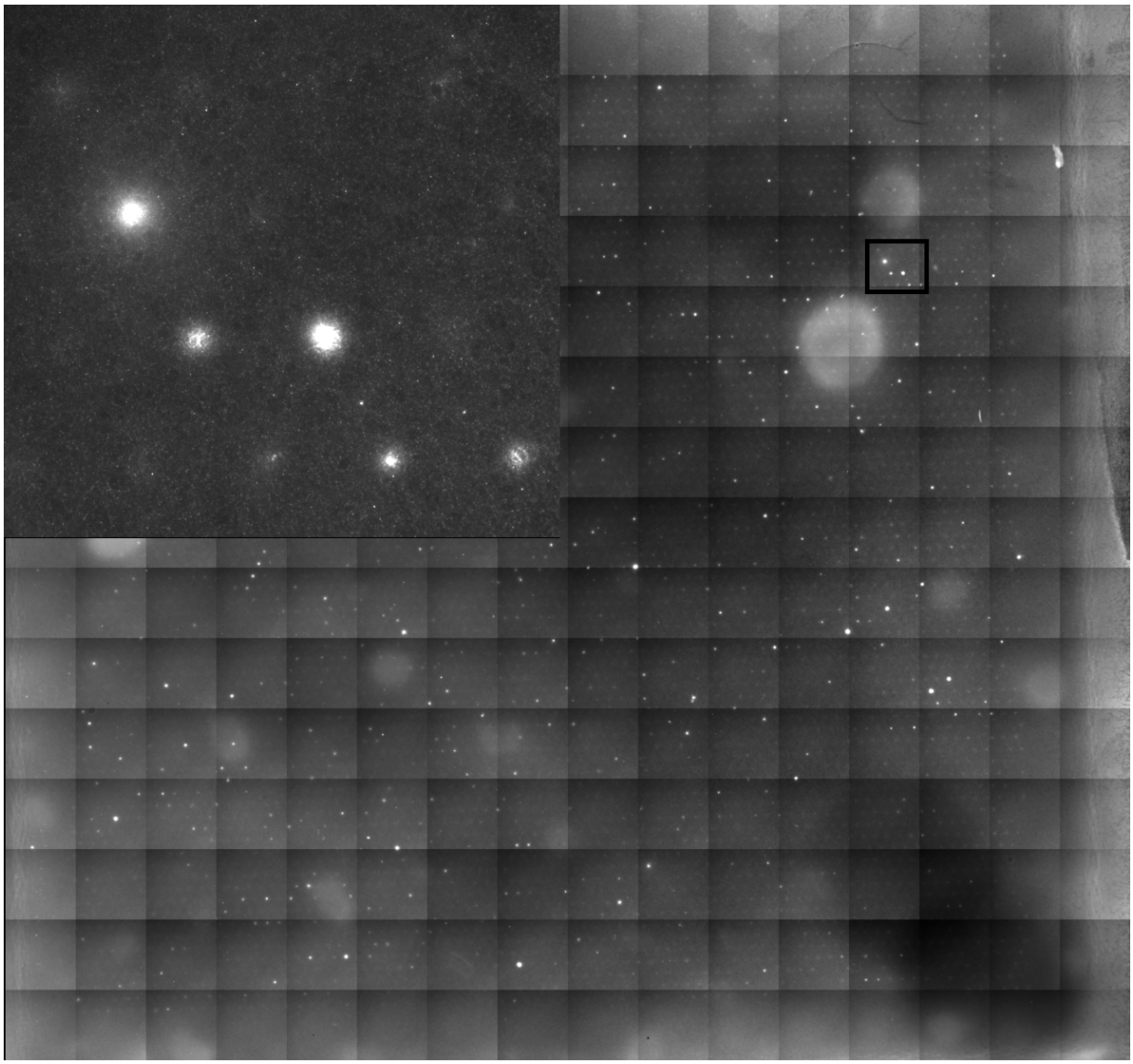

Figure 42: Condition 'Cells seeded on chip'. 6K cells were seeded on a chip with 5 mbar pressure. This chip was put in a clamper unit and was placed above a mouse antibody anti-PSA coated membrane which made contact via a drop of medium. They incubated for a day. Then the membrane was removed and washed, followed by staining with Rabbit polyclonal antibody to PSA, which on turn was stained with Goat antibody to rabbit IgG (PE). The well imprint is seen which is needed for analysis. Dots with increased fluorescence intensity are seen.

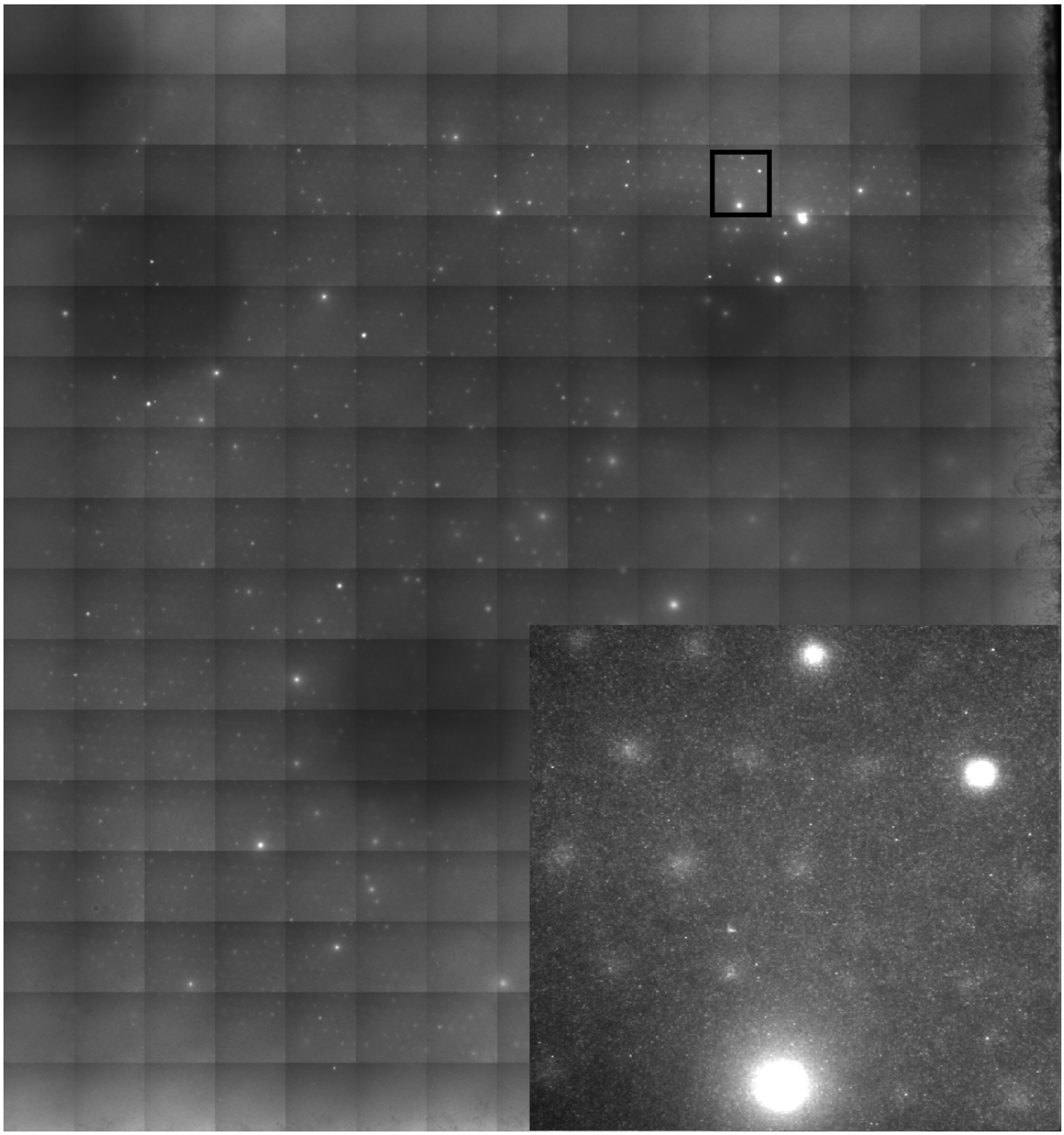

Figure 43: Condition 'Cells-FF seeded on chip'. 6K enriched cells were seeded on a chip with 5 mbar pressure. This chip was put in a clamper unit and was placed above a mouse antibody anti-PSA coated membrane which made contact via a drop of medium. They incubated for a day. Then the membrane was removed and washed, followed by staining with Rabbit polyclonal antibody to PSA, which on turn was stained with Goat antibody to rabbit IgG (PE). The well imprint is seen which is needed for analysis. Dots with increased fluorescence intensity are seen. However, the picture appears blurry.

No signal was seen when only FF were put on a membrane. PSA secretion of the cells seeded on the membrane was visible on a same level as PSA secretion of cells enriched by FF was visible. Moreover, the chip isolated tumour cells and then was able to have PSA staining patterns on its membrane. This is important for our next experiment series that builds up towards visualising CTC enriched with FF from a PCa patient DLA sample.

5.4.2 PSA secretion

LNCaP

PSA secretion from the cells from the cell line LNCaP was clearly visible when directly seeded on the membrane, see Figure 44. Secretion was also visualized when cells were seeded on the chip which was put over a membrane, see Figure 45. Professionals of VYCAP recognized this as secretion. However, spots were not bright enough for analysis with the software next to a large part of the outer edges not being visible which need to be selected for the software to work.

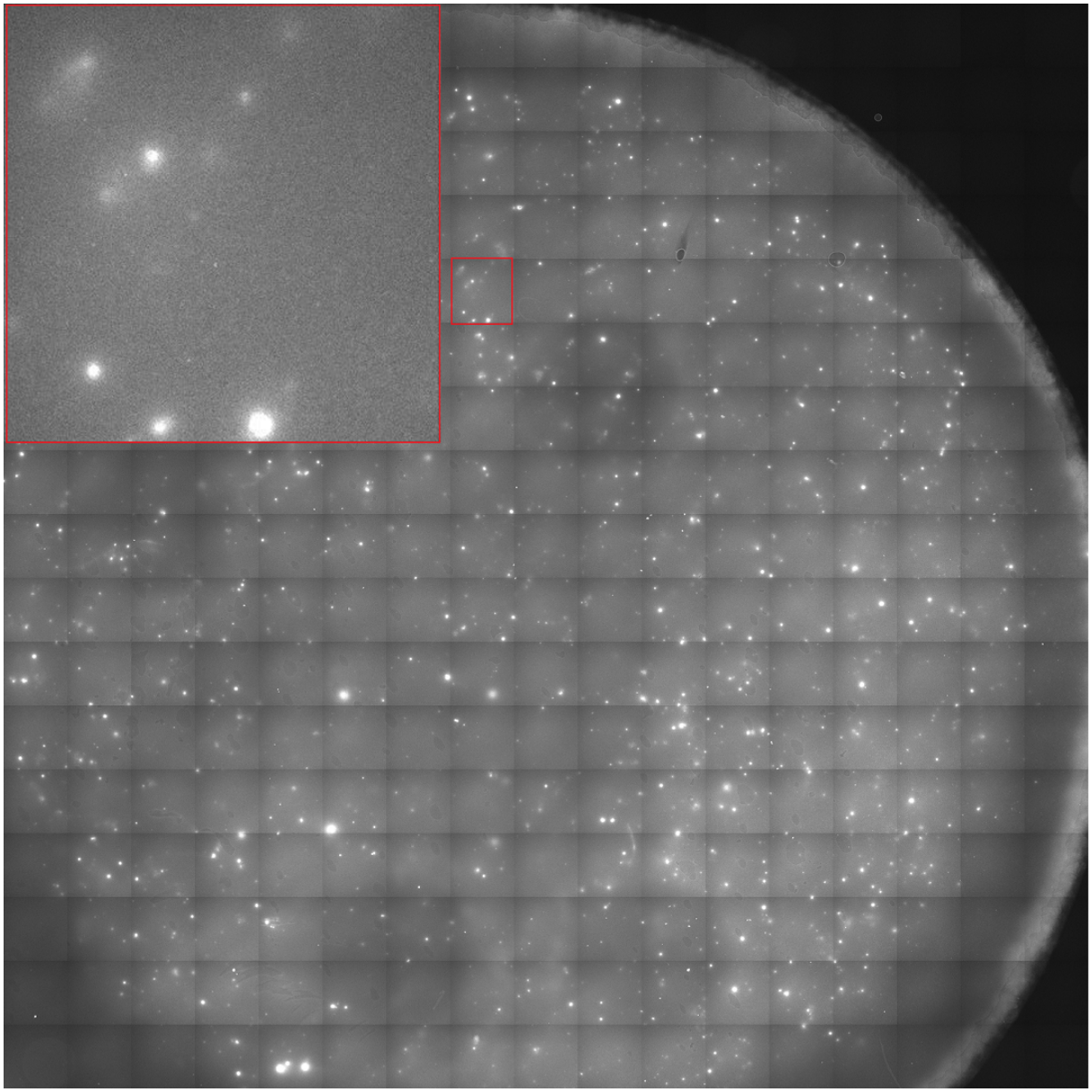

Figure 44: 6K LNCaP cells directly seeded on a mouse antibody anti-PSA coated membrane. They incubated for a day. Were washed off, and the membrane was stained with Rabbit polyclonal antibody to PSA, which on turn was stained with Goat antibody to rabbit IgG (PE). The condition that was incubated for 16 hours looked similar.

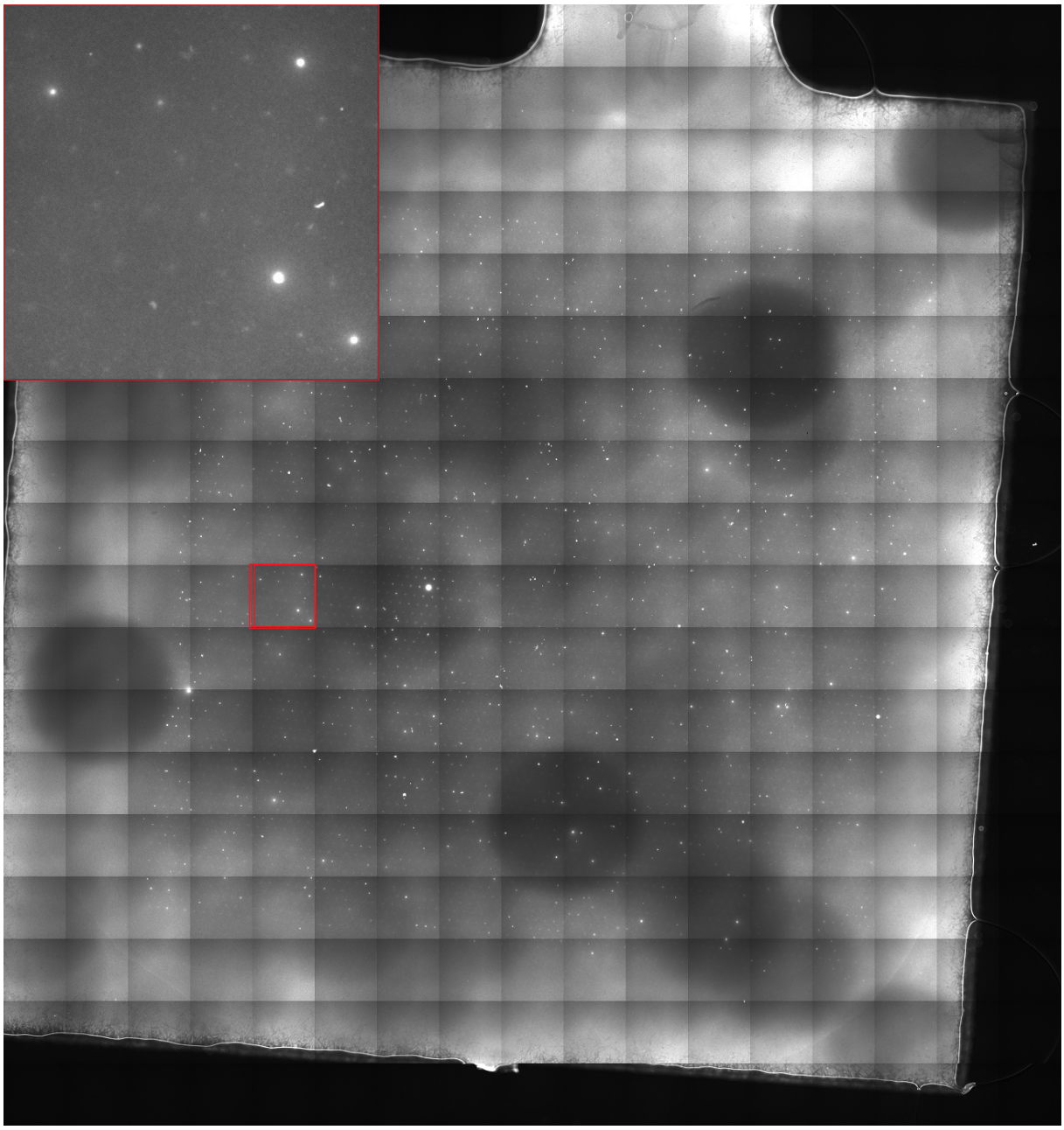

Figure 45: 6K LNCaP cells seeded on a chip which was put above a mouse antibody anti-PSA coated membrane. They incubated for a day. The membrane was stained with Rabbit polyclonal antibody to PSA, which on turn was stained with Goat antibody to rabbit IgG (PE). The experiment was done in duplo. Spots are visible. However, they were smaller than in Figure 44 what caused focusing to take longer, which immediately resulted in more photo-bleaching which can be seen as the slightly darker round circles. The condition that was incubated for 16 hours looked similar.

Direct seeding clearly worked. Seeding on the chip also worked, however not yet as good as we hoped. Nevertheless we moved on to the next stage, spiked blood samples.

Spiked blood

Spiked blood samples which underwent enrichment gave similar results in intensity as cells from the LNCaP cell line. However less cells were found. Also the imprint of the wells on the membrane was fading, which needed to be resolved.

Since a solution on the loss of well imprint was not quickly found, we experimented with tracing cells when directly seeded on the membrane. We imaged the cells stained with HO-3-BV421 and PSMA-PE while they were on the membrane, see Figure 46B and C. Then we went on with the standard procedure of washing and staining of the secreted PSA. Cells were washed away and PSA secretion was detected, see Figure 46A. Secretion spots were present in the same pattern as the cells were present, see the arrows in Figure 46.

Darker spots can be seen within the secretion spots, where no secretion got attached to the membrane, see Appendix 8.20 Figure 76. This is were cells were situated on the membrane before washing.

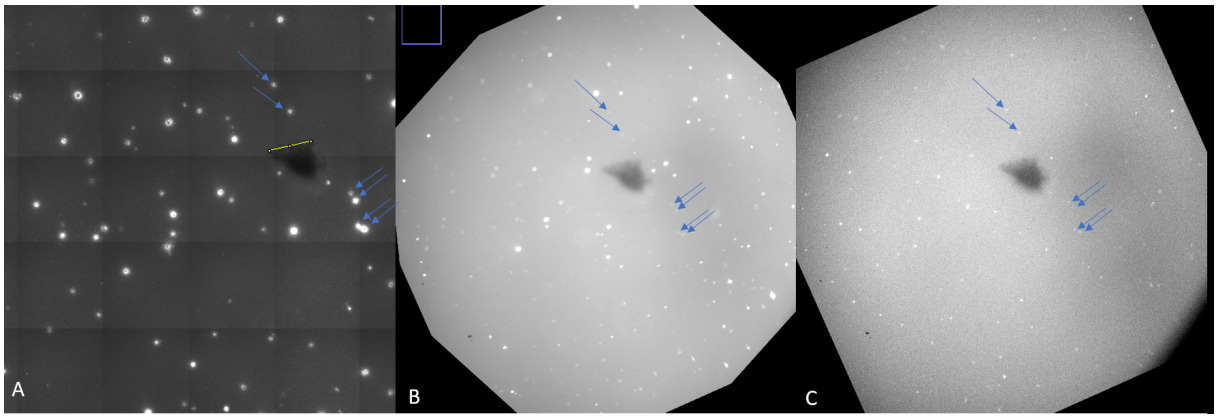

Figure 46: Enriched blood sample seeded directly on a mouse antibody anti-PSA coated membrane. The arrows indicate secretion spots which were present in the same pattern as the cells were present. A: PSA secretion imaged in with a PE filter. The membrane was stained with Rabbit polyclonal antibody to PSA, which on turn was stained with Goat antibody to rabbit IgG (PE). B: Cells imaged with the DAPI filter. Cells were stained with EpCAM-BV421. Right: Cells imaged with the PE filter. Cells were stained with PSMA-PE.

Again, seeding directly on the membrane gave good results. The experiments on chip went similar, however the issue with the imprint of the wells was unresolved. Therefore, software analysis could not be used. But tumour cells could still be found in blood samples. We moved on to the final stage, the PCa patient DLA samples.

PCa DLA and spiked breast cancer DLA

PSA secretion from the enriched CTCs from the PCa patient DLA sample was in small numbers clearly visible when directly seeded on the membrane, see Figure 47. Direct seeding worked for the automated Cell Search enrichment procedure as for the manual procedure. A breast cancer sample with extra spiked LNCaP cells showed more visible cells.

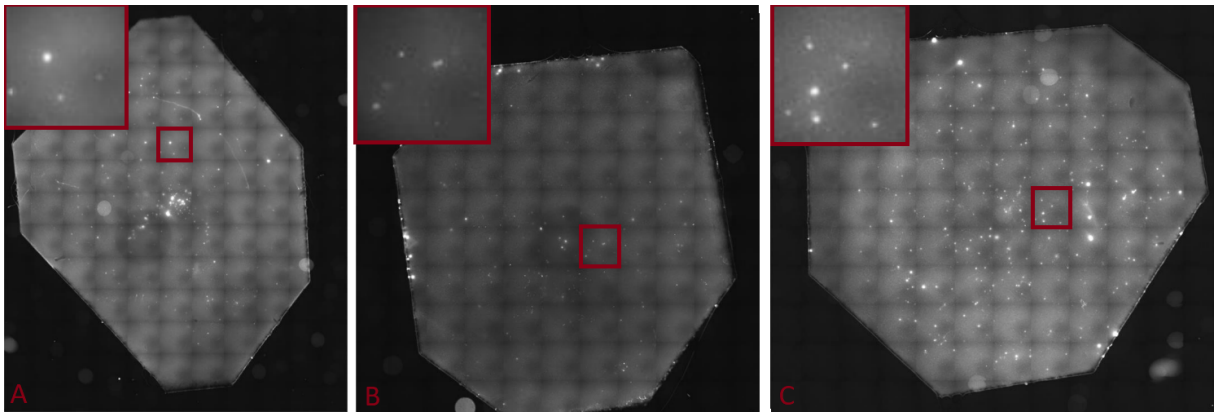

Figure 47: Enriched CTCs seeded on a chip which was put above a mouse antibody anti-PSA coated membrane. A: enriched was done with the manual procedure on a DLA sample of a PCa patient. B: enrichment was done with the automated Cell Search procedure on a DLA sample of a PCa patient. C: A spiked breast cancer DLA sample. They incubated for a day. The membrane was stained with Rabbit polyclonal antibody to PSA, which on turn was stained with Goat antibody to rabbit IgG (PE).

Secretion was not visualized when enriched CTCs from the PCa patient DLA sample were seeded on the chip which was put over a membrane, see Figure 48. It was not visible for both the automated Cell Search enrichment procedure as for the manual procedure. Spiked DLA samples were not tested with the chip. The second DLA samples from PCa patients gave similar results, visibility when seeded directly on the membrane, but not via the chip.

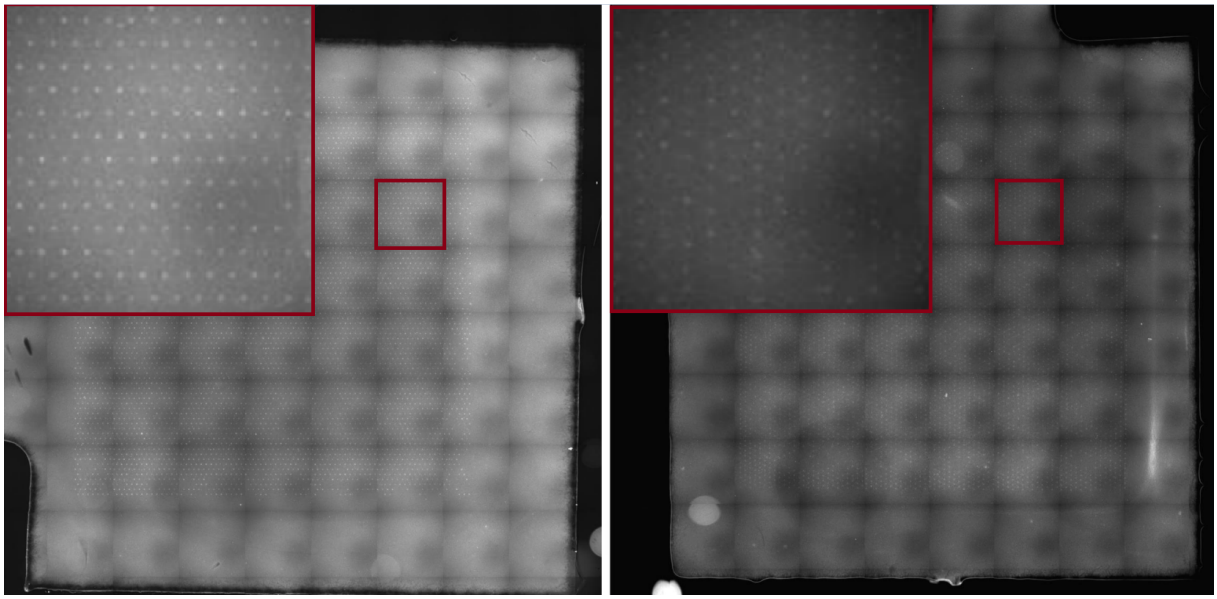

Figure 48: Enriched CTCs from a PCa patients DLA sample, seeded on a chip which was put above a mouse antibody anti-PSA coated membrane. No PSA secretion was, however there was a proper imprint of all the wells of the chip. Left: enrichment was done with the manual procedure. Right: enrichment was done with the automated Cell Search procedure. They incubated for a day. The membrane was stained with Rabbit polyclonal antibody to PSA, which on turn was stained with Goat antibody to rabbit IgG (PE).

Therefore we looked into if we could find the CTC on the chip. Cells were stained with the markerpanel. No CTC were found when scanning the first of the seeded chips for PSMA or EpCAM bound fluorescent antibodies. There were lots of Leukocytes detected which had CD45, see Appendix 8.26 Figure 83. However, 2 supposed CTCs were found in the second chip, see Figure 49. This is still a very low number and more were expected. A good explanation might be that al wells were already occupied or blocked. We found lots of debris but moreover, 74% of wells was already filled with 1 or often multiple leukocytes.

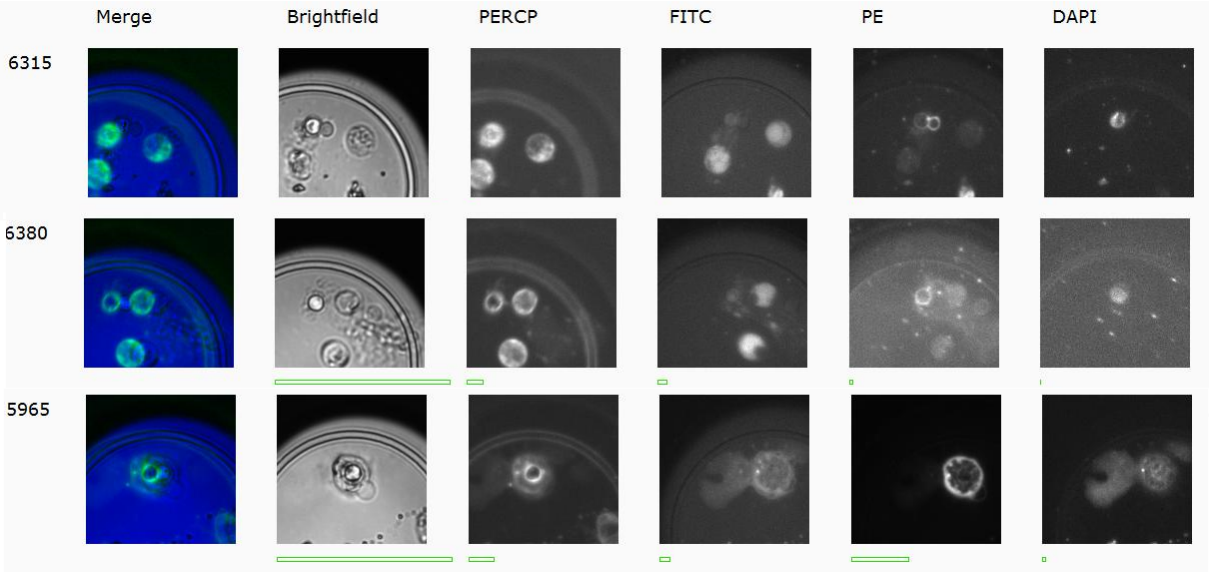

Figure 49: Examples of cells found in the chip. The top 2 rows are leukocytes and debris. The bottom row is a CTC. In total 2 CTC were identified. Lots of leucocytes were identified. From left to right. The well number. Merge: multiple channels. Brightfield, the chip, cells, and debris. PERCP: CD45. FITC: Calcein. PE: PSMA. DAPI: EpCAM.

5.5 Conclusion & Discussion

5.5.1 Conclusions

FF influence on secretion

The basis is there for determining if the enrichment of cells does influence their secretion patterns. The images obtained from cells directly seeded on membranes do not show differences. For proper analysis, cells need to be separated which can be done with the chip. This experiment is done successfully but only once. Therefore, more repeats are necessary.

Visualising secretion of PSA by isolated cells

Secretion of PSA can be visualised with the methods used in this report. However, the intensity of the signal was to dim for analysis with the software. Secretion from cells harvested from cell lines was visualized, Secretion in spiked blood samples was visualised. Secretion of CTCs is unsure if it is visualised due to the very dim fluorescence we could not use the software to identify if it were indeed CTCs secreting.

5.5.2 Discussion

Clustering of FF

Larger fluorescent spots are seen at the condition 'Cells-FF directly seeded at the membrane' which do not like contamination, see the arrow at Figure 40. This is likely due to clustering of the FF which causes multiple cells to accumulate together resulting in overlapping spots which is visually seen as 1 bigger spot of fluorescence. The aggregation of FF once they become bigger or part of a bigger overall is described by literature[149], they can be found in different shapes and sizes[150].

Tested differences

Since we did have contamination like patterns in the wells, plus we lost the visuals of the imprint of all the individual wells, many different factors were tested that could potentially influence the outcome of the experiments. Since only 2 chips were used at the same time. All these experiments stand for 3 days of lab work. Factors that were tested but did not result in a positive outcome:

1. Coating: Cells might not like the chemical properties of the chip surface. The morphology of cells kept looking bad. Cells often look not viable anymore after incubating in the chip for 1 day or more. Therefore experiments with coating with Poly-L-Lysine were conducted since literature states that cells 'like' this coating in order to keep the cells more viable. Implementation of poly-L-lysine has been used to stimulate cell growth[151]. It is also looked into in application of transplantation for its bio-compatibility, cell adhesion properties and ability to retain shape[152].

2. New PDMS: PDMS might be contaminated since it looked really old and had a brown colour.

3. New O-ring: O-rings might be contaminated.

4. Confluency: Confluence might influence cell behaviour, for example whole cell mechanical behaviour is dependent on confluency[153, 154]. Overgrown cells might not grow much after passaging. There is no clear difference between cells that were harvested at 50% confluency versus cells that were harvested at 100% confluency and then seeded directly on membranes. Both have the same height of intensity peaks. There might be a different spreading pattern, however repeats should be done to investigate if this is due to cell behaviour or due to the methods (all membranes slightly vary

and sometimes are differently orientated in the wells of the wells plate in which they are kept). See Figure 51 for these results.

5. Seeding pressure: The seeding pressure was experimented with, and afterwards standard lowered from 10-20 mbar to 5 mbar. However, this might not have been sufficient, as later literature research pointed out that specifically LNCap cells (the cell line we worked with in this Chapter) are highly influenced by shear stress[155]. There, Du145, LNCaP, and PC3 were tested on their response to 10 short pulses of 3950 dyn/cm^2 (395 Pa, or 3.95 mbar). LNCaP and PC3 cells both showed a significant increase in their late apoptotic populations, see Figure 50.

6. Drug stimulation: If there are cells, maybe they don't secrete much. With stimulating we could find out if it was just a matter of enough secretion by the cells. Cells were 24h incubated under standard conditions, then 24h while being stimulated, finally 24h with inhibiting drugs.

7. dry vs. wet imaging of the membrane: We tried imaging the membranes dry and wet. Since both methods could be used, we tested if there was a problem.

8. filtering all solution: The solution could be contaminated. Since you can't heat most solution without changing their properties, all solution were filtered by filters that would not allow bacteria or fungi to come through.

9. degassing procedures: For degassing we needed to switch labs. This came with a lot of dangerous manoeuvres sterility wise. We tried to reduce these.

10. gamma radiated chips: The chips could be delivered contaminated. Therefore, we requested gamma radiated chips which were sure to be clean.

11. Passage number: The passage number of the cells could influence cell behaviour and possibly secretion. Since we were working with high passage numbers, we went back to the lowest passage number we had in house and repeated experiments with those cells after 2 weeks of culturing them.

12. Seeding time: the original protocol said 1 day of incubation. We often counted the end of the day in which we started incubating, to the start of the day we started staining as 1 day. This was however often around 16 hours. We tested if there were visual differences when actually waiting 24 hours as might have been indicated by the original protocol. This experiment was done once and no clear differences were observed. Therefore, we kept using the much more practical (for standard working hours of the researchers) 16 hours incubation as '1 day incubation'.

It might of course have been a combination these factors, however they were tested one by one and not as combinations.

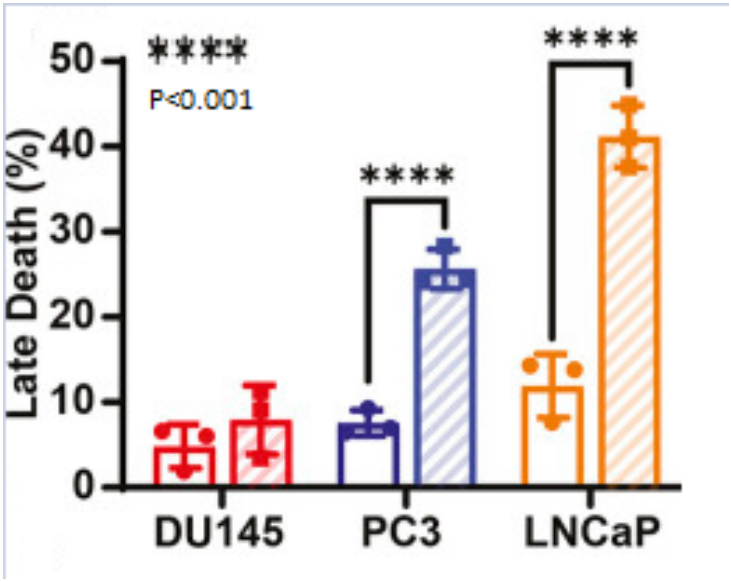

Figure 50: Reprinted from Hope et al, 2021[155]. Average early late apoptotic populations for cancer cells treated with 0 (left) or 10 (right) pulses of FSS.

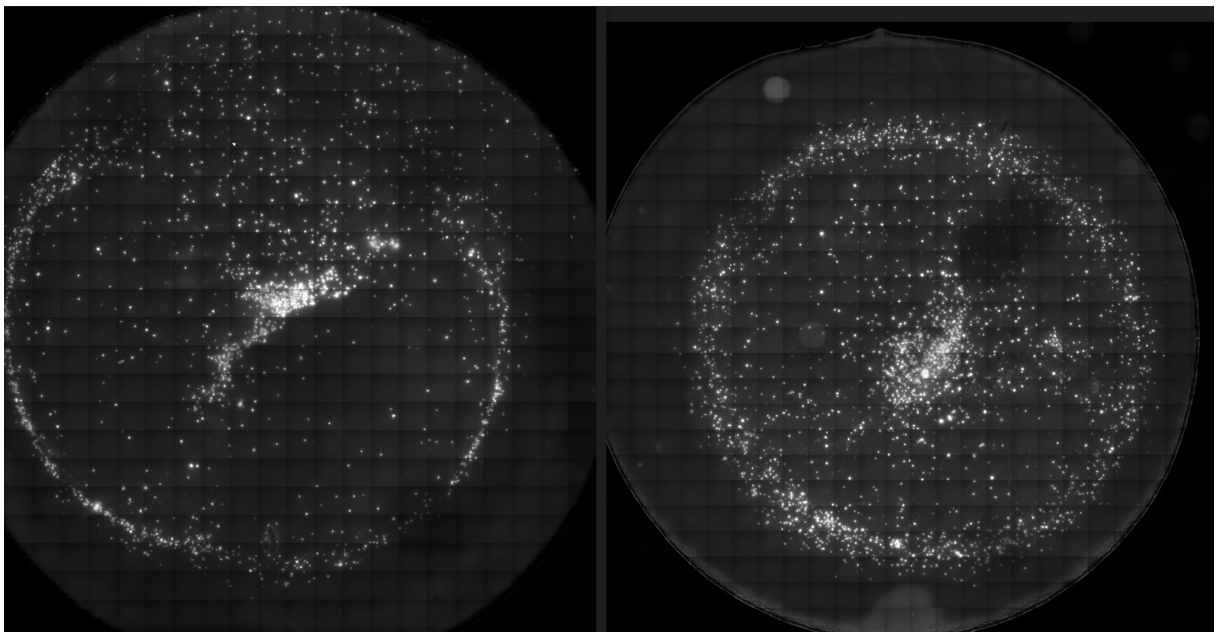

Figure 51: Left: low Confluency at harvesting (50%). Right: high Confluency at harvesting (completely overgrown, 100%). There is no clear difference. Both have the same height of intensity peaks. There might be a different spreading pattern visible however, repeats should be done to investigate if this is due to cell behaviour or due to the methods.

PDMS

When investigating how to get a better imprint and also in search of possible contamination, we came across the PDMS part inside of the clamper that hold the membrane up. Since these were old and way more often used than recommended by the professionals from VYCAP, we decided to produce new ones. This is done in the same way as standard PDMS chips are being produced, see Appendix 8.13 for the procedure. However after this VYCAP provided us with new PDSM bottoms regularly so we didn't have to do it ourselves. As a rule you could change the PDMS bottom every 5 times. When you want to be sure or for important experiments, change it every 2 or 3 times. We found no improvements after

changing the PDMS layers for new ones.

Quantification

For quantification of the PSA secretion, plots could be made. An attempt has been made, but never resulted in reliable results. That might have been concluded to abruptly or under the wrong assumption that there would be a linear relation between concentration and fluorescence intensity. This has been done before with anti-EpCAM antibodies printed on PVDF membrane[146] and even though individual measurements do seem to be unreliable, the overal results in an calibration curve that could be used for quantification.

Seeding

While seeding cells keep track of how many seconds it takes for a droplet to pass. When it takes more than 3 minutes, the chip is likely almost full. Also, when wetting the chip, without pre-wetting in the vacuum-pump beforehand, light tapping of the pump unit helps.

Chip

The chip has a very low throughput. Preparation of the chip plus the seeding takes a long time which will prevent applying these technologies on a bigger level.

The samples that we aim at, DLA samples of cancer patients, are very precious and should be handled with care. We should be sure a chip will work since we can not waste a sample. Chips are often faulty. They are broken and or not properly attached. This causes sample to flow next to the chip without catching any cells.

The wetting procedure of the chip is laborious and often takes several tries, this should be optimized. When applying vacuum to get the ethanol to enter the wells, often the set up needs to be shaken to get rid of bubbles. Also often vacuum needs to be reapplied in order to reach good wetting. It often takes long before wetting has taken place, however ethanol evaporates which causes the risk of the chip becoming dry, which will ruin the wetting process.

The seeding procedure is laborious, the chip needs to be constantly watched if there is still liquid flowing (if drops keep on falling). When you feel like the liquid is stopping, the chip is likely full and seeded. Then you have to take the chip out and check under the microscope if the chip is seeded. When this is not the case, the chip should be put back in the pump and seeding continuous. This should all be done while keeping the chip sterile.

The biggest problem of the chip is that there is only one chip. There are no controls with the same complexity level. This makes it hard to check the many steps of all the protocols. The best controls we can use is seeding directly on a membrane. This leaves all possible errors which come with the chip (seeding, putting it on the clamp unit, proper contact between chips and membranes, imaging of the chip) without proper control. That makes is difficult to determine where a problem might be if one arises, which is often the case in research.

Good hardware is needed. The computers we used often struggled with handling the obtained data since we work with pictures of up to 3 GB per channel. With overlaying channels this could go up to 15 GB. Therefore, this could only be done with compromised pictures, which reduced the quality of the pictures and the identification of the 6400 wells and the possible cells within. When new hardware came combined with software to progress the pictures, this became already better.

Good hardware is also needed to decrease scanning times. When scanning more than 3 channels, there was a change that chips would become dry during the last scans which ruins the scans, the chip,

and the cells. When using a cover slip, evaporation was slower but eventually air bubbles formed under it which scattered the light and ruined the scans. When using no cover slips, evaporation was even faster.

5.5.3 Future research

Multiple secretion product analysis

Right now we only look at one secretion product. However, there are techniques to look into multiple secretion products at the same time, like using ELIspot for multi-level analysis in fluorospot assays. The use of this is already demonstrated with multiple fluorophores and with the use of filters[147]. It is the same principal used for the imaging of the cells, but then applied on secretion products.

Further isolation

The cells who are proven to be CTCs can be further isolated by the punch system. A needle can punch out the bottom of a microwell by only touching the corners and thereby leaving the cell on top of the pore in the middle intact.[144] This gives the option of culturing these CTCs after isolation and then do tests with drugs in order to see which will work. Next to that this will also give the possibility to look into the DNA, RNA, and protein expression of these CTCs. Thereby gaining more knowledge about CTCs, but moreover work towards more individualised medicine.

Cell line type

Experiments were done with LNCaP cells. Which have very low stiffness (less than half of DU145, and significantly less stiff than PC-3 cells) and thus are more fluid-like[155]. Using other cell lines might result in higher catch rates.

Enrichment not sufficient

The chips with the PCa patient DLA samples were filled with leukocytes. Only sometimes were there CTCs found. This is likely due to al the debris and already full wells. Therefore, the enrichment procedure does not seem sufficient enough if the Vycap chip is used. An extra cleaning step needs to be implemented to get rid of everything that is not a CTC. A technique already used in this report which can also be applied in sorting cells is flowcytometry in the form of Fluorescence Activated Cell Sorting (FACS). PSMA can be used to select CTC, CD45 can be used to deselect leukocytes, and DAPI can be used to get rid of dead cells.

There are in house experiments with optimization of the FF enrichment, by simply doing it multiple times. Which does result in some loss of CTC but also major decreases in leukocytes.

6 General discussion

We tried to make a step towards more personalised medicine for metastasized PCa Patients because of their relative poor survival conditions (32% 5 year survival rate) and the large number of PCa patients. Treatment options increased rapidly and more secure guidance is needed to tackle the heterogeneity of PCa, which can be provided by CTCs. However, it is ofcourse not only PCa patients at which these techniques will be applicable. With the right target biomarkers, FF can be designed for any sort of CTC of different origin, the self seeding microwell chip works for any CTC, and the secretion analysis method only requires good literature reviews in order to determine which secretion product is of interest.

We looked into epitope compatibility. However later on we realised that the FF might pose a larger problem because of their size and possible steric hindrance. This was seen due to the opposite results of Chapter 3 and Chapter 5.1.2. Which reported positively about using two targeting antibodies as combination, and showed negative results while using it with the combination of FF and fluorophores, respectively. Downsizing on the FF might be of interest. When their size decrease influences their enrichment capacities, looking into option to bind multiple FF to each other for enrichment and afterwards breaking these bonds might be of interest. Also instead of staining the cells, staining the FF proved to work well. We recommend that method in combination with CD45 staining to weed out false positives.

We measured the decreased cell viability due to the FF, but also saw that the metabolic activity was not changed. Since viability is a factor that influences metabolic activity, more research should be done. We recommend looking into other methods that tell something about cell behaviour like looking into mitochondrial activity or directly measuring cells dying due to apoptosis by lactate dehydrogenase.

We made the first steps towards single cell secretion analysis. However a lot of optimization has to be done before there will be any results that might be useful. Next to that, an extra enrichment step should be added and we recommend using the in this research often used flowcytometer to sort cells based upon fluorescence signal. Sort positive for PSMA, sort negative for CD45. If wanted, dead or apoptotic cells can be filtered out by sorting negative on for example DAPI and Apotracker. We did however prove that we can catch CTC's from PCa patient samples, so there is definitely a step made towards more personalised medicine to improve the life expectancy of metastatic PCa patients by delivering correct, responsive treatment for their disease.

7 General conclusion

When targeting EpCAM like we do for enrichment, the epitopes for HO3 and VU1D9 can be targeted at the same time without interference of each other. These antibodies can be attached to a fluorophore and by increasing the threshold for FSC at flowcytometry, can be used as a reliable staining. When choosing between the fluorophores to attach, choose BV421 above BV605. However, there might be steric hindrance of the FF, since we get worse signal from the EpCAM antibodies when cells are enriched and measuring with flowcytometry. When looking with fluorescence microcopy in chips we have very dim (it at all any) fluorescence. Therefore, staining the FF might be interesting with a counterstain for CD45 to rule out false positives.

While using EpCAM as a target for enrichment, keep in mind that CTCs might have varying EpCAM expression levels, depending on the sort of cancer and the heterogeneity of the cancer, as demonstrated with the higher EpCAM expression on LNCaP cells versus PC-3 cells.

Flowcytometry is reliable when looking at viability influence of FF due to the enrichment procedure. The best performing staining was DAPI which proved a significant difference between cells (exposed or non-exposed to the magnet) and cells bound by FF in which FF do decrease cell viablity. Trypan blue shows this same significant reduction in viability due to FF. However most interestingly, according to our Alamar Blue Assays metabolic activity was not significantly reduced due to the enrichment procedure. This is surprisingly since there was cell death, which is a factor that would naturally also be present in the metabolic activity studies.

The basis has been established for determining if the enrichment of cells does influence their secretion patterns. With the Vycap chip we can isolate cells and these cells do show secretion patterns visible on our membranes. For future research, optimizing protocol will likely result in sufficient intense secretion patterns to be compared in order to determine if FF influence these secretion pattern.

Secretion of PSA of individual cells is seen when looking at isolated single cells from the cell line LNCaP. Secretion patterns can also be seen of DLA samples from PCa patients when the enriched CTCs are directly seeded on the membrane. More optimization has to be done to get images of isolated CTC secretion patterns.

References

[1] Marieb EN, Hoehn K. Human anatomy physiology. Pearson; 2013.

[2] Stamey TA, Yang N, Hay AR, McNeal JE, Freiha FS, Redwine E. Prostate-specific antigen as a serum marker for adenocarcinoma of the prostate. The New England journal of medicine. 1987 10;317:909–916.

[3] Moreira DM, Abern MR. Prostate cancer: Overview, detection, treatment. Encyclopedia of Reproduction. 2018 1:474–478.

[4] Bhandari R, Thomas V, Giri S, Kumar PP, Cook-Glenn C. Small Cell Carcinoma of the Prostate: A Case Report and Review of the Literature. 2020.

[5] Wang W, Epstein JI. Small cell carcinoma of the prostate: A morphologic and immunohistochemical study of 95 cases. American Journal of Surgical Pathology. 2008 1;32:65–71.

[6] Munoz F, Franco P, Ciammella P, Clerico M, Giudici M, Filippi AR, et al. Squamous cell carcinoma of the prostate: long-term survival after combined chemo-radiation. Radiation Oncology (London, England). 2007 4;2:15.

[7] Moskovitz B, Munichor M, Bolkier M, Lime PM. Squamous cell carcinoma of the prostate. Urologia internationalis. 1993;51:181–183.

[8] Malik RD, Ba B, Dakwar G, Hardee ME, Sanfilippo NJ, Rosenkrantz AB, et al. Squamous Cell Carcinoma of the Prostate. Reviews in Urology. 2011;13:56.

[9] Gangadharan V, Prakash G, Eswari V, Kannan I. Primary urothelial carcinoma of prostate: A rare case report. International Journal of Medical Research Health Sciences. 2014;3:212.

[10] Hardeman SW, Soloway MS. Transitional cell carcinoma of the prostate: Diagnosis, staging and management. World Journal of Urology. 1988 12;6:170–174.

[11] Collins S. Types of Prostate Cancer; 2021. Available from: `https://www.webmd.com/prostate-cancer/types-prostate-cancer`.

[12] The Surveillance E, (NIH) ERSNCI. Prostate Cancer Cancer Stat Facts; 2022. Available from: `https://seer.cancer.gov/statfacts/html/prost.html`.

[13] Gillessen S, Attard G, Beer TM, Beltran H, Bjartell A, Bossi A, et al. Management of Patients with Advanced Prostate Cancer: Report of the Advanced Prostate Cancer Consensus Conference 2019. European Urology. 2020 4;77:508–547.

[14] Gandaglia G, Abdollah F, Schiffmann J, Trudeau V, Shariat SF, Kim SP, et al. Distribution of metastatic sites in patients with prostate cancer: A population-based analysis. The Prostate. 2014 2;74:210–216.

[15] McDougall JA, Bansal A, Goulart BHL, McCune JS, Karnopp A, Fedorenko C, et al. The Clinical and Economic Impacts of Skeletal-Related Events Among Medicare Enrollees With Prostate Cancer Metastatic to Bone. The Oncologist. 2016 3;21:320–326.

[16] Tangirala K, Appukkuttan S, Simmons S. Costs and Healthcare Resource Utilization Associated with Hospital Admissions of Patients with Metastatic or Nonmetastatic Prostate Cancer. American Health Drug Benefits. 2019 10;12:306.

[17] Yang C, Xia BR, Jin WL, Lou G. Circulating tumor cells in precision oncology: clinical applications in liquid biopsy and 3D organoid model. Cancer Cell International 2019 19:1. 2019 12;19:1–13.

[18] Nagrath S, Sequist LV, Maheswaran S, Bell DW, Irimia D, Ulkus L, et al. Isolation of rare circulating tumour cells in cancer patients by microchip technology. Nature 2007 450:7173. 2007 12;450:1235–1239.

[19] Salsbury AJ. The significance of the circulating cancer cell. Cancer Treatment Reviews. 1975 3;2:55–72.

[20] de Bono JS, Scher HI, Montgomery RB, Parker C, Miller MC, Tissing H, et al. Circulating Tumor Cells Predict Survival Benefit from Treatment in Metastatic Castration-Resistant Prostate Cancer. Clinical Cancer Research. 2008 10;14:6302–6309.

[21] Cho H, Oh CK, Cha J, Chung JI, Byun SS, Hong SK, et al. Association of serum prostate-specific antigen (PSA) level and circulating tumor cell-based PSA mRNA in prostate cancer. Prostate International. 2022 3;10:14.

[22] Fischer JC, Niederacher D, Topp SA, Honisch E, Schumacher S, Schmitz N, et al. Diagnostic leukapheresis enables reliable detection of circulating tumor cells of nonmetastatic cancer patients. 2013.

[23] Cunningham D, You Z. In vitro and in vivo model systems used in prostate cancer research. Journal of Biological Methods. 2015;2:17.

[24] Horoszewicz JS, Leong SS, Chu TM, Wajsman ZL, Friedman M, Papsidero L, et al. The LNCaP cell line–a new model for studies on human prostatic carcinoma. Progress in clinical and biological research. 1980;37:115–132.

[25] Horoszewicz JS, Leong SS, Kawinski E, Karr JP, Rosenthal H, Chu TM, et al. LNCaP Model of Human Prostatic Carcinoma. Cancer Research. 1983;43.

[26] Wu X, Gong S, Roy-Burman P, Lee P, Culig Z. Current mouse and cell models in prostate cancer research. Endocrine-related cancer. 2013 8;20.

[27] Bokhoven AV, Varella-Garcia M, Korch C, Johannes WU, Smith EE, Miller HL, et al. Molecular Characterization of Human Prostate Carcinoma Cell Lines. Prostate. 2003 11;57:205–225.

[28] Webber. Immortalized and tumorigenic adult human prostatic epithelial cell lines: Characteristics and applications part 2. Tumorigenic cell lines; 1997. Available from: `https://onlinelibrary-wiley-com.ezproxy2.utwente.nl/doi/pdf/10.1002`.

[29] Culig Z, Hoffmann J, Erdel M, Eder IE, Hobisch A, Hittmair A, et al. Switch from antagonist to agonist of the androgen receptor blocker bicalutamide is associated with prostate tumour progression in a new model system. British Journal of Cancer. 1999;81:242.

[30] Wu TT, Sikes RA, Cui Q, Thalmann GN, Kao C, Murphy CF, et al. ESTABLISHING HUMAN PROSTATE CANCER CELL XENOGRAFTS IN BONE: INDUCTION OF OSTEOBLASTIC REACTION BY PROSTATE-SPECIFIC ANTIGEN-PRODUCING TUMORS IN ATHYMIC AND SCID/bg MICE USING LNCaP AND LINEAGE-DERIVED METASTATIC SUBLINES. J Cancer. 1998;77:887–894.

[31] Kaighn ME, Narayan KS, Ohnuki Y, Lechner JF, Jones LW. Establishment and characterization of a human prostatic carcinoma cell line (PC-3). Investigative Urology. 1979;17:16–23.

[32] Xu Y, Zhao H, Hou J. Correlation between overexpression of EpCAM in prostate tissues and genesis of androgen-dependent prostate cancer. Tumour biology : the journal of the International Society for Oncodevelopmental Biology and Medicine. 2014;35:6695–6700.

[33] Pettaway CA, Pathak S, Greene G, Ramirez E, Wilson MR, Killion JJ, et al. Selection of Highly Metastatic Variants of Different Human Prostatic Carcinomas Using Orthotopic Implantation in Nude Mice1. Clinical Cancer Research. 1996;2:627.

[34] Korenchuk S, Lehr JE, McLean L, Lee YG, Whitney S, Vessella R, et al. VCaP, a cell-based model system of human prostate cancer. In Vivo (Athens, Greece). 2001 3;15:163–168.

[35] Stone KR, Mickey DD, Wunderli H, Mickey GH, Paulson DF. Isolation of a human prostate carcinoma cell line (DU 145). International Journal of Cancer. 1978 3;21:274–281.

[36] Scaccianoce E, Festuccia C, Dondi D, Gucrini V, Bologna M, Motta M, et al. Characterization of prostate cancer DU145 cells expressing the recombinant androgen receptor. Oncology research. 2003;14:101–112.

[37] Klein KA, Reiter RE, Redula J, Moradi H, Zhu XL, Brothman AR, et al. Progression of metastatic human prostate cancer to androgen independence in immunodeficient SCID mice. Nature Medicine. 1997;3:402–408.

[38] Bello D, Webber MM, Kleinman HK, Wartinger DD, Rhim JS. Androgen responsive adult human prostatic epithelial cell lines immortalized by human papillomavirus 18 useful cell culture models for studies on prostate growth regulation and carcinogenesis. Carcinogenesis. 1997;18:1215–1223.

[39] Lee YG, Korenchuk S, Lehr J, Whitney S, Vessela R, Pienta KJ. Establishment and characterization of a new human prostatic cancer cell line: DuCaP. In Vivo (Athens, Greece). 2001 3;15:157–162.

[40] Thalmann GN, Anezinis PE, Chang SM, Zhau HE, Kim EE, Hopwood VL, et al. Androgen-independent Cancer Progression and Bone Metastasis in the LNCaP Model of Human Prostate Cancer. 1994.

[41] Nagabhushan M, Miller CM, Pretlow TP, Giaconia JM, Edgehouse NL, Schwartz S, et al. CWR22: The First Human Prostate Cancer Xenograft with Strongly Androgen-dependent and Relapsed Strains Both in Vivo and in Soft Agar1. CANCER RESEARCH. 1996;56:3042–3046.

[42] Sramkoski RM, Pretlow TG, Giaconia JM, Pretlow TP, Schwartz S, Sy MS, et al. A new human prostate carcinoma cell line, 22Rv1. In vitro cellular developmental biology Animal. 1999;35:403–409.

[43] Macleod RAF, Dirks WG, Matsuo Y, Kaufmann M, Milch H, Drexler HG. WIDESPREAD INTRASPECIES CROSS-CONTAMINATION OF HUMAN TUMOR CELL LINES ARISING AT SOURCE. J Cancer. 1999;83:555–563.

[44] Bokhoven AV, Varella-Garcia M, Korch C, Hessels D, Miller GJ. Widely used prostate carcinoma cell lines share common origins. The Prostate. 2001 4;47:36–51.

[45] Varella-Garcia M, Boomer T, Miller GJ. Karyotypic similarity identified by multiplex-FISH relates four prostate adenocarcinoma cell lines: PC-3, PPC-1, ALVA-31, and ALVA-41. Genes, Chromosomes and Cancer. 2001 8;31:303–315.

[46] Webber M. Immortalized and tumorigenic adult human prostatic epithelial cell lines: Characteristics and applications part I. Cell markers and immortalized nontumorigenic cell lines; 1996. Available from: `https://onlinelibrary-wiley-com.ezproxy2.utwente.nl/doi/pdf/10.1002`.

[47] Alberts B, Bray D, Johnson A, Lewis J, Raff M, Roberts K, et al. Essential Cell Biolog. W.W. Norton Company; 2013.

[48] Springer TA. Adhesion receptors of the immune system. Nature. 1990;346:425–434.

[49] Petruzzelli L, Takami M, Humes HD. Structure and function of cell adhesion molecules. American Journal of Medicine. 1999;106:467–476.

[50] Hosono H, Ohishi T, Takei J, Asano T, Sayama Y, Kawada M, et al. The antiepithelial cell adhesion molecule (EpCAM) monoclonal antibody EpMab16 exerts antitumor activity in a mouse model of colorectal adenocarcinoma. Oncology Letters. 2020 12;20:1–1.

[51] Litvinov SV, Velders MP, Bakker HAM, Fleuren GJ, Warnaar SO. Ep-CAM: A Human Epithelial Antigen Is a Homophilic Cell-Cell Adhesion Molecule. The Journal Of Cell Biology. 1994;125.

[52] Pavi M, Gunar G, Djinovi-Carugo K, Lenari B. Crystal structure and its bearing towards an understanding of key biological functions of EpCAM. Nature Communications. 2014 8;5.

[53] Sharma S, Zhuang R, Long M, Pavlovic M, Kang Y, Ilyas A, et al. Circulating Tumor Cell Isolation, Culture, and Downstream Molecular Analysis. Biotechnology advances. 2018 7;36:1063.

[54] Danila DC, Heller G, Gignac GA, Gonzalez-Espinoza R, Anand A, Tanaka E, et al. Circulating Tumor Cell Number and Prognosis in Progressive Castration-Resistant Prostate Cancer. Clinical Cancer Research. 2007 12;13:7053–7058.

[55] Kim MS, Sim TS, Kim YJ, Kim SS, Jeong H, Park JM, et al. SSA-MOA: a novel CTC isolation platform using selective size amplification (SSA) and a multi-obstacle architecture (MOA) filter. Lab on a Chip. 2012 7;12:2874–2880.

[56] Cohen SJ, Punt CJA, Iannotti N, Saidman BH, Sabbath KD, Gabrail NY, et al. Relationship of circulating tumor cells to tumor response, progression-free survival, and overall survival in patients with metastatic colorectal cancer. Journal of clinical oncology : official journal of the American Society of Clinical Oncology. 2008;26:3213–3221.

[57] Raimondi C, Nicolazzo C, Gradilone A. Circulating tumor cells isolation: the post-EpCAM era. Chinese Journal of Cancer Research. 2015 10;27:461.

[58] Mashhadi SMY, Kazemimanesh M, Arashkia A, Azadmanesh K, Meshkat Z, Golichenari B, et al. Shedding light on the EpCAM: An overview. Journal of Cellular Physiology. 2019 8;234:12569–12580.

[59] Lei Z, Maeda T, Tamura A, Nakamura T, Yamazaki Y, Shiratori H, et al. EpCAM contributes to formation of functional tight junction in the intestinal epithelium by recruiting claudin proteins. Developmental Biology. 2012 11;371:136–145.

[60] Münz M, Murr A, Kvesic M, Rau D, Mangold S, Pflanz S, et al. Side-by-side analysis of five clinically tested anti-EpCAM monoclonal antibodies. Cancer Cell International. 2010 11;10:1–12.

[61] Andree K. Circulating Tumor Cells a Real-Time Liquid Biopsy; 2019.

[62] Andree KC, Barradas AMC, Nguyen AT, Mentink A, Stojanovic I, Baggerman J, et al. Capture of Tumor Cells on Anti-EpCAM-Functionalized Poly(acrylic acid)-Coated Surfaces. ACS Applied Materials and Interfaces. 2016 6;8:14349–14356.

[63] Brilliant Violet;. Available from: `https://www.biolegend.com/en-us/brilliant-violet`.

[64] Helms V. Principles of computational cell biology : from protein complexes to cellular networks. 2019;second edition:440.

[65] Scientific T. Fluorescence SpectraViewer;. Available from: `https://www.thermofisher.com/order/fluorescence-spectraviewer?SID=srch-svtool&UID=2762ph8#!/`.

[66] Suthanthiraraj PPA, Graves SW. Fluidics. Current protocols in cytometry / editorial board, J Paul Robinson, managing editor [et al]. 2013;0 1:Unit.

[67] McKinnon KM. Flow Cytometry: An Overview. Current protocols in immunology. 2018 2;120:5.1.1.

[68] Sabban S. Development of an in vitro model system for studying the interaction of Equus caballus IgE with its highaffinity FcRI receptor; 2011.

[69] ThermoFisher. DAPI Protocol for Fluorescence Imaging - NL. Available from: https://www.thermofisher.com/uk/en/home/references/protocols/cell-and-tissue-analysis/protocols/dapi-imaging-protocol.html.

[70] Thermofisher. DAPI (4',6-diamidino-2-phenylindole) | Thermo Fisher Scientific - NL;. Available from: https://www.thermofisher.com/nl/en/home/life-science/cell-analysis/fluorophores/dapi-stain.html.

[71] BioLegend. Brilliant Violet 421 Streptavidin;. Available from: https://www.biolegend.com/it-it/products/brilliant-violet-421-streptavidin-7297.

[72] Tan YH, Liu M, Nolting B, Go JG, Gervay-Hague J, Liu GY. A Nanoengineering Approach for Investigation and Regulation of Protein Immobilization. ACS nano. 2008 11;2:2374.

[73] Schnell U, Cirulli V, Giepmans BNG. EpCAM: Structure and function in health and disease. Biochimica et Biophysica Acta (BBA) - Biomembranes. 2013 8;1828:1989–2001.

[74] Molter CW, Muszynski EF, Tao Y, Trivedi T, Clouvel A, Ehrlicher AJ. Prostate cancer cells of increasing metastatic potential exhibit diverse contractile forces, cell stiffness, and motility in a microenvironment stiffness-dependent manner. Frontiers in Cell and Developmental Biology. 2022 9;0:1862.

[75] Zhang X, Lin Y, Gillies RJ. Tumor pH and its measurement. Journal of nuclear medicine : official publication, Society of Nuclear Medicine. 2010 8;51:1167.

[76] Huang S, Tang Y, Peng X, Cai X, Wa Q, Ren D, et al. Acidic extracellular pH promotes prostate cancer bone metastasis by enhancing PC-3 stem cell characteristics, cell invasiveness and VEGF-induced vasculogenesis of BM-EPCs. Oncology reports. 2016 10;36:2025–2032.

[77] Gires O, Pan M, Schinke H, Canis M, Baeuerle PA. Expression and function of epithelial cell adhesion molecule EpCAM: where are we after 40 years?. Springer; 2020.

[78] Voit W, Kim DK, Zapka W, Muhammed M, Rao KV. Magnetic behavior of coated superparamagnetic iron oxide nanoparticles in ferrofluids. MRS Online Proceedings Library (OPL). 2001;676:Y7.8.

[79] Helmenstine AM. How to Synthesize Ferrofluid (Liquid Magnets); 2020. Available from: https://www.thoughtco.com/how-to-make-liquid-magnets-606319.

[80] Molday RS, Yen SPS, Rembaum A. Application of magnetic microspheres in labelling and separation of cells. Nature. 1977;268:437–438.

[81] Molday RS, Mackenzie D. Immunospecific ferromagnetic iron-dextran reagents for the labeling and magnetic separation of cells. Journal of immunological methods. 1982 8;52:353–367.

[82] Miltenyi S, Müller W, Weichel W, Radbruch A. High gradient magnetic cell separation with MACS. Cytometry. 1990;11:231–238.

[83] Thomas TE, Abraham SJR, Otter AJ, Blackmore EW, Lansdorp PM. High gradient magnetic separation of cells on the basis of expression levels of cell surface antigens. Journal of Immunological Methods. 1992 10;154:245–252.

[84] Waseem S, Udomsangpetch R, Bhakdi SC. Buffer-optimized high gradient magnetic separation: Target cell capture efficiency is predicted by linear bead-capture theory. Journal of Magnetics. 2016;21:125–132.

[85] Bohmer N, Demarmels N, Tsolaki E, Gerken L, Keevend K, Bertazzo S, et al. Removal of Cells from Body Fluids by Magnetic Separation in Batch and Continuous Mode: Influence of Bead Size, Concentration, and Contact Time. ACS Applied Materials and Interfaces. 2017 9;9:29571–29579.

[86] Hejazian M, Li W, Nguyen NT. Lab on a chip for continuous-flow magnetic cell separation. Lab on a Chip. 2015 2;15:959–970.

[87] Liu P, Jonkheijm P, Terstappen LWMM, Stevens M. Magnetic particles for ctc enrichment. MDPI AG; 2020.

[88] Thermofisher. Calcein, AM, cell-permeant dye;. Available from: https://www.thermofisher.com/order/catalog/product/C1430.

[89] Czepluch FS, Olieslagers SJF, Waltenberger J. Monocyte function is severely impaired by the fluorochrome calcein acetomethylester. Biochemical and Biophysical Research Communications. 2007 9;361:410–413.

[90] Liminga G, Nygren P, Dhar S, Nilsson K, Larsson R. Cytotoxic effect of calcein acetoxymethyl ester on human tumor cell lines drug delivery by intracellular trapping; 1995.

[91] Jonsson B, Liminga G, Csoka K, Fridborg H, Dhar S, Nygren P, et al. Cytotoxic activity of calcein acetoxymethyl ester (Calcein/AM) on primary cultures of human haematological and solid tumours. European journal of cancer (Oxford, England : 1990). 1996;32A:883–887.

[92] Lv Y, Liu R, Xie S, Zheng X, Mao J, Cai Y, et al. Calcein-acetoxymethy ester enhances the antitumor effects of doxorubicin in nonsmall cell lung cancer by regulating the TopBP1/p53RR pathway. Anti-Cancer Drugs. 2017 6;28:861–868.

[93] Gatti R, Belletti S, Orlandini G, Bussolati O, Dall'Asta V, Gazzola GC. Comparison of annexin V and calcein-AM as early vital markers of apoptosis in adherent cells by confocal laser microscopy. Journal of Histochemistry and Cytochemistry. 1998 6;46:895–900.

[94] Probes IM. MP 03224 LIVE/DEAD ő Viability/Cytotoxicity Kit Product Information. 2005.

[95] Thermofisher. Propidium Iodide | Thermo Fisher Scientific - NL;. Available from: `https://www.thermofisher.com/nl/en/home/life-science/cell-analysis/fluorophores/propidium-iodide.html`.

[96] Wallberg F, Tenev T, Meier P. Analysis of Apoptosis and Necroptosis by Fluorescence-Activated Cell Sorting. Cold Spring Harbor Protocols. 2016 4;2016:pdb.prot087387.

[97] Strober W. Trypan Blue Exclusion Test of Cell Viability. Current Protocols in Immunology. 1997 3;21:A.3B.1–A.3B.2.

[98] Tran SL, Puhar A, Ngo-Camus M, Ramarao N. Trypan Blue Dye Enters Viable Cells Incubated with the Pore-Forming Toxin HlyII of Bacillus cereus. PLoS ONE. 2011;6.

[99] Hantz HL, Young LF, Martin KR. Physiologically Attainable Concentrations of Lycopene Induce Mitochondrial Apoptosis in LNCaP Human Prostate Cancer Cells:. https://doiorg/101177/153537020523000303. 2016 11;230:171–179.

[100] Strober W. Trypan Blue Exclusion Test of Cell Viability. Current protocols in immunology. 2015 11;111:A3.B.1.

[101] Huaman J, Naidoo M, Zang X, Ogunwobi OO. Fibronectin Regulation of Integrin B1 and SLUG in Circulating Tumor Cells. Cells. 2019;8.

[102] BioLegend. Apotracker Green;. Available from: `https://www.biolegend.com/fr-fr/products/apotracker-green-18527?GroupID=GROUP22`.

[103] Biologicals N. Phosphatidylserine Externalization in Apoptosis;. Available from: `https://www.novusbio.com/research-topics/apoptosis/phosphatidylserine-externalization`.

[104] Rampersad SN. Multiple Applications of Alamar Blue as an Indicator of Metabolic Function and Cellular Health in Cell Viability Bioassays. Sensors (Basel, Switzerland). 2012 9;12:12347.

[105] Thermofisher. alamarBlue Assays for Cell Viability | Thermo Fisher Scientific - NL;. Available from: `https://www.thermofisher.com/nl/en/home/life-science/cell-analysis/fluorescence-microplate-assays/microplate-assays-cell-viability/alamarblue-assay-cell-viability.html`.

[106] Invitrogen. alamarBlueő Cell Viability Reagent protocol;.

[107] Invitrogen. MP 03224 LIVE/DEAD ő Viability/Cytotoxicity Kit Product Information.

[108] McHugh ML. Multiple comparison analysis testing in ANOVA; 2011.

[109] Thermofisher. Ethidium Homodimer-1 (EthD-1);. Available from: `https://www.thermofisher.com/order/catalog/product/E1169`.

[110] Thermofisher. CyQUANT LDH Cytotoxicity Assay;. Available from: `https://www.thermofisher.com/order/catalog/product/C20301`.

[111] Kumar P, Nagarajan A, Uchil PD. Analysis of Cell Viability by the Lactate Dehydrogenase Assay. Cold Spring Harbor protocols. 2018 6;2018:465–468.

[112] Foss CA, Mease RC, Cho SY, Kim HJ, Pomper MG. GCPII imaging and cancer. Current medicinal chemistry. 2012 2;19:1346–1359.

[113] Chang SS. Overview of Prostate-Specific Membrane Antigen. Reviews in Urology. 2004;6:S13.

[114] Gordon IO, Tretiakova MS, Noffsinger AE, Hart J, Reuter VE, Al-Ahmadie HA. Prostate-specific membrane antigen expression in regeneration and repair. Modern Pathology. 2008 12;21:1421–1427.

[115] Dou D, Silva DVD, Nordholm J, Wang H, Daniels R. Type II transmembrane domain hydrophobicity dictates the cotranslational dependence for inversion. Molecular Biology of the Cell. 2014 11;25:3363–3374.

[116] Kiess AP, Banerjee SR, Mease RC, Rowe SP, Rao A, Foss CA, et al. Prostate-specific membrane antigen as a target for cancer imaging and therapy. The quarterly journal of nuclear medicine and molecular imaging : official publication of the Italian Association of Nuclear Medicine (AIMN) [and] the International Association of Radiopharmacology (IAR), [and] Section of the Society of. 2015 9;59:241.

[117] Spatz S, Tolkach Y, Jung K, Stephan C, Busch J, Ralla B, et al. Comprehensive Evaluation of Prostate Specific Membrane Antigen Expression in the Vasculature of Renal Tumors: Implications for Imaging Studies and Prognostic Role. Journal of Urology. 2018 2;199:370–377.

[118] Tan N, Bavadian N, Calais J, Oyoyo U, Kim J, Turkbey IB, et al. Imaging of Prostate Specific Membrane Antigen Targeted Radiotracers for the Detection of Prostate Cancer Biochemical Recurrence after Definitive Therapy: A Systematic Review and Meta-Analysis. Journal of Urology. 2019 8;202:231–240.

[119] Juzeniene A, Stenberg VY, Øyvind Sverre Bruland, Larsen RH. Preclinical and Clinical Status of PSMA-Targeted Alpha Therapy for Metastatic Castration-Resistant Prostate Cancer. Cancers 2021, Vol 13, Page 779. 2021 2;13:779.

[120] Boinapally S, Ahn HH, Cheng B, Brummet M, Nam H, Gabrielson KL, et al. A prostate-specific membrane antigen (PSMA)-targeted prodrug with a favorable in vivo toxicity profile. Scientific Reports 2021 11:1. 2021 3;11:1–10.

[121] Rajasekaran AK, Anilkumar G, Christiansen JJ. Is prostate-specific membrane antigen a multifunctional protein? American Journal of Physiology - Cell Physiology. 2005 5;288:975–981.

[122] Staniszewska M, Costa PF, Eiber M, Klose JM, Wosniack J, Reis H, et al. Enzalutamide enhances psma expression of psma-low prostate cancer. International Journal of Molecular Sciences. 2021 7;22:7431.

[123] Ruigrok EAM, van Vliet N, Dalm SU, de Blois E, van Gent DC, Haeck J, et al. Extensive preclinical evaluation of lutetium-177-labeled PSMA-specific tracers for prostate cancer radionuclide therapy. European Journal of Nuclear Medicine and Molecular Imaging. 2021 5;48:1339.

[124] Gong MC, Chang SS, Sadelain M, Bander NH, Heston WDW. Prostate-specific membrane antigen (PSMA)-specific monoclonal antibodies in the treatment of prostate and other cancers. Cancer metastasis reviews. 1999;18:483–490.

[125] of Medicine NNL. PTPRC protein tyrosine phosphatase receptor type C [Homo sapiens (human)] - Gene - NCBI;. Available from: `https://www.ncbi.nlm.nih.gov/gene?Db=gene&Cmd=ShowDetailView&TermToSearch=5788`.

[126] Holmes N. CD45: all is not yet crystal clear. Immunology. 2006 2;117:145.

[127] Barashdi MAA, Ali A, McMullin MF, Mills K. Protein tyrosine phosphatase receptor type C (PTPRC or CD45). Journal of Clinical Pathology. 2021 9;74:548–552.

[128] Rheinländer A, Schraven B, Bommhardt U. CD45 in human physiology and clinical medicine. Immunology Letters. 2018 4;196:22–32.

[129] Zhao Y, Huang Z, Lazzarini P, Wang Y, Di A, Chen M. A unique human blood-derived cell population displays high potential for producing insulin. Biochemical and Biophysical Research Communications. 2007 8;360:205–211.

[130] Saunders AE, Johnson P. Modulation of immune cell signalling by the leukocyte common tyrosine phosphatase, CD45. Cellular signalling. 2010 3;22:339–348.

[131] Schuette V, Embgenbroich M, Ulas T, Welz M, Schulte-Schrepping J, Draffehn AM, et al. Mannose receptor induces T-cell tolerance via inhibition of CD45 and up-regulation of CTLA-4. Proceedings of the National Academy of Sciences of the United States of America. 2016 9;113:10649–10654.

[132] Matthews DC, Appelbaum FR, Eary JF, Fisher DR, Durack LD, Hui TE, et al. Phase I Study of 131I-Anti-CD45 Antibody Plus Cyclophosphamide and Total Body Irradiation for Advanced Acute Leukemia and Myelodysplastic Syndrome. Blood. 1999 8;94:1237–1247.

[133] Nemecek ER, Matthews DC. Antibody-based therapy of human leukemia. Current opinion in hematology. 2002;9:316–321.

[134] Plant D, Prajapati R, Hyrich KL, Morgan AW, Wilson AG, Isaacs JD, et al. Replication of association of the PTPRC gene with response to antitumor necrosis factor therapy in a large UK cohort. Arthritis Rheumatism. 2012 3;64:665–670.

[135] Ferreiro-Iglesias A, Montes A, Perez-Pampin E, Cañete JD, Raya E, Magro-Checa C, et al. Replication of PTPRC as genetic biomarker of response to TNF inhibitors in patients with rheumatoid arthritis. Pharmacogenomics Journal. 2016 4;16:137–140.

[136] Pentyala S, Whyard T, Pentyala S, Muller J, Pfail J, Parmar S, et al.. Prostate cancer markers: An update (Review). Spandidos Publications; 2016.

[137] Robert M, Gibbs BF, Jacobson E, Gagnon C. Characterization of prostate-specific antigen proteolytic activity on its major physiological substrate, the sperm motility inhibitor precursor/semenogelin I. Biochemistry. 1997 4;36:3811–3819.

[138] Balk SP, Ko YJ, Bubley GJ. Biology of prostate-specific antigen. Journal of Clinical Oncology. 2003 1;21:383–391.

[139] Lilja H, Oldbring J, Rannevik G, Laurell CB. Seminal Vesicle-secreted Proteins and Their Reactions during Gelation and Liquefaction of Human Semen. 1987.

[140] Magklara A, Scorilas A, Stephan C, Kristiansen GO, Hauptmann S, Jung K, et al. Decreased concentrations of prostate-specific antigen and human glandular kallikrein 2 in malignant versus nonmalignant prostatic tissue. Urology. 2000 9;56:527–532.

[141] Pretlow TG, Pretlow TP, Yang B, Kaetzel CS, Delmoro CM, Kamis SM, et al. Tissue concentrations of prostate-specific antigen in prostatic carcinoma and benign prostatic hyperplasia. International Journal of Cancer. 1991 11;49:645–649.

[142] Downing S, Bumak C, Nixdorf S, Ow K, Russell P, Jackson P. Elevated Levels of Prostate-Specific Antigen (PSA) in Prostate Cancer Cells Expressing Mutant p53 is Associated with Tumor Metastasis. Molecular Carcinogenesis. 2003 11;38:130–140.

[143] Webber MM, Waghray A, Bello D. Prostate-specific Antigen, a Serine Protease, Facilitates Human Prostate Cancer Cell Invasion1. 1995;1:1089–1094.

[144] Swennenhuis JF, Tibbe AGJ, Stevens M, Katika MR, Dalum JV, Tong HD, et al. Self-seeding microwell chip for the isolation and characterization of single cells. Lab on a Chip. 2015 7;15:3039–3046.

[145] Cho E, Kim C, Kook JK, Jeong YI, Kim JH, Kim YA, et al. Fabrication of electrospun PVDF nanofiber membrane for Western blot with high sensitivity. Journal of Membrane Science. 2012 2;389:349–354.

[146] Abali F, Broekmaat J, Tibbe A, Schasfoort RBM, Zeune L, Terstappen LWMM. A microwell array platform to print and measure biomolecules produced by single cells. Lab on a Chip. 2019 5;19:1850–1859.

[147] Janetzki S, Rueger M, Dillenbeck T. Stepping up ELIspot: Multi-level analysis in fluorospot assay. Cells. 2014 11;3:1102–1115.

[148] VyCAP. Single cell analysis - VyCAP;. Available from: `https://www.vycap.com/product_cat/single-cell-analysis/`.

[149] Voit W, Kim DK, Zapka W, Muhammed M, Rao KV. Magnetic behavior of coated superparamagnetic iron oxide nanoparticles in ferrofluids. MRS Online Proceedings Library 2001 676:1. 2011 3;676:781–786.

[150] Botet R, Trohidou KN, Blackman JA, Kechrakos D. Scaling laws in magneto-optical properties of aggregated ferrofluids. American Physical Society. 2001.

[151] Culebras M, Grande CJ, Torres FG, Troncoso OP, Gomez CM, Bañó MC. Optimization of Cell Growth on Bacterial Cellulose by Adsorption of Collagen and Poly-L-Lysine. http://dxdoiorgezproxy2utwentenl/101080/009140372014958829. 2015 9;64:411–415.

[152] Haque T, Chen H, Ouyang W, Martoni C, Lawuyi B, Urbanska A, et al. Investigation of a New Microcapsule Membrane Combining Alginate, Chitosan, Polyethylene Glycol and Poly-L-Lysine for Cell Transplantation Applications. https://doi-orgezproxy2utwentenl/101177/039139880502800612. 2018 1;28:631–637.

[153] Jaasma MJ, Jackson WM, Keaveny TM. The effects of morphology, confluency, and phenotype on whole-cell mechanical behavior. Annals of Biomedical Engineering. 2006 5;34:759–768.

[154] Efremov YM, Dokrunova AA, Bagrov DV, Kudryashova KS, Sokolova OS, Shaitan KV. The effects of confluency on cell mechanical properties. Journal of Biomechanics. 2013 4;46:1081–1087.

[155] Hope JM, Bersi MR, Dombroski JA, Clinch AB, Pereles RS, Merryman WD, et al. Circulating prostate cancer cells have differential resistance to fluid shear stress-induced cell death. Journal of Cell Science. 2021 2;134.

8 Appendix

8.1 Appendix A: membrane preparation and activation

1. Cut or order membranes that they fit exactly into a well of a 24 wells plate.
2. Under sterile conditions (in hood), place membranes in the wells. Incubate membranes in 500ul of methanol (100%), and ensure that the membranes are completely covered for 1 minute.
3. Wash membranes with 1X PBS, twice.
4. Place a sterile 'O'-ring in the wells on top of the membranes. Membranes will not float, and less antibodysolution will be needed.
5. Prepare anti-PSA antibody solutions of concentration 25ug/ml (Calculate for 150 ul of anti-PSA solution for each membrane).
6. Coat membrane with 150ul of prepared Anti-PSA solutions. Ensure the entire surface is covered.
7. Incubate the membrane in 4deg C overnight.

8.2 Appendix B: membrane blocking

1. Remove the wells plate from 4deg C and aspirate out the antibody solution.
2. Prepare sterile BSA in 1X PBS solution (3%w/v). Work under sterile conditions and use a syringe with 0.2 filter to filter the solution afterwards.
3. Add 200-300ul of BSA solution to block the membrane for 1 hour.
4. Wash with 1X PBS. Leave the membranes in PBS if they are not immediately used.

8.3 Appendix C: Cell seeding and culturing on membranes

1. Make sure the 'O'-rings are still in place.
2. If cells need to be tracked, follow the corresponding staining protocol. *
3. Put the sample on the membranes. If simultaneously cells are seeded on chips, make sure the same number of cells is put on the membranes. Ideally use 500uL.
4. Place the 24 wells plate in the incubator for 1 day.

* Optional steps

8.4 Appendix D: Cell seeding on Chip

1. Get the tube, remove the lid and secure the tube in the holder.
2. Aspirate ethanol, but do not let the chip get dry, so a little bit of ethanol remains on the chip.
3. Pour PBS on the chip, completely immerse the chip and shake the chip a little.
4. Pour some PBS inside of the tube, especially the blue part (the soft material), needs to be washed.
5. Place the chip in the tube, push it softly in.
6. Pour some PBS on top of the chip.
7. Wash with PBS, ideal seeding pressure is maximum 10 mbar, but for washing with PBS pressure as high as 100 mbar can be used.
8. Check if drops come through, and never let the chip go dry.
9. Wash with standard culture medium if seeding cell lines (special medium if working with DLA samples), approx. 2mL
10. If filtrate analysis is wanted, stop the pump system. Change tubes and clean as done in step 4. End with a little bit of medium, and empty the tube before placing the chip.
11. Add the sample with a pipet in the chip. Prepare the sample in such a manner that between 0.1 and 1 mL of the sample dilution is sufficient.
12. Add some medium on top. Approx. 1 mL.
13. Use a pressure of max. 10 mbar.
14. If needed, add some more medium, especially at the sides in order for potential cells there to not get stuck.
15. After seeding, or when the chip gets stuck possibly due to blockage, take the chip out and put it in a sterile petridish.
16. Check under the microscope if an appropriate number of cells is present in the chip. If not, repeat procedure starting at step 11.

8.5 Appendix E: Preparing for imaging and imaging of seeded chips

1. Start the software.
2. Place a sterile chipholder in the puncher system.
3. Get a sterile glass coverslide. *
4. Add PBS on top of the coverslide. *
5. Place the coverslide on top of the chip. *
6. Remove excess liquid, and dry the bottom of the chip via the corners.
7. Place chip in the chipholder.
8. In the software, select 'load/align slide'
9. In the software, insert name and date.
10. Set the exposure time for the real time image on the software inbetween 50-200ms.
11. Find the chip, direct the chipholder with chip directly under the objective.
12. Find focus, in such a way that individual wells are seen, focus on the bottom of the wells.
13. Find the left corner of the chip(where wells are still present). Select the uttermost left corner well.
14. Repeat for the bottom right and top right corner wells. Then click 'accept'.
15. Three spots on the chip in-between the just selected corners are shown one after another. Check the focus, very quick checks in other filter channels can be done but be sure not to bleach. Then select 'accept'.
16. Select the exposure times for all different channels. Do very quick checks the first time when imaging what are the best exposure times and if signal is visible. Then stick with those values and fill those in every time.
17. Click 'start imaging' and the software will collect the data channel by channel.
18. After imaging, remove the chip from the chipholder.
19. Remove the coverslide from the chip.

* Optional steps

8.6 Appendix F: Culturing on chip while collecting secretion

1. Get the seeded and imaged chip.
2. Get the sterile clamper, make sure a sterile 'o'ring and a sterile PDMS mold are present.
3. Get a sterile, anti-PSA coated, PVDF membrane.
4. Pull the lever on the clamper up and take of the top of the clamper.
5. Place the PDMS mold in the bottom of the clamper.
6. Place the 'o' ring in top of the clamper.
7. Wet the PDMS molt with a drop of culture medium. *
8. Dry the membrane, then place it on top of the wetted PDMS molt. Make sure you'll remember the orientation of the membrane. Best is to pick and stick with a certain orientation.
9. Place the chip in the top of the clamper, you can slide it in. Make sure it is tight.
10. Put the top of the clamper (with the chip) back on the bottom of the clamper(with the membrane) by very carefully sliding it back on.
11. Check if the membrane didn't move, by moving the top back and forth a bit and checking if there is no movement.
12. Pull the lever gently, this will press the membrane on the chip.
13. Put medium in the round hole of the clamper, so directly on top of the chip. Stop if the hole is full.
14. Get a small, sterile petridish and put the lid on top of the clamper. The lid will fit perfectly on top of the clamper, which will prevent the chip from drying out.
15. Place the clamper in a special box for clamping units. *
16. Place it in the incubator for 1 day.

* These steps are optional.

8.7 Appendix G: Membrane staining

1. Take membranes out of incubation after 24 hours.
2. Wash membranes with 1% tween in PBS
3. Wash with 1% BSA in PBS for 1 hour OR 3 times 5 minutes
4. Prepare primary antibody (code Ab 19554), Rabbit polyclonal Ab to PSA , stock = 7.58mg/ml (500ug). Dilutions prepared = 2ul in 1ml of 1%BSA in PBS solution. (vortex Ab before using it).
5. Add 150ul in all the wells with 'o'-rings and 250ul in all the wells without 'o'-ring. Incubate for 1 hour on shaker (300rpm).
6. Wash with 1% BSA in PBS solution 3 times for 5min.
7. Prepare secondary antibody, Goat Ab to Rabbit IgG (PE) , stock = 0.1mg/ml (100ug). Dilutions prepared 2ul in 1ml of 1%BSA in PBS solution. (vortex Ab before using it).
8. Add 150ul in all the wells with 'o'-rings and 250ul in all the wells without 'o'-ring. Incubate for 1 hour on shaker(300rpm).
9. Wash with 1% BSA in PBS solution 3 times for 5min.
10. Wash membranes with milli Q so no salts will be on the membrane when they dry. Alternatively, place membranes in PBS, cover in Al foil and place in 4degC for later use.

8.8 Appendix H: Preparing and imaging of the membranes with the Puncher microscope

Preparation of the membrane for imaging:

1. Dry membrane by holding one or multiple corners of the membrane against a dry tissue.
2. Get a glass slide and put 1 drop of mounting medium on top of it.
3. Put the membrane on the glass slide.
4. Put 1 drop of mounting medium on top of the membrane.
5. Put another glass plate on top, tape the glass slides together and image immediately.

Imaging of the membranes:

1. Start the software.
2. Place a sterile holder for glass slides in the puncher system.
3. In the software, select 'load/align slide'
4. In the software, insert name and date.
5. Set the exposure time for the real time image on the software.
6. Find the membrane, direct the holder for the glass slide with membrane directly under the objective.
7. Find focus, in such a way that individual imprint of wells can be seen, work quickly since bleaching occurs rapidly.
8. Find the left corner of the membrane (or if possible the imprint of the wells on the membrane.
9. Repeat for the bottom right and top right corners. Then click 'accept'.
10. Three spots on the membrane in-between the just selected corners are shown one after another. Check the focus. Then select 'accept'.
11. Select the exposure times for all different channels.
12. Click 'start imaging' and the software will collect the data channel by channel.
13. After imaging, remove the glass slide with the membrane from the holder.

8.9 Appendix I: Staining protocol used in Chapter 3 and Chapter 4

1. Start with 100.000 cells in each tube/condition.
2. Centrifuge tubes 300 rpm, 5 minutes.
3. Aspirate off liquid.
4. Add 100 ţl of antibody 1 solution to each sample. Depending on the experiment, stainings solution can be added at the same time. (Keep in mind the working concentration when preparing the solution)
5. Incubate at 37 degrees for about 30 min.
6. Add 2 ml of wash buffer.
7. Centrifuge tubes 300 rpm, 5 minutes. (possibly repeat 3x if necessary)
8. Aspirate off liquid.
9. Add 100 ţl of secondary antibody (diluted in wash buffer).
10. Incubate at 37 degrees for about 30 min.
11. Add 2 ml of wash buffer.
12. Centrifuge tubes 300 rpm, 5 minutes.
13. Aspirate off liquid. (repeat step 11, 12, and 13 another 2x)
14. Add 250 ţl wash buffer.
15. Measure with FACS machine and/or visualize with the fluorescence microscope.

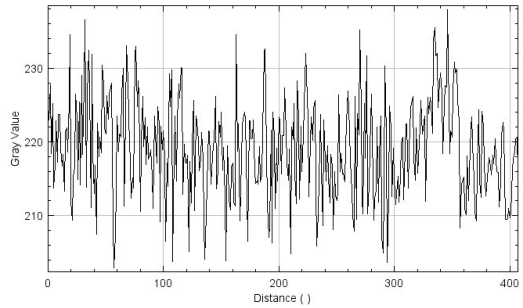

Figure 52: Plot of the intensity of 2 randomly selected cells in the PE channel of the 'HO3-BV421' condition. Only background is clearly seen.

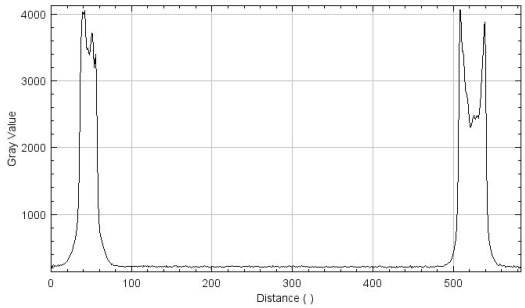

Figure 53: Plot of the intensity of 2 randomly selected cells in the PE channel of the 'VU1D9-PE' condition. Both cells are clearly seen.

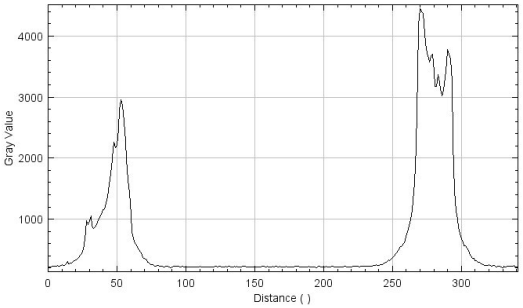

Figure 54: Plot of the intensity of 2 randomly selected cells in the PE channel of the 'both' condition. Both cells are clearly seen.

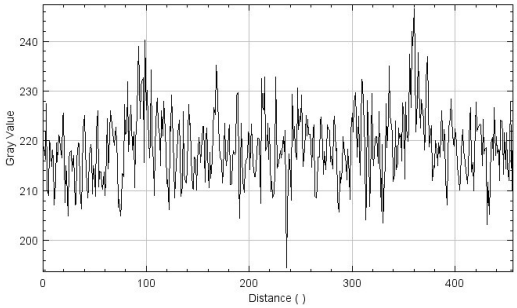

Figure 55: Plot of the intensity of 2 randomly selected cells in the PE channel of the 'control' condition. Only background is clearly seen.

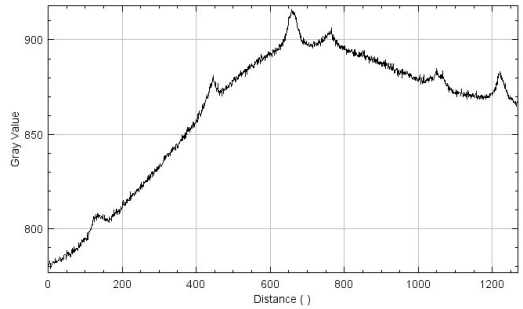

Figure 56: Plot of the intensity of 6 selected cells in the DAPI channel of the 'both' condition. All 6 cells are clearly seen. The 3rd and 6th peak are most intense relatively to the background.

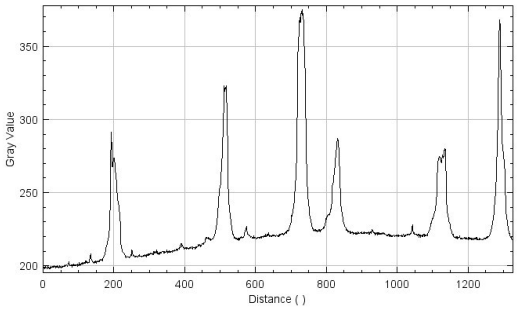

Figure 57: Plot of the intensity of 6 selected cells in the PE channel of the 'both' condition. All 6 cells are clearly seen. The 3rd and 6th peak are most intense.

8.10 Appendix J: Intensity plots of the epitope compatibility study

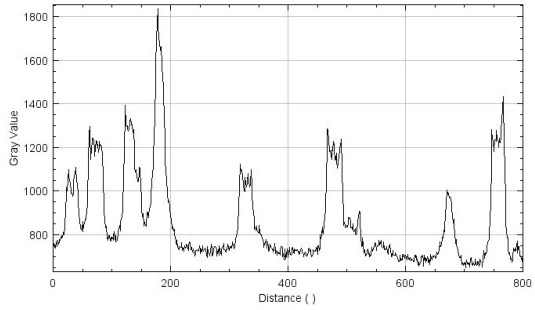

Figure 58: Plot of the intensity of 8 randomly selected cells in the DAPI channel of the HO3-BV421 stained LNCaPs. Cells are clearly visible.

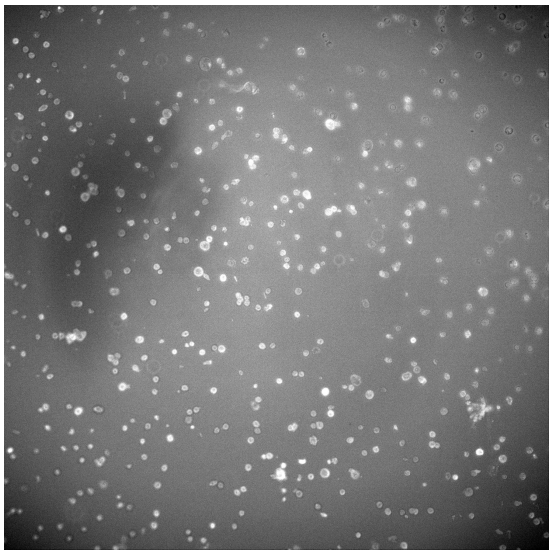

Figure 60: Images taken from Lncap cells stained by HO3 antibodies attached to BV605 imaged with the BV605 filter. Cells are clearly visible.

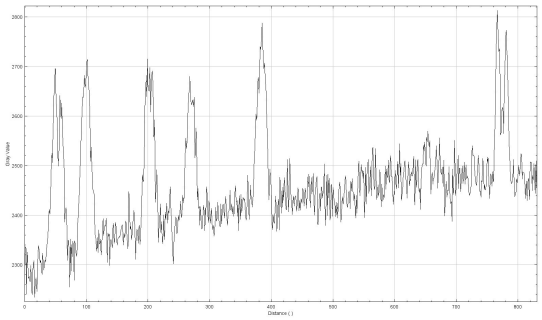

Figure 62: Plot of the intensity of 6 randomly selected cells in the BV605 channel of the HO3-BV605 stained LNCaPs. Cells are clearly visible.

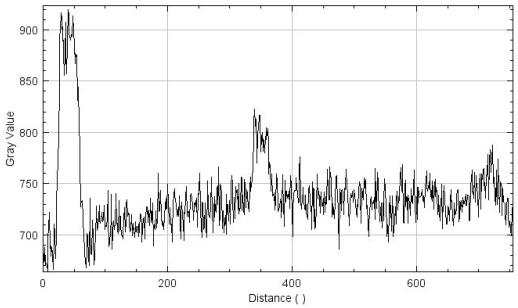

Figure 59: Plot of the intensity of 8 randomly selected cells in the DAPI channel of the HO3-BV421 stained PC3 cells. Some cells are hard to distinguish since they are only slightly above background level.

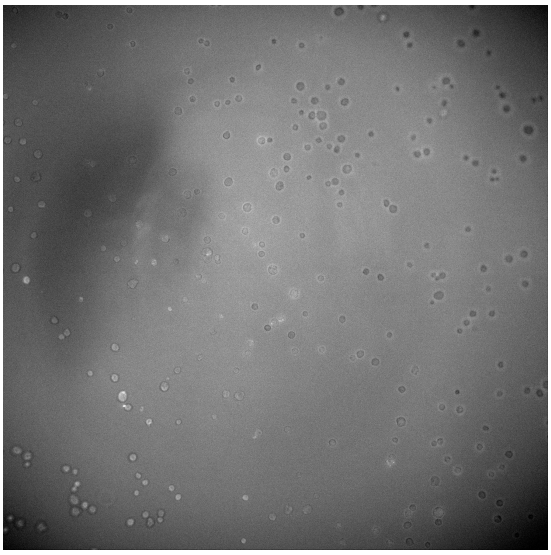

Figure 61: Images taken from PC3 cells stained by HO3 antibodies attached to BV605 imaged with the BV605 filter. Some cells are hard to distinguish since they are only slightly above background level.

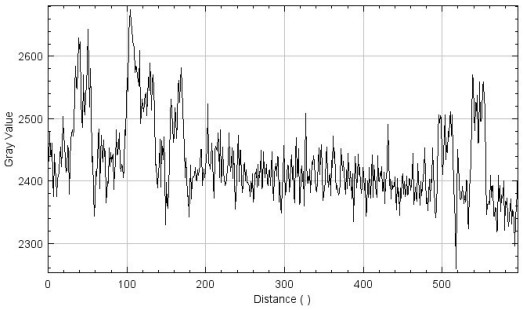

Figure 63: Plot of the intensity of 5 randomly selected cells in the BV605 channel of the HO3-BV421 stained PC3 cells. Some cells are hard to distinguish since they are only slightly above background level.

8.11 Appendix K: Intensity plots of the cell line EPCAM expression comparison

8.12 Appendix L: Degassing of chips

1. Place the chip in a petri dish
2. Add ethanol, make sure there is plenty since ethanol will evaporate
3. Place in Vacuum dome
4. Close the valve on top
5. Turn it on
6. Wait 15 minutes
7. Check if the chip is degassed, shake a little to see if bubbles come out. Maybe undo the vacuum and start again if some bubbles are stuck.
8. Undo to vacuum very slowly, otherwise incoming air will disrupt everything inside(Black line on the valve pointed towards the degasser, to slowly let air out).

8.13 Appendix M: PDMS layer production

1. Clean the mold. Use the N2 gun.
2. Prepare the PDMS solution by mixing the PDMS curing agent with the PDMS, in a concentration of around 1:10.
3. Put the solution in the vacuum pump to get rid of the bubbles.
4. Pour the PDMS in the mold.
5. If needed, punch any new bubbles.
6. Put it in the oven on 80 degrees Celsius for approximately 15 minutes (the higher the temperature, the stiffer the end product).
7. Take the newly produced PDMS layers out of the mold.

8.14 Appendix N: Manual magnetic incubation and separation

Incubation protocol:

1. Reduce DLA volume to 1 mL by centrifugation at 400g for 5m (if needed)
2. Use FACS tubes,
3. Enter 2 mL in each tube when not working with DLA samples. Otherwise, put the 1mL in the FACS tube.
4. Before adding FF, vortex them.
5. Add FF.
6. Put the tubes against the magnet for 5 minutes, then turn the tubes, mix, and repeat. (X3)
7. Add 1 ml buffer (casein:non-casein = 1:1, this is anti-fouling, sort of PBS/BSA).

Separation protocol:

1. Add 1mL, this makes is less viscous.
2. Tape it against the magnet.
3. Wait 20 minutes.
4. Remove the liquid with a pasteur pipette.
5. Place the pipette at the bottom of the tube.
6. Remove all liquid very slowly without disturbing the layer that formed of cells and FF on the side of the magnet (you might also use a pump at 1ml/min for more controlled removal).
7. Collect the caught cells with a medium and volume of choice.

8.15 Appendix O: Examples of flowcytometer results

Examples of flowcytometer results stained with DAPI, with at Figure 64 the 'Cells' condition, at Figure 65 the 'Cells exposed to magnet' condition, and at Figure 66 the 'Cells enriched by use of FF' condition.

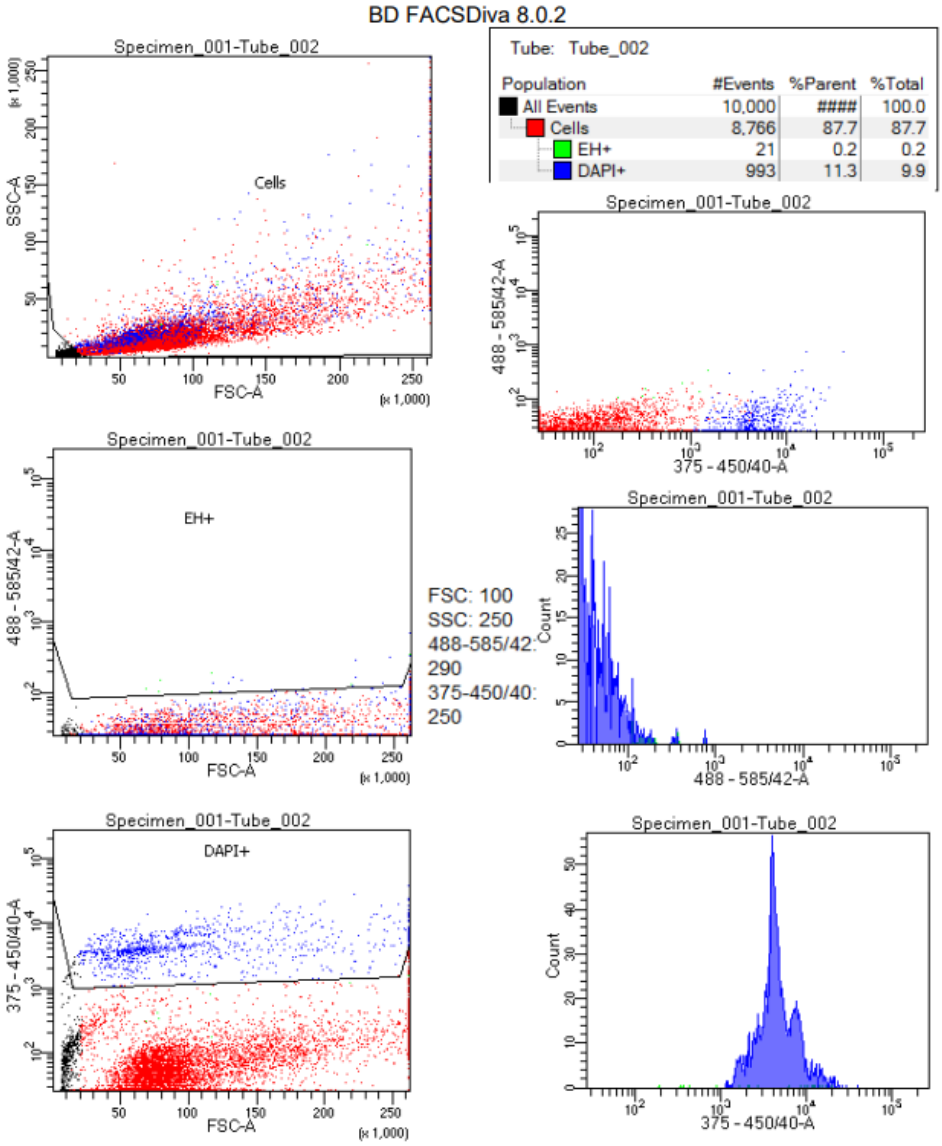

Figure 64: Flowcytometer measurements of 'Cells' condition with DAPI+ staining.

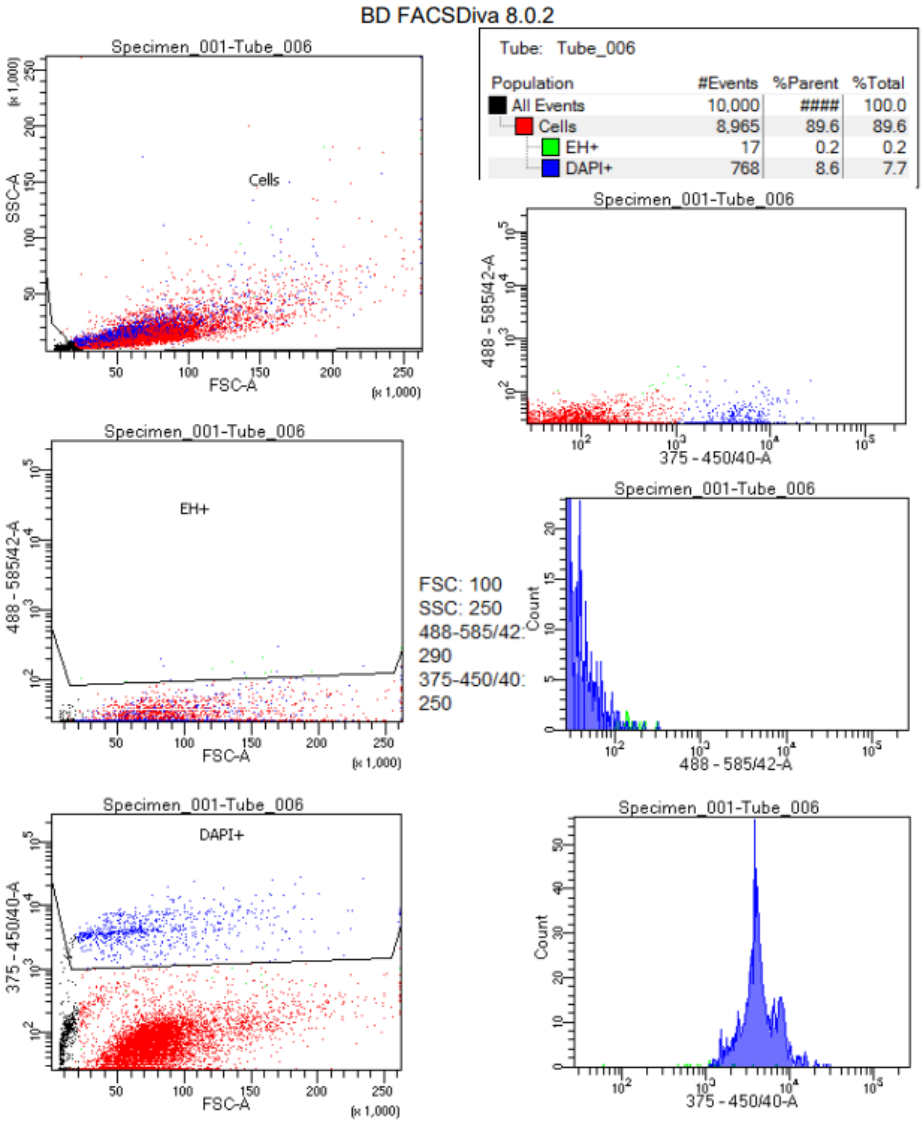

Figure 65: Flowcytometer measurements of 'Cells exposed to magnet' condition with DAPI+ staining.

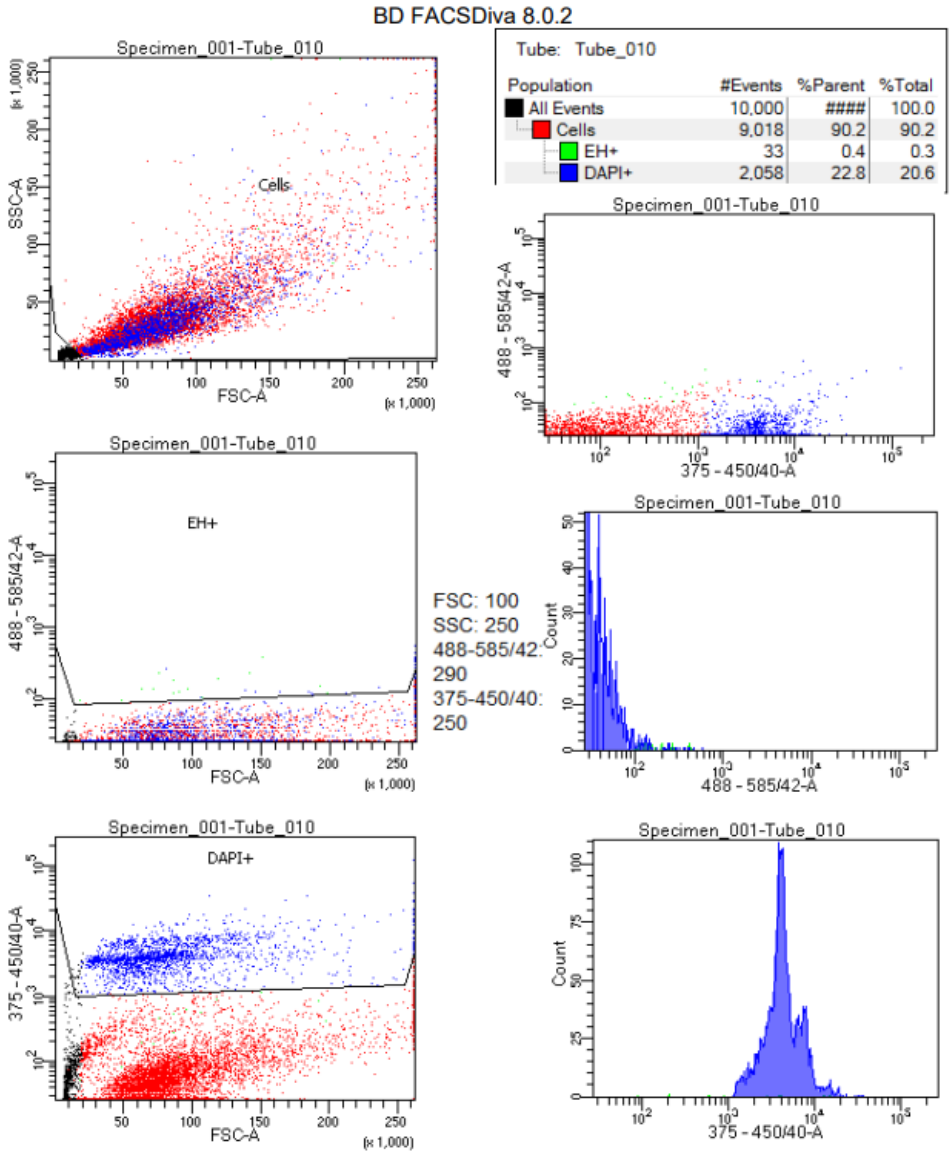

Figure 66: Flowcytometer measurements of 'Cells enriched by use of FF' condition with DAPI+ staining.

8.16 Appendix P: Flowcytometer results of killed cells

Examples of flowcytometer results of with 70% ethanol killed cells. Stained with DAPI, EH, or both. DAPI does stain the majority, whereas EH does not stain the majority. Likely the staining was not present in a sufficient concentration for such a quantity of cells.

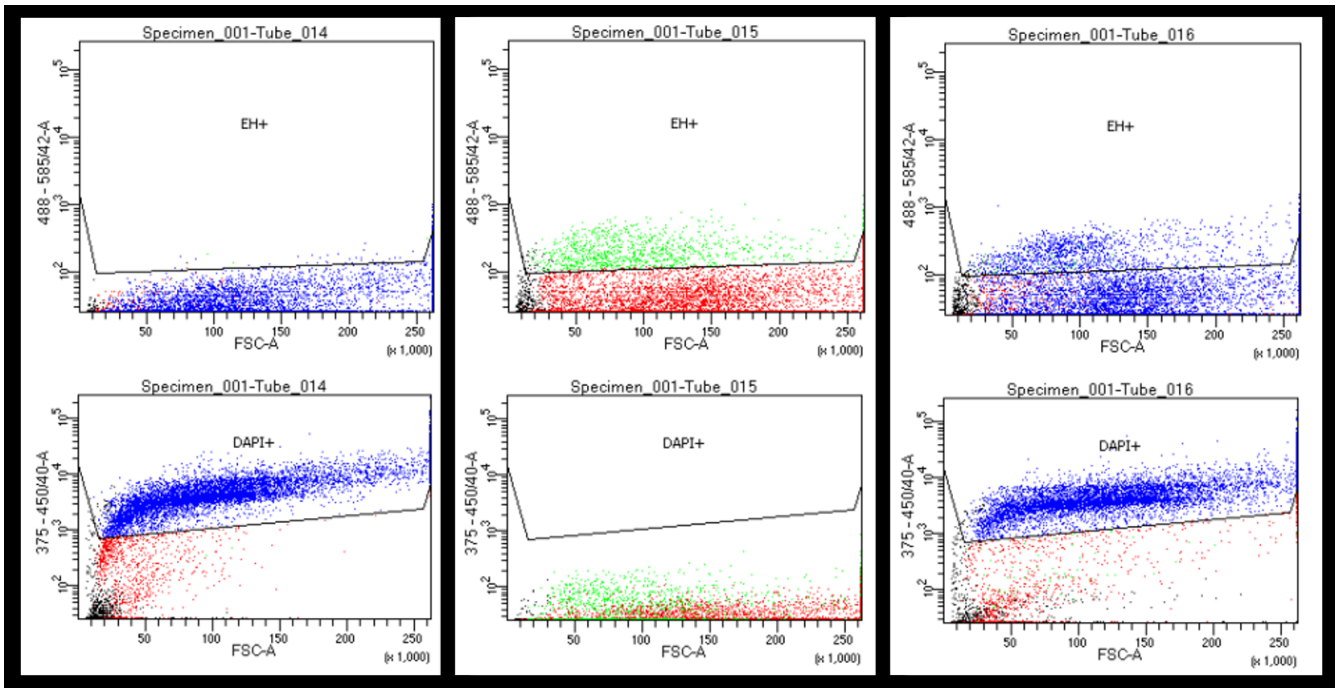

Figure 67: Examples of flowcytometer results of with 70% ethanol killed cells. Stained with DAPI, EH, or both. DAPI does stain the majority, whereas EH does not stain the majority. Likely the staining was not present in a sufficient concentration for such a quantity of cells. Left: DAPI+, EH-. Middle: DAPI-, EH+. Right: DAPI+, EH+.

8.17 Appendix Q: Flowcytometer results Calcein AM, and PI

LNCaP cells stained with 20nM Calcein AM. 2 subpopulations that stain positive are formed, see Figure 68. LNCaP cells stained with the standard concentration recommended by the manufacturer of PI (left) and EH (right). The intensity of the EH signal is higher, see Figure 69.

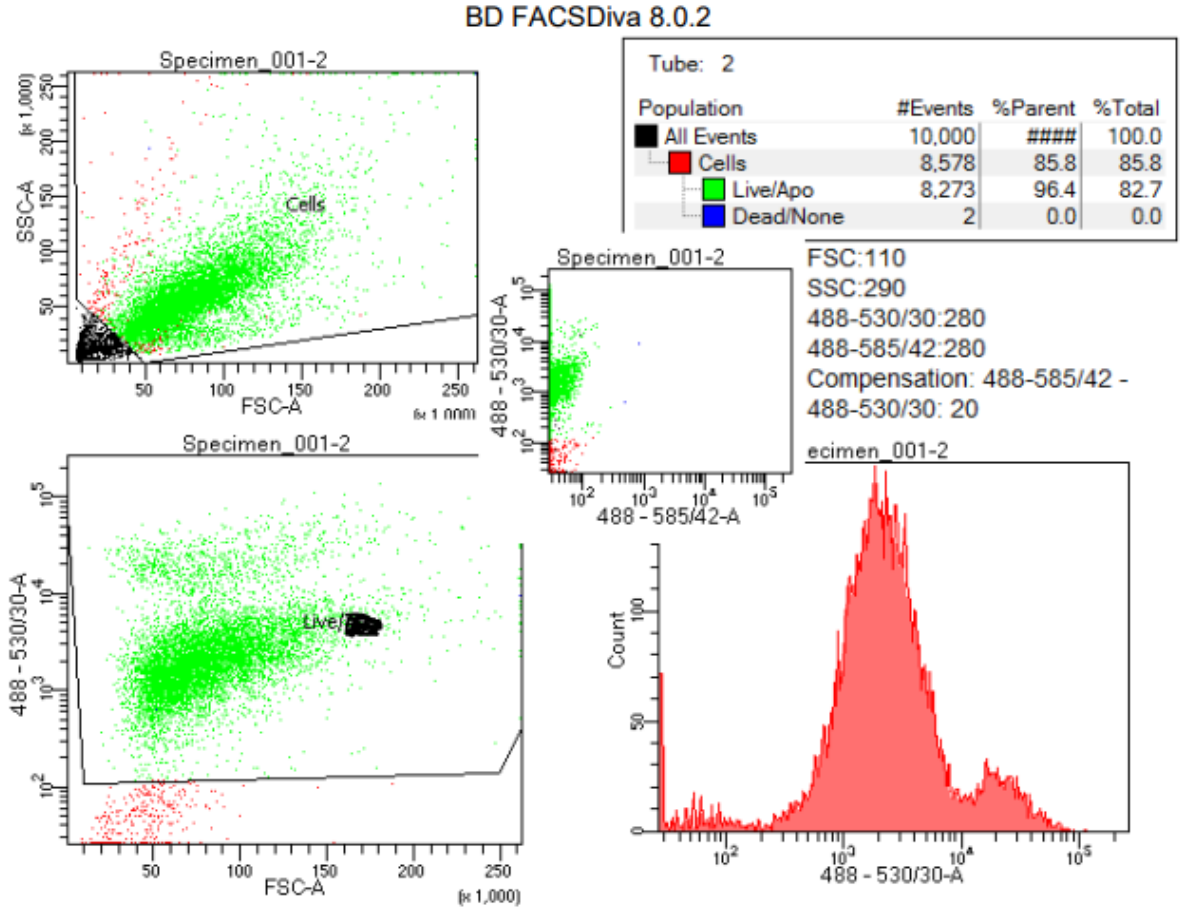

Figure 68: LNCaP cells stained with 20nM Calcein AM. 2 subpopulations that stain positive are formed.

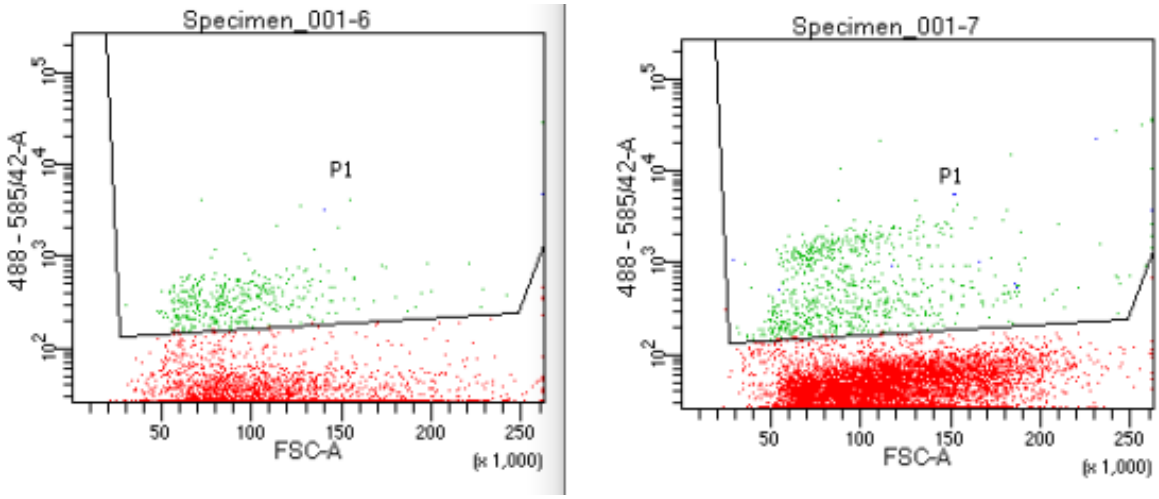

Figure 69: LNCaP cells stained with the standard concentration recommended by the manufacturer of PI (left) and EH (right). The intensity of the EH signal is higher.

8.18 Appendix R: Zoomed in at the peaks of the metabolic activity graphs from the Alamar Blue Assays

Looking at the peaks of the graphs for more clarity. Graphs start at 90% metabolic activity.

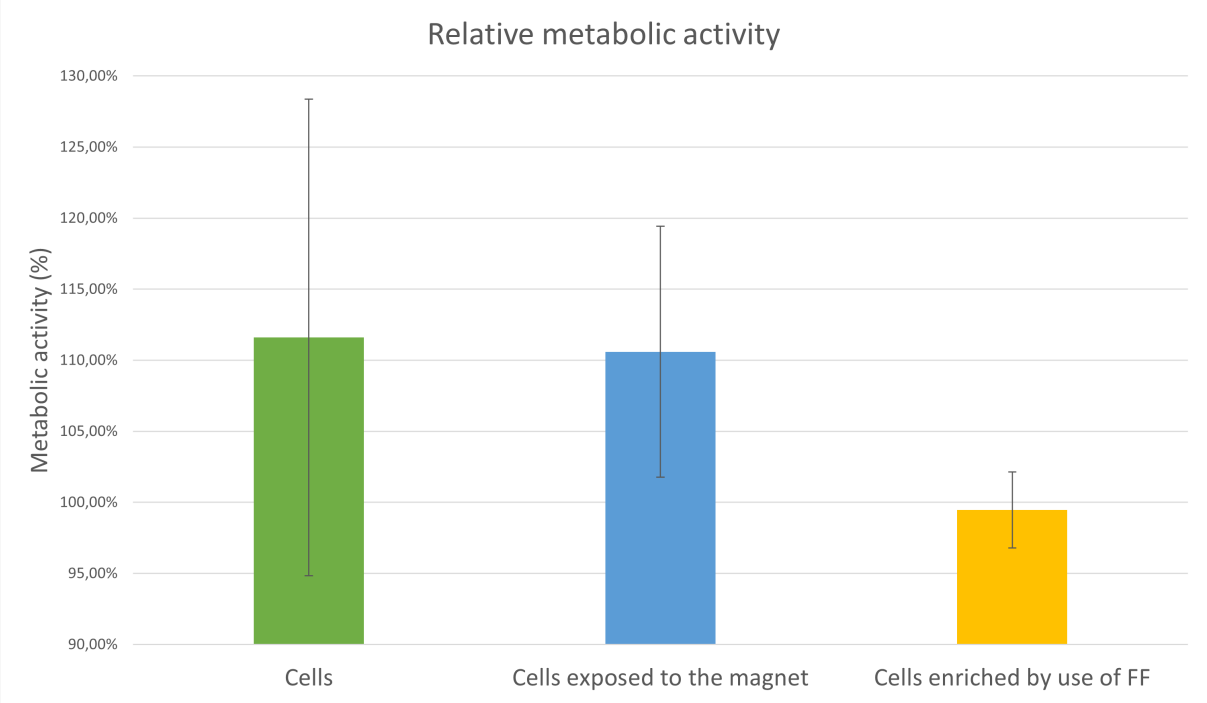

Figure 70: Figure 23 but zoomed in, the Y-axes starts at 90%. Relative metabolic activity of the conditions of Cells(green), Cells exposed to the magnet(blue), and cells enriched by use of FF(yellow) and their standard deviation. They have a respective relative metabolic activity of 111,6, 110,6 and 99,5%. This is relative to the highest seeded density of untreated cells. All relative densities were taken together for each one of the 3 conditions. These are the last 3 experiments, after the protocol was optimized and the procedure was well under control. The conditions are not significantly different from each other (P=0.52549, p>0.05).

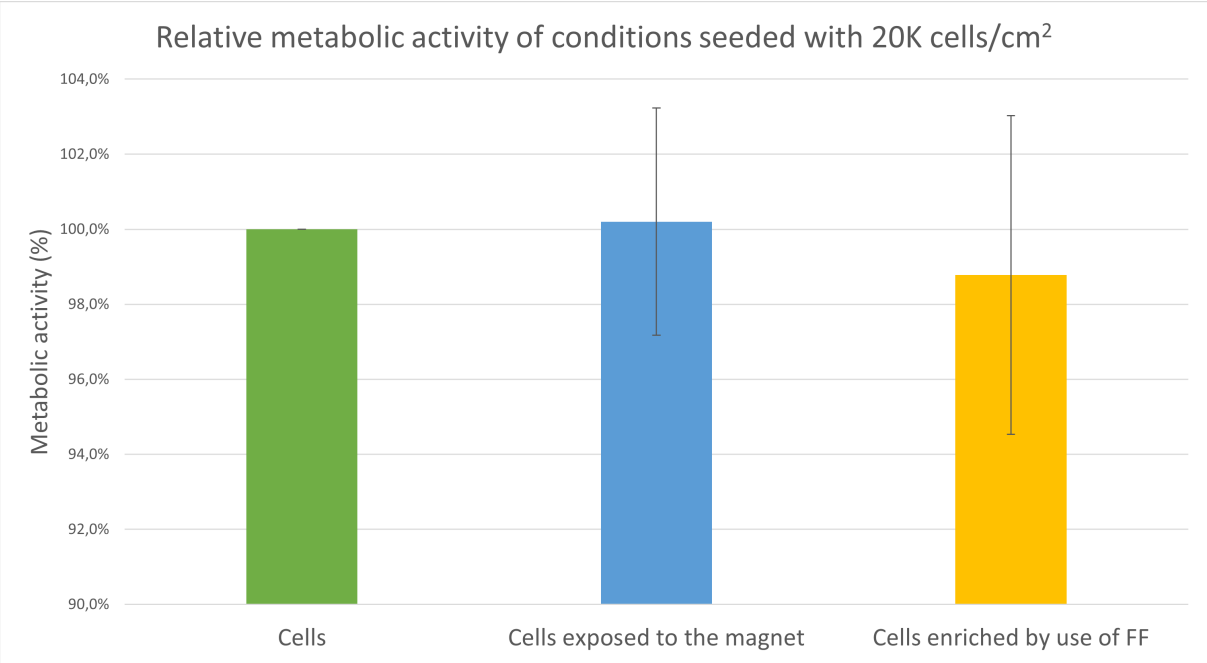

Figure 71: Figure 24 but zoomed in, the Y-axes starts at 90%. Only relative metabolic activity of conditions seeded with 20K cells/cm^2 are taken into account and their standard deviation. Cells(green), Cells exposed to the magnet(blue), and cells enriched by use of FF(yellow) have a respective relative metabolic activity of 100.0, 100.2 and 98.8%. This is relative to the highest seeded density of untreated cells, which is the 20K cells/cm^2 conditions(therefore it was set in every experiment as 100%). The difference between conditions was even less significant (P=0.721358, P>0.05).

8.19 Appendix S: Full results of the flowcytometer results from tests looking into interactions between staining and FF

Looking at the peaks of the graphs for more clarity. Graphs start at 90% metabolic activity.

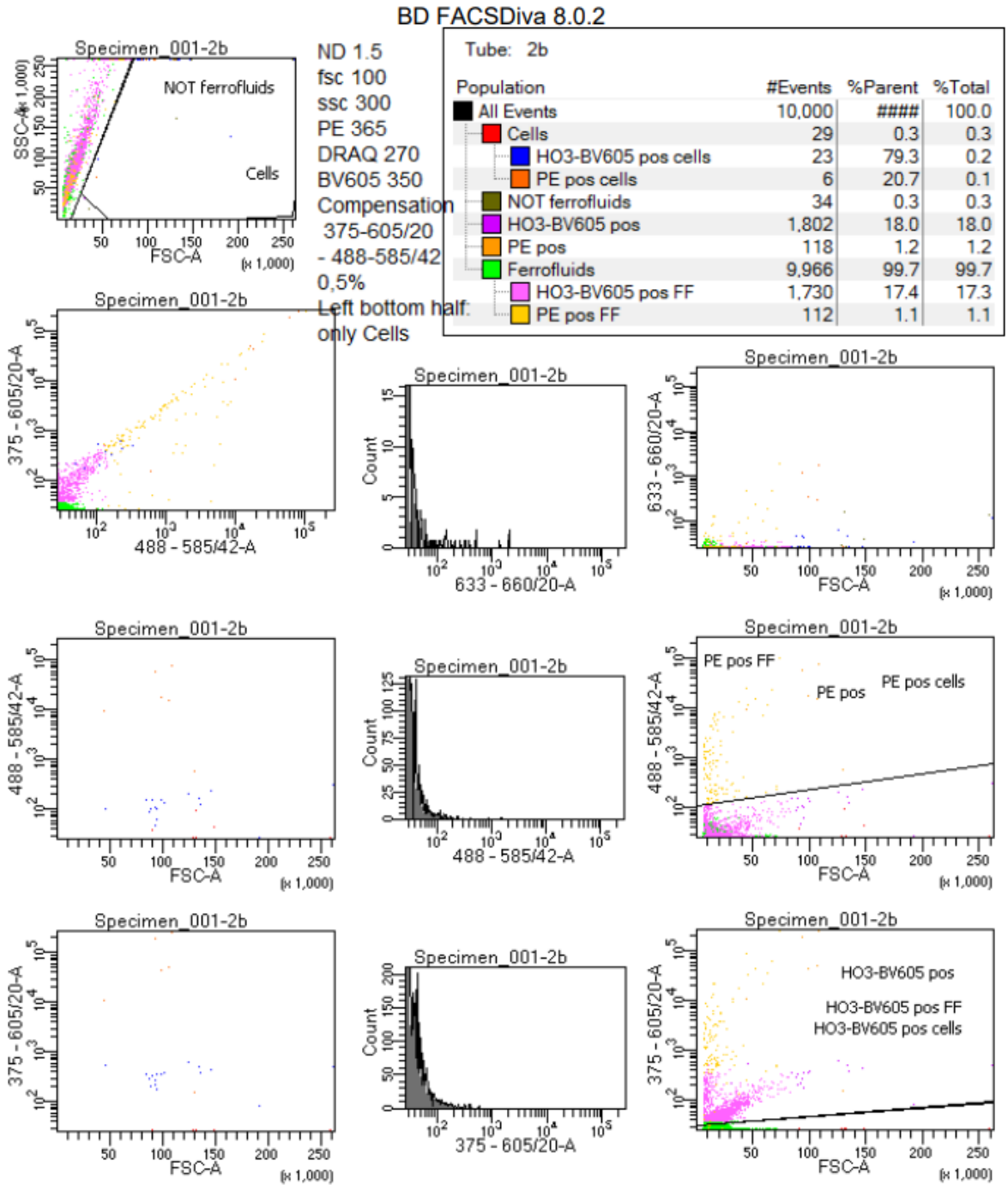

Figure 72: Flowcytometer results of FF mixed with HO3-BV605 which stains EpCAM at cells. 17.4% of FF was stained positive for HO3-BV605. HO3-BV605 was measured with the 375-605/20 filter and results are depicted in the graph at the right bottom. The graph at the left top shows the FSC vs. SSC and the gates set to differentiate between cells and FF.

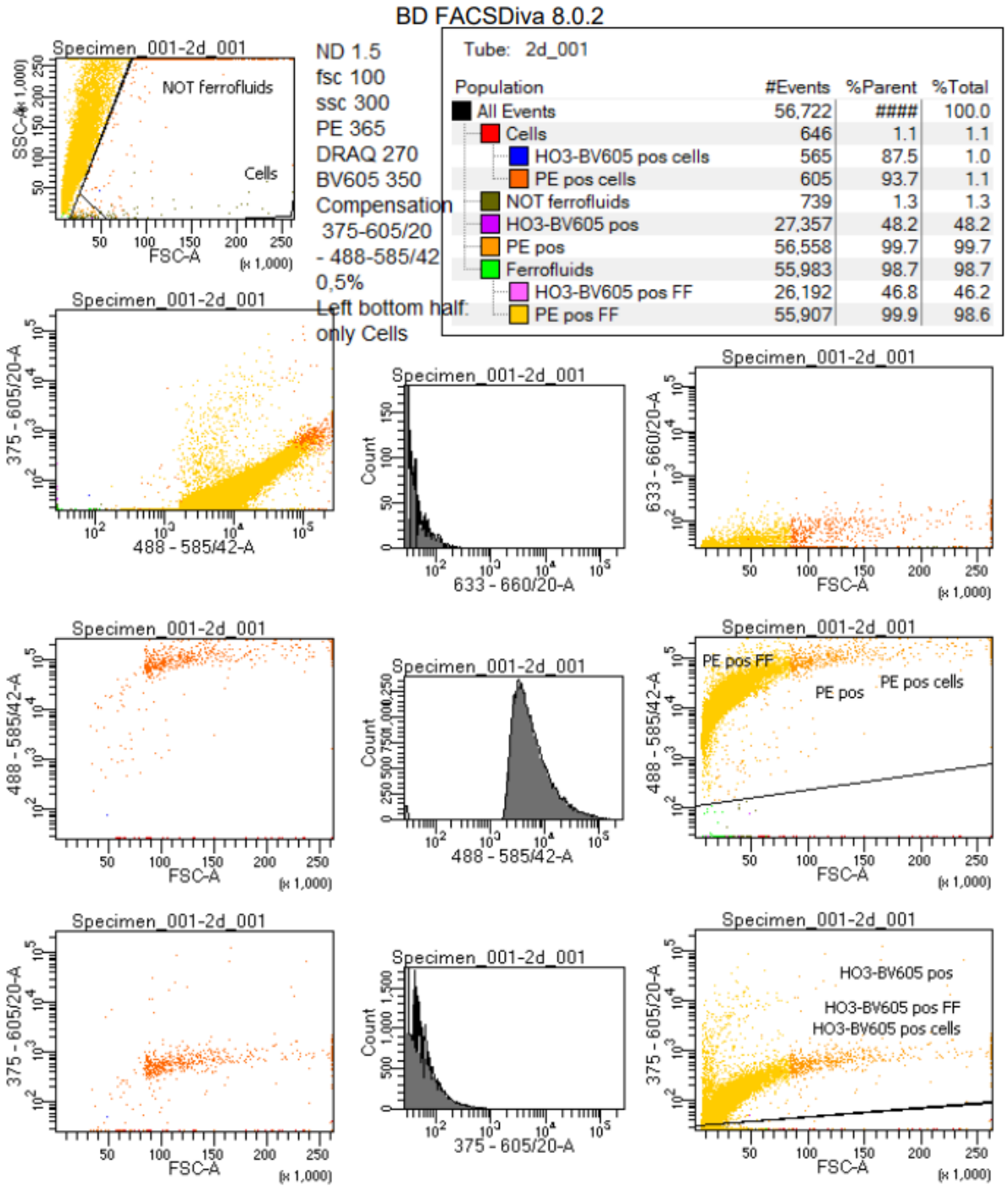

Figure 73: Flowcytometer results of FF mixed with HO3-BV605 which stains EpCAM at cells and PE anti-mouse which stains the FF. 46.8% of FF was stained positive for HO3-BV605. HO3-BV605 was measured with the 375-605/20 filter and results are depicted in the graph at the right bottom. PE anti-Mouse was measured with 488-585/42. The graph at the left top shows the FSC vs. SSC and the gates set to differentiate between cells and FF.

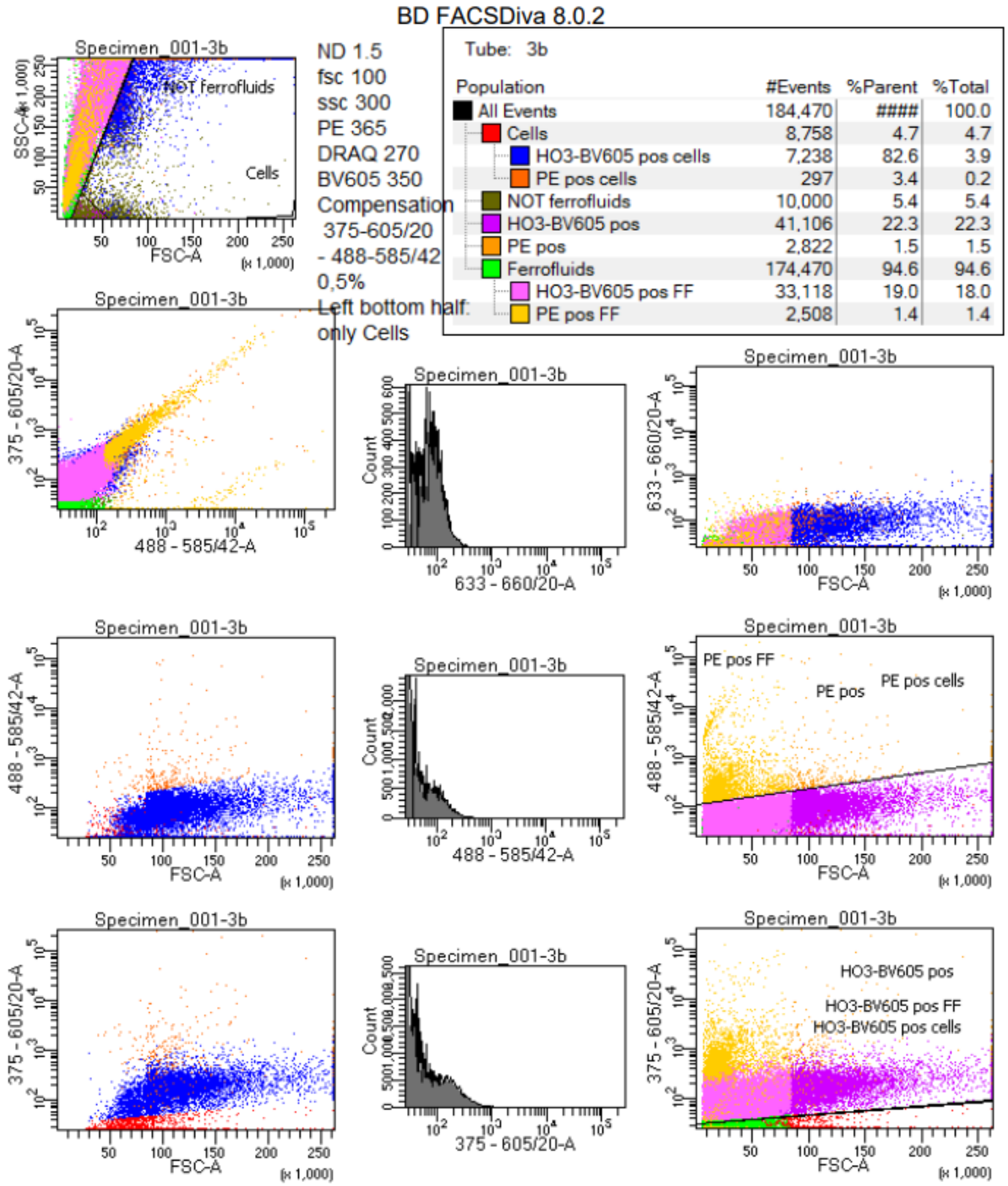

Figure 74: Flowcytometer results of cells enriched with FF. Then mixed with HO3-BV605 which stains EpCAM at cells. 82.6% of cells was stained positive for HO3-BV605. HO3-BV605 was measured with the 375-605/20 filter and results are depicted in the graph at the right bottom. The graph at the left top shows the FSC vs. SSC and the gates set to differentiate between cells and FF.

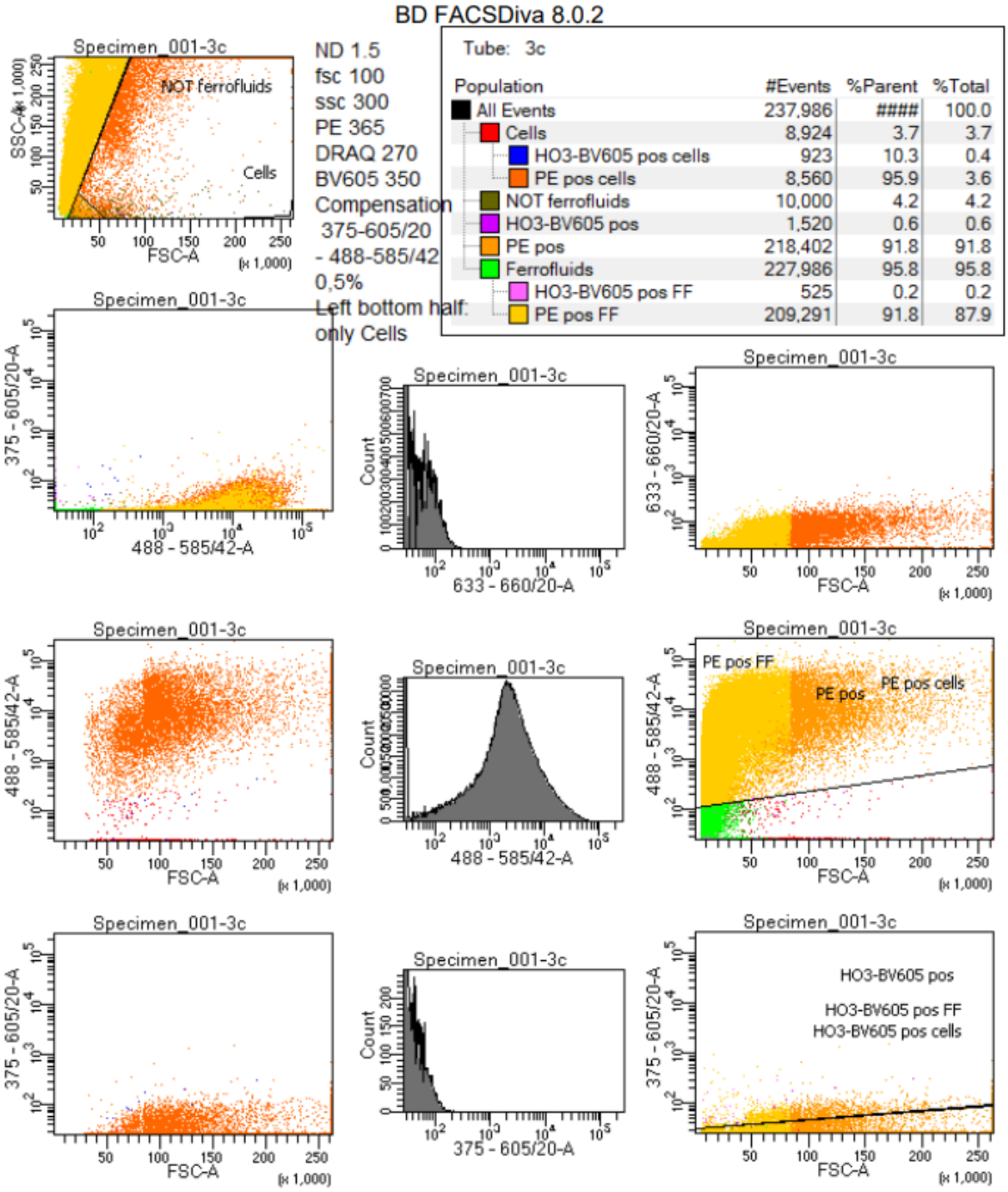

Figure 75: Flowcytometer results of cells enriched with FF. Then mixed with PE anti-mouse which stains the FF. 95.9% of cells was stained positive for PE anti-mouse. PE anti-Mouse was measured with 488-585/42. The graph at the left top shows the FSC vs. SSC and the gates set to differentiate between cells and FF.

8.20 Appendix T: Example of PSA secretion of cells directly seed on a membrane

Darker spots are visible within the secretion spots. This is were cells were attached to the membrane.

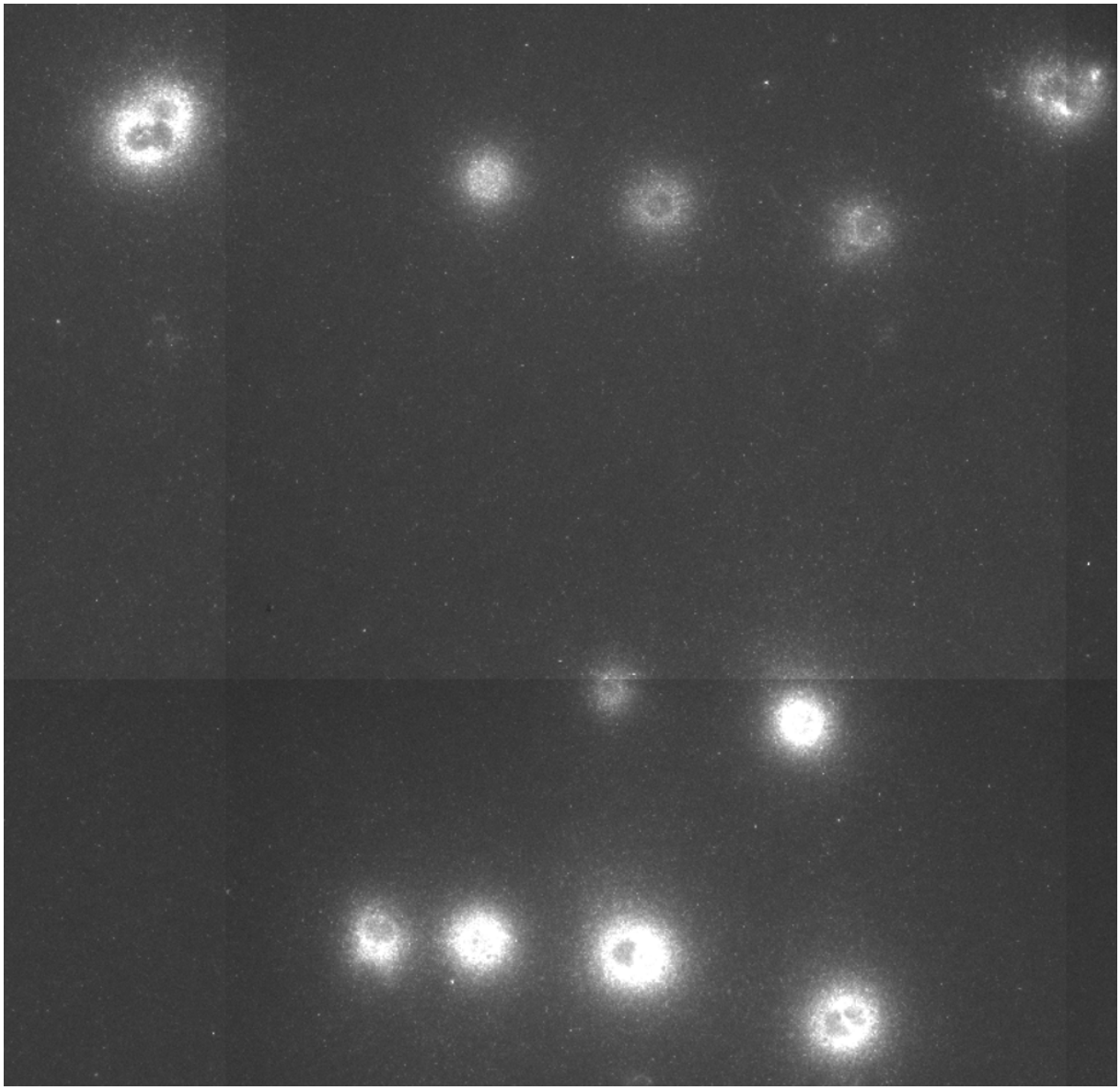

Figure 76: PSA secretion spots with darker spots within them. This is were cells were attached on the membrane. Enriched blood sample seeded directly on a mouse antibody anti-PSA coated membrane. PSA secretion imaged in with a PE filter. The membrane was stained with Rabbit polyclonal antibody to PSA, which on turn was stained with Goat antibody to rabbit IgG (PE).

8.21 Appendix U: Example of the chip seeded with enriched cells stained with CTO

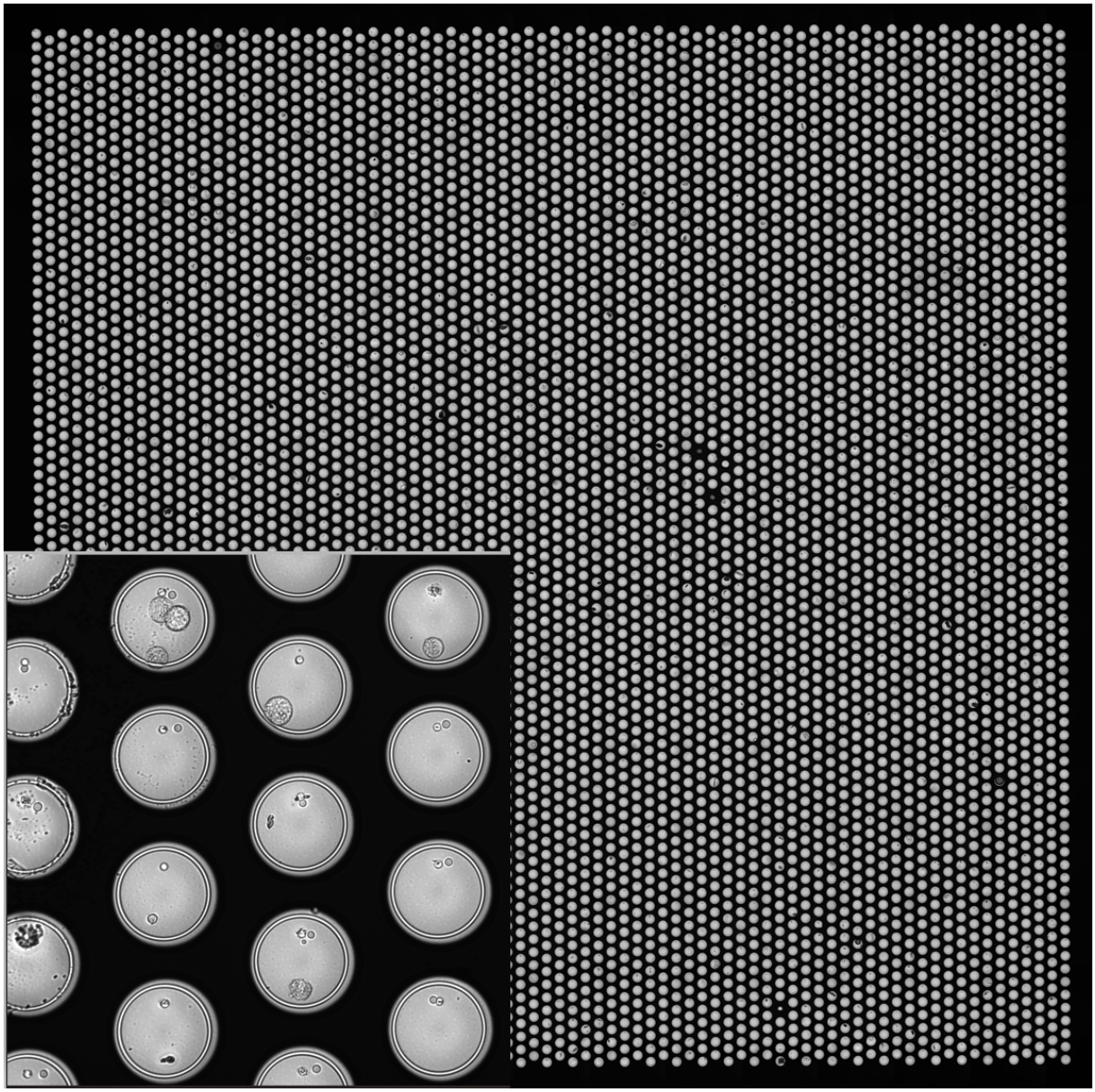

Figure 77: Condition 'Cells-FF seeded on chip', the chip imaged with brightfield. 6K enriched cells were seeded on a chip with 5 mbar pressure. Most wells are visible. When zooming in on wells, cells and debris can be seen

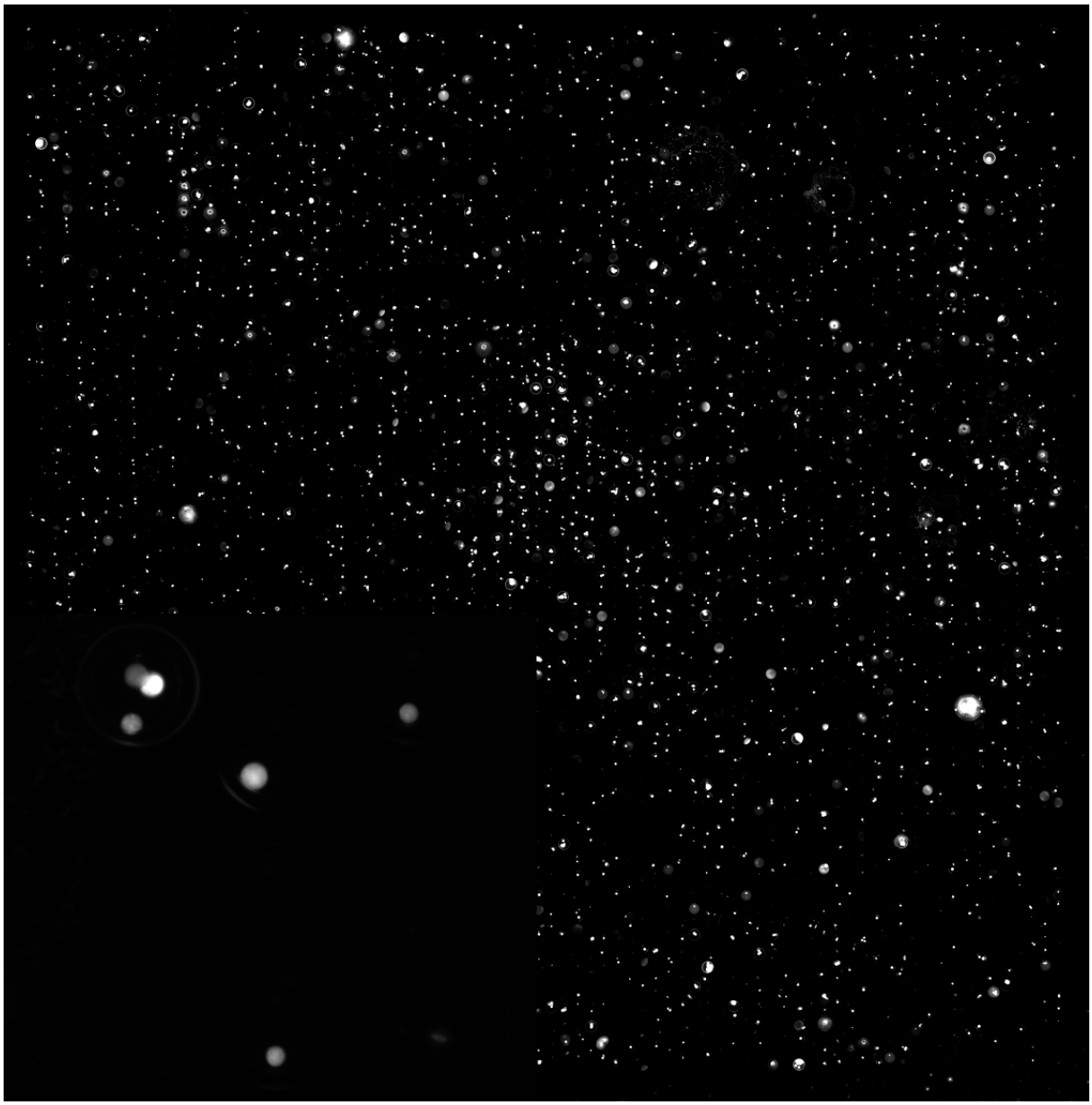

Figure 78: Condition 'Cells-FF seeded on chip', the chip imaged with PE. Cells were stained with CTO. Approximately 2600 wells gave PE signal of which approximately 90% was from cells. Therefore 2340 wells (37%) was seeded with a cell. 6K enriched cells were seeded on a chip with 5 mbar pressure. This means the chip was already 'full' (not flowing anymore under pressure) or some cells have were not caught by the chip. Most wells are visible. When zooming in on wells, cells and debris can be seen.

8.22 Appendix V: Example of the chip seeded with enriched cells stained with PE-PSMA and APC-CD45

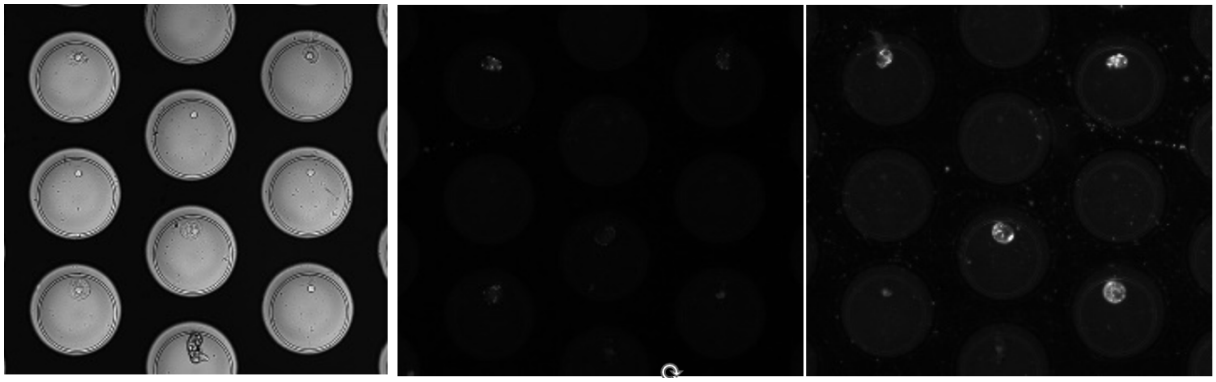

Figure 79: LNCaP cells seeded in a chip. Left: brightfield. Middle: APC (CD45). Right: PE (PSMA).

8.23 Appendix W: Flowcytometer results of optimizing the staining protocol

Table 6: Overview of the flowcytometer results of the incubation time and light exposure experiment. The median fluorescence intensity decreased of CTO after longer incubation times. This decrease were also seen in the percentage of cells that were selected as positive for a staining. In orange the most important results for CTO have been shown. On the left the stainings used are indicated; a - means not used, a + means used.

CTO+, BV605+	Median Intensity CTO	% intensity vs. 1h dark inc.	% CTO+ cells
4h light exposure	2910	28,0%	60,30%
4h dark incubation	3470	33,4%	69,60%
1h dark incubation	10394	100,0%	97,30%

CTO-, BV605+			
4h light exposure	386	54,7%	2,90%
4h dark incubation	454	64,3%	8,50%
1h dark incubation	706	100,0%	5,40%

CTO+, BV605-			
4h light exposure	4748	27,3%	88,50%
4h dark incubation	7435	42,8%	97,90%
1h dark incubation	17386	100,0%	99,40%

CTO-, BV605-			
4h light exposure	111	71,6%	0,40%
4h dark incubation	158	101,9%	0,10%
1h dark incubation	155	100,0%	0,30%

Table 7: Overview of the flowcytometer results of the incubation time and light exposure experiment. The median fluorescence intensity decreased of BV605 after longer incubation times. The decreases was also seen in the percentage of cells that were selected as positive for a staining. In purple the most important results for BV605 have been shown. On the left the stainings used are indicated; a - means not used, a + means used.

CTO+, BV605+	Median Intensity BV605	% intensity vs. 1h dark inc.	% BV605 + cells
4h light exposure	1367	46,3%	86,40%
4h dark incubation	1384	46,9%	86,50%
1h dark incubation	2953	100,0%	96,10%

CTO-, BV605+			
4h light exposure	1514	57,2%	86,70%
4h dark incubation	1338	50,5%	81,80%
1h dark incubation	2647	100,0%	91,30%

CTO+, BV605-			
4h light exposure	10	-7,3%	8,70%
4h dark incubation	-11	8,0%	9,10%
1h dark incubation	-137	100,0%	4,00%

CTO-, BV605-			
4h light exposure	26	63,4%	0,50%
4h dark incubation	32	78,0%	0,10%
1h dark incubation	41	100,0%	0,10%

8.24 Appendix X: Flowcytometer results of Eh and DAPI staining

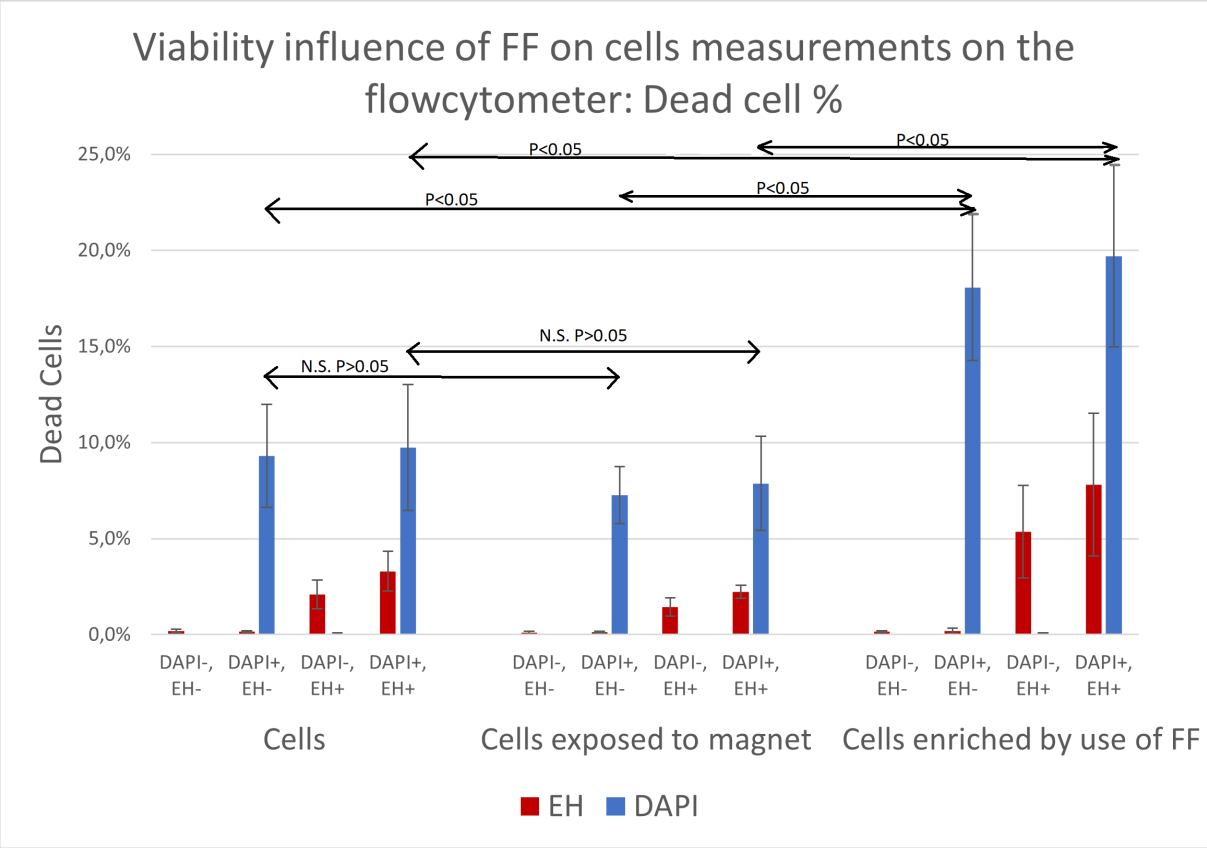

Figure 80: Flowcytometer measurements of cell dead levels and their standard deviation. Measurements were done with DAPI and EH. Significant difference was shown with DAPI staining between the 'Cells' and 'Cells enriched by use of FF'(for both DAPI+/EH- and DAPI+/EH+ staining)(P<0.05). Also significant difference was shown between the 'Cells exposed to the magnet' and 'Cells enriched by use of FF'(for both DAPI+/EH- and DAPI+/EH+ staining)(P<0.05). No significant difference was seen when looking at the EH results(P>0.05).

8.25 Appendix Y: Chips after seeding: debris and cell movement

Cell debris can be seen in both figures. In figure 82 a chip can be seen before and after seeding, with cells that still move around since they are not directly attached after seeding. In Figure 81 cells can be seen that remained in place before and after incubation.

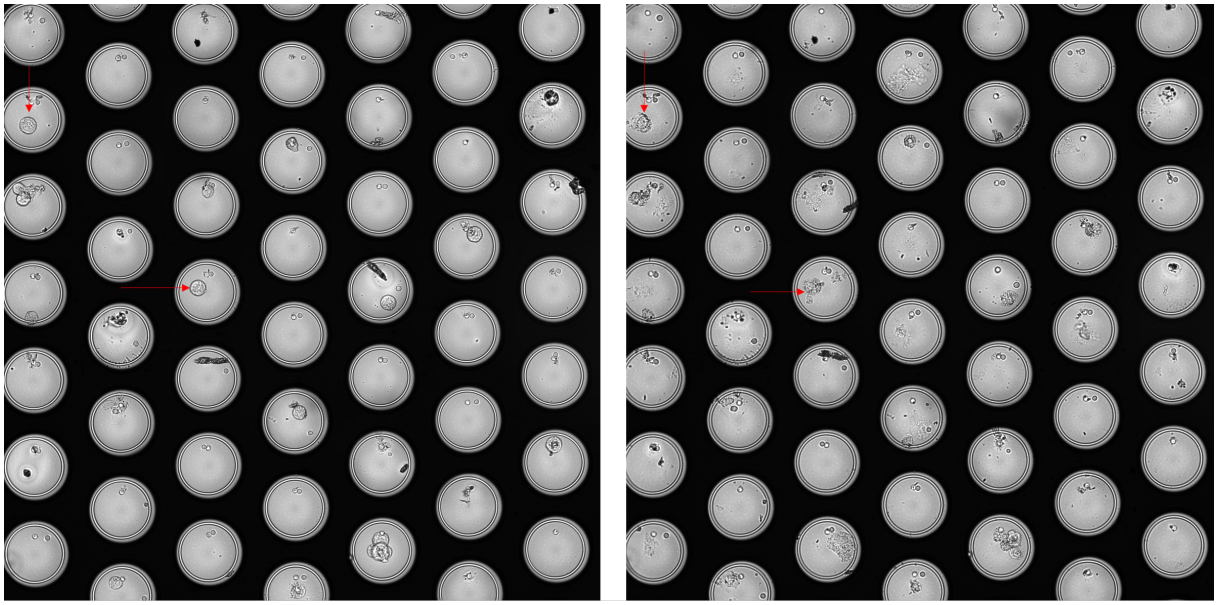

Figure 81: Condition 'Cells-FF seeded on chip'. 6K enriched cells were seeded on a chip with 5 mbar pressure. isolate cells can be seen at the arrow. They remained in place during incubation.

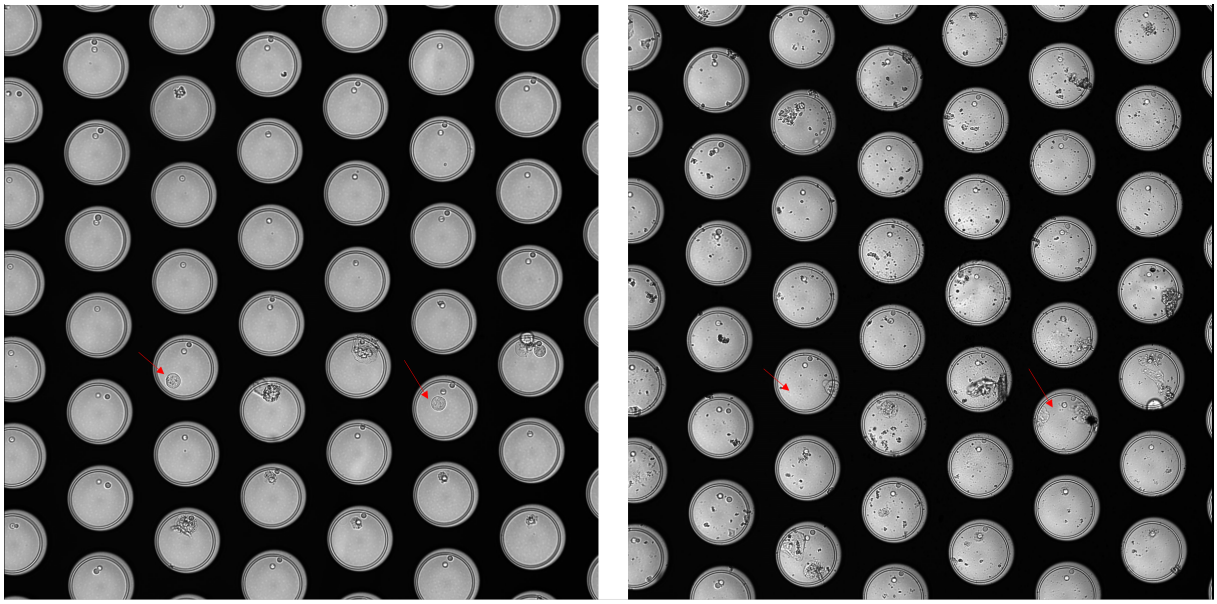

Figure 82: Condition 'Cells-FF seeded on chip'. 6K enriched cells were seeded on a chip with 5 mbar pressure. isolate cells can be seen at the arrow. They did not remain in place during incubation.

8.26 Appendix Z: scans of all channels used in the markerpanel of a DLA sample without CTCs but with leukocytes.

PE was slightly out of focus. No CTCs were found. Leukocytes were found.

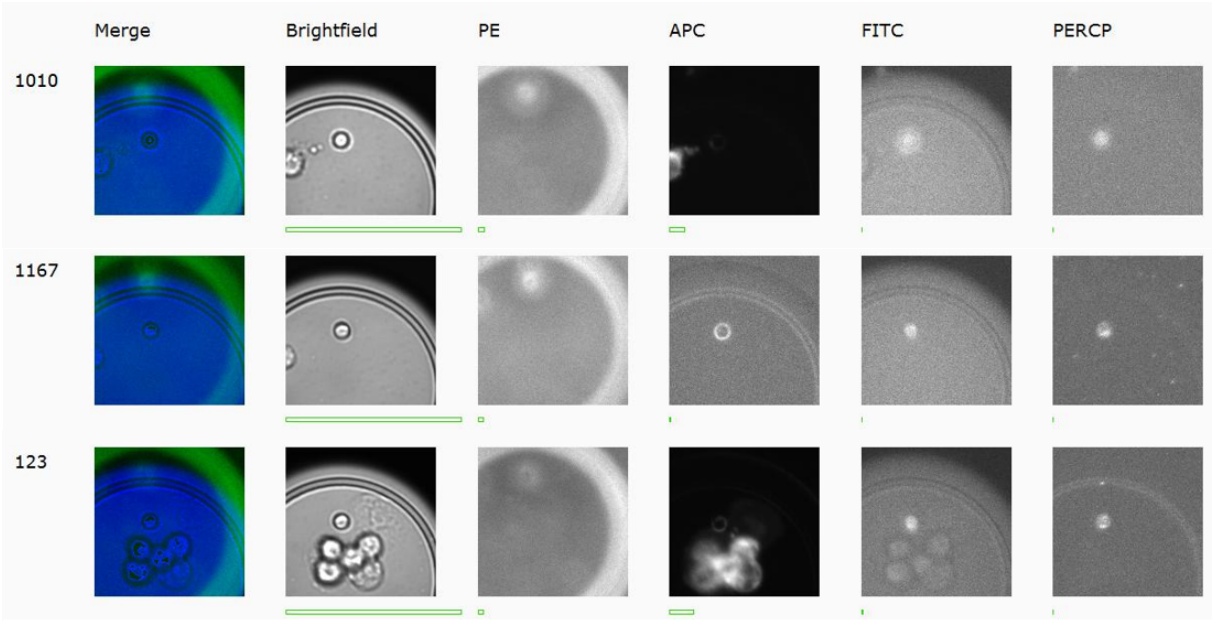

Figure 83: Examples of cells found in the chip. No CTC were identified. Lots of leucocytes were identified. Left the well number. PE: PSMA. APC: CD45. FITC: Calcein. PERCP: EpCAM.